Supporting Information for Martinoid: The Peptoid Martini Force Field

Hamish W. A. Swanson, Alexander Van Teijlingen, King Hang Aaron Lau, and Tell Tuttle

Department of Pure and Applied Chemistry, University of Strathclyde, 295 Cathedral Street, Glasgow G1 1XL, UK.

Corresponding author address: aaron.lau@strath.ac.uk, tell.tuttle@strath.ac.uk

1. Peptoid Monomer Synthesis

Peptoids were prepared by either Zuckermann's solid phase submonomer protocol[1] or by liquid phase synthesis based on a one step S_N2 reaction initially described by Salaun et al.[2] All solvents and reagents received from the manufacturers specified below were used without further purification.

1.1. Solid Phase Synthesis (SPS)

0.74 g of Rink Amide polystyrene resin (scale 0.66 mM, Merck-Novabiochem, MBHA Rink Amide 0.89 mM/g loading) was swollen by successive washes with 1 x DCM (Fischer Scientific, HPLC Gradient Grade) and 2 x DMF (Honeywell, peptide synthesis grade). The resin was then deprotected with two washes of 5 mL 20 % piperidine (Fisher Scientific, Reagent Grade) in NMP (Honeywell, peptide synthesis grade) each with a duration of 20 minutes. After washing the resin with DMF six times, the resin was treated with bromoacetic acid (8.8 mL, 1.5 M, Merck-Sigma Aldrich) and DIC in DMF (4.13 mL, 50:50 /v, Fluorochem, Glossop, UK) for 40 minutes with shaking. The resin was subsequently filtered and washed four times with DMF and two times with NMP. The resin was then treated with the amine required for each type of sidechain (Table S1) dissolved in NMP (8.8 mL, 1.5 M) with shaking for 40 minutes. The resin was then alternately washed with methanol and DCM three times and dried. The resin was twice treated with cleavage solution (95 % TFA: 2.5 % H2O : 2.5 % TIPS) with shaking for 20 minutes each time. The two batches of TFA with the cleaved peptoid was separately collected, and the TFA was removed by rotary evaporation leaving a yellow oil, this was solubilised in a mixture of H2O and acetonitrile, transferred to a pre-weighed vial, and freeze-dried.

Table S1 – Synthesis and work up details for SPS.

Species	Name*	Amine in Stock (mL)	Crude Mass (g)	Pure Material (g)	Yield (%)
Nf	N-Benzyl amine	1.44	0.1161	0.0687	41.8
Nfe	2-(phenylethyl)amine	1.66	0.1215	0.0626	35.1
Nfes	(S)-(-)-1-Phenylethylamine	1.66	0.1902	0.0795	44.6

*Note: all amines used in SPS were purchased from Apollo Scientific.

Preparative reverse phase HPLC (RP-HPLC) was used to purify the peptoids. Stock solutions of the crude material were prepared in mixtures of H_2O (Fischer Scientific, HPLC Gradient Grade) and acetonitrile (Fischer Scientific, HPLC Gradient Grade) which were filtered through 0.2-micron syringe filters to remove any solids. Preparative RP-HPLC was performed on a Jupiter C18 column (Phenomenex, 90 Å, 250 x 10.0 mm) to purify the material using an isocratic eluent mixture of 2 % acetonitrile: 98 % H_2O with 0.1 % TFA. Higher acetonitrile percentages were found to preclude material partitioning onto the solid phase, with the material eluting as the injection peak. 1 mL of crude stock at concentrations from 2 – 25 mg/mL were injected across different preparative runs and fractions were collected every 30 or 60 seconds. The HPLC fractions with matching UV absorbance peak features (data at 220 nm and 254 nm) were combined, and solvent was removed successively by a centrifugal evaporation (heating at 30^{o}C; to reduce volume to a few millilitres) and by freeze-drying. A fluffy white crystalline solid was obtained for Nfe and Nfes, while for the product for Nfe was more granular in nature. The identity and final purity of the product was characterized by NMR (see section 2).

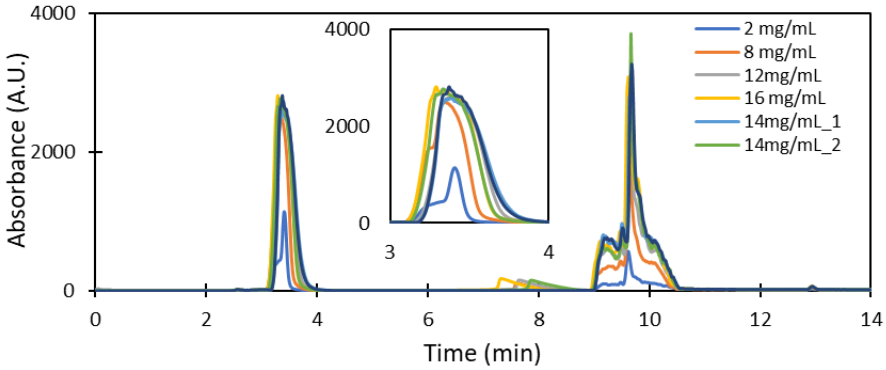

Figure S1 – All fractions of Nf obtained by isocratic HPLC with 2 % acetonitrile: 98 % H_2O with 0.1 % TFA. Fractions collected between 3 – 4 minutes were combined giving pure material as evidenced by NMR spectroscopy (see section 2).

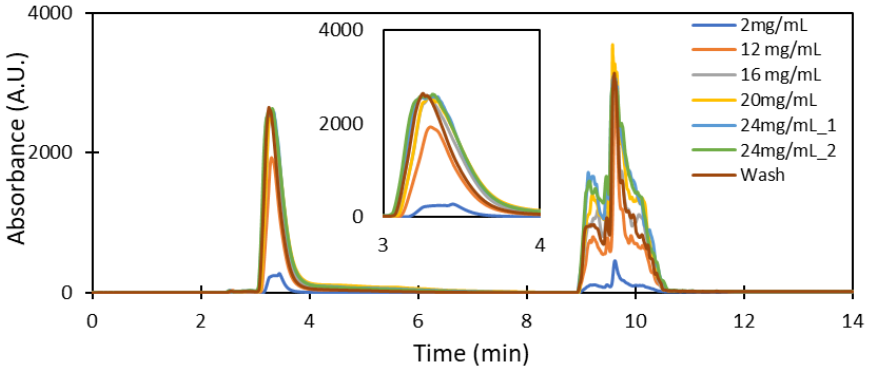

Figure S2 – All fractions of Nfe obtained by isocratic HPLC with 2 % acetonitrile: 98 % H_2O with 0.1 % TFA. Fractions collected between 3 – 4 minutes were combined giving pure material as evidenced by NMR spectroscopy (see section 2).

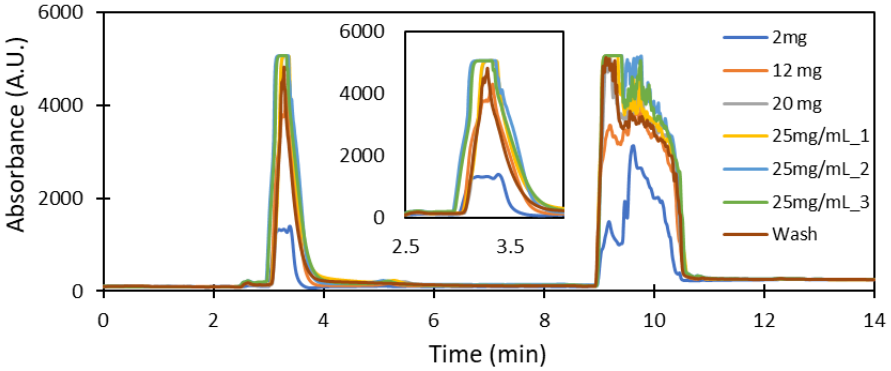

Figure S3 – All fractions of Nfes obtained by isocratic HPLC with 2 % acetonitrile: 98 % H_2O with 0.1 % TFA. Fractions between 3 – 4 minutes were combined giving pure material as evidenced by NMR spectroscopy (see section 2).

1.2. Liquid Phase Synthesis

It was found that the cleavage of single monomers without bulky aromatic groups from the Rink Amide resin using TFA resulted in chemical decomposition. For Nk and Nke this was particularly acute, with it not being possible to obtain pure material. It was suspected that this occurred through a slow C-terminal cyclization reaction observed in some peptoids, as described by Seo et al.[3] While the peptoids incorporating Nk and Nke residues are generally stable even under acidic conditions (e.g., neat TFA), it is thought that the small size of the monomeric form and the prolonged TFA exposure associated with resin cleaving and HPLC purification may have promoted cyclization.

To access monomers of this description it was decided instead to begin liquid phase synthesis with the 2-bromoacetamide as the starting material and perform S_N2 reactions with the primary amine sidechain. 2-bromoacetamide (Sigma Aldrich) was dissolved in acetonitrile (HPLC Gradient Grade, Fisher Scientific) at a concentration of 0.25 M with stirring (typically 1 – 2 mmol scale). 1 amine equivalent was then added, leading to an intensification in the yellow solution colour. All reagents, suppliers and final yields are shown in Tables S2.

Acetonitrile was selected as the preferred polar aprotic solvent as several of the monomer products precipitated in this solvent which was convenient for work-up. In initial synthesis batches, 1 equivalent of diisopropylethylamine (DIPEA, Alfa Aesar) was used as a complementary base to neutralise the equivalent of hydrogen bromide formed by the reaction. Through X-ray crystallography characterization, it was confirmed that the final product was a bromide salt (results not shown).

It was found in subsequent batches that similar yields could be obtained with the omission of DIPEA, as well as resulting in faster precipitate formation and reduced adhesion to glassware. For all batches, after 12 – 24 h the precipitate was recrystallised in hot acetonitrile:methanol (approximately 2:1 /v). For Nke it was necessary to use acetone as the recrystallisation solvent. Although this monomer is unstable in acetone over extended periods (suspected imine formation), it is found to be sufficiently stable for our protocol with a short recrystallisation step (e.g., rapid transfer of hot liquor into ice-bath). All solids were filtered and washed with the relevant recrystallization solution.

Table S2 – Species, monomer, supplier and recovered yield for liquid phase reactions.

Species	**Amine**	**Supplier**	**Yield (%)**
Nab.HBr	1-butylamin*e*	Alfa Aesar	22.0
Nfe[4Cl].HBr	2-(4-Chlorophenyl) ethylamine	Tokyo Chemical Industry	26.3
boc-Nk.HBr	*t*-butyl N-(4-aminobutyl) carbamate	Apollo Scientific	57.4
boc-Nab.HBr	Ethane-1,2-diamine (N-Boc Protected)	Apollo Scientific	28.4

2. Peptoid Monomer Characterisation

It was found that obtaining ^{13}C NMR data was challenging, with many scans yielding poor quality data. It was proposed that this was due to the nitrogen atoms within the structures, which can supress ^{13}C signals. For this reason, we decided to use both ^{1}H – ^{13}C Heteronuclear Single Quantum Coherence (HSQC) and Heteronuclear Multiple Bond Correlation (HMBC) to infer the chemical shifts of ^{13}C atoms. The most important inference made possible by HMBC is the cross-peak between the C_α of the peptoid monomer and the amide C-terminus, which cannot be identified due to proton exchange of protonated nitrogen atoms which occurs due to D_2O exchange. In all cases the inferences obtained are consistent with the expected structures (Figures S4 – S24).

2.1. Nf

^{1}H NMR

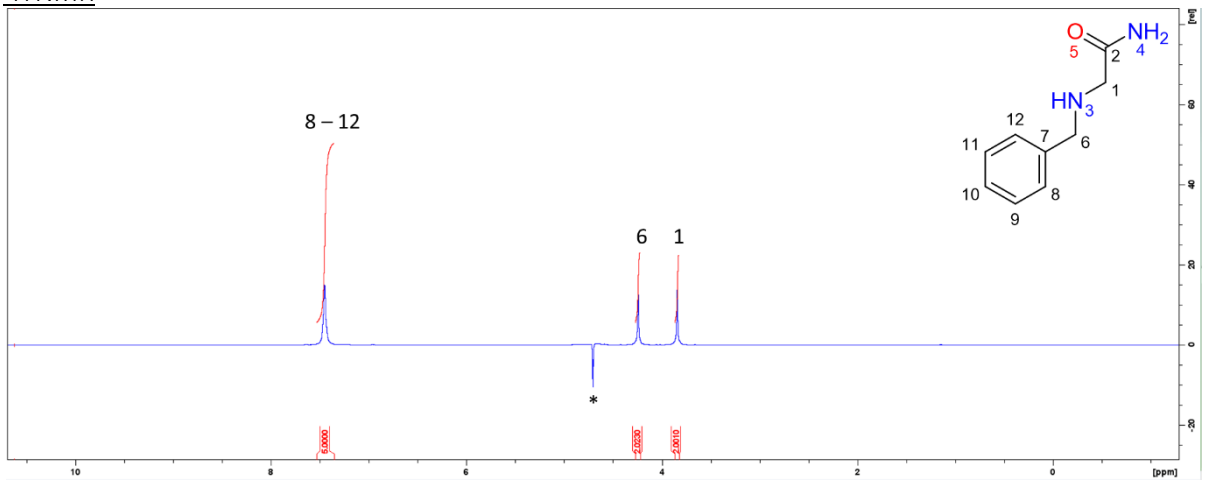

Figure S4 – Nf ^{1}H NMR (400 MHz, D_2O) δ (ppm): 7.47 – 7.43 (m, 5H), 4.24 (s, 2H), 3.84 (s, 2H). * is H_2O

$^{1}H - {}^{13}C$ HSQC NMR

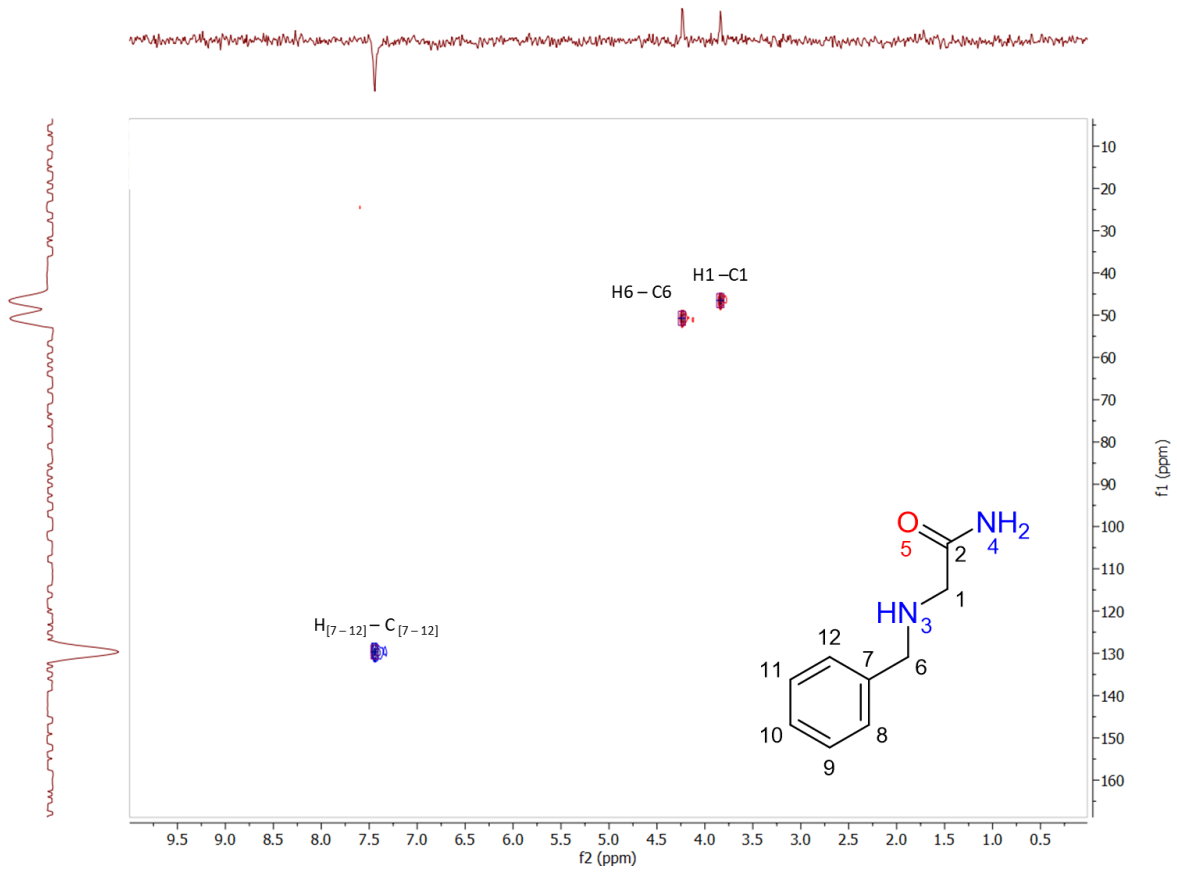

Figure S5 – Nf HSQC ($^{1}H - {}^{13}C$, 400 MHz, D_2O).

Table S3 – Nf HSQC cross peaks.

F1 Carbon Shift (ppm)	F2 Proton Shift (ppm)	Assigned Carbon
130.52	7.47 – 7.43	8 – 12
46.53	3.84	1
50.73	4.24	6

$^{1}H - {}^{13}C$ HMBC NMR

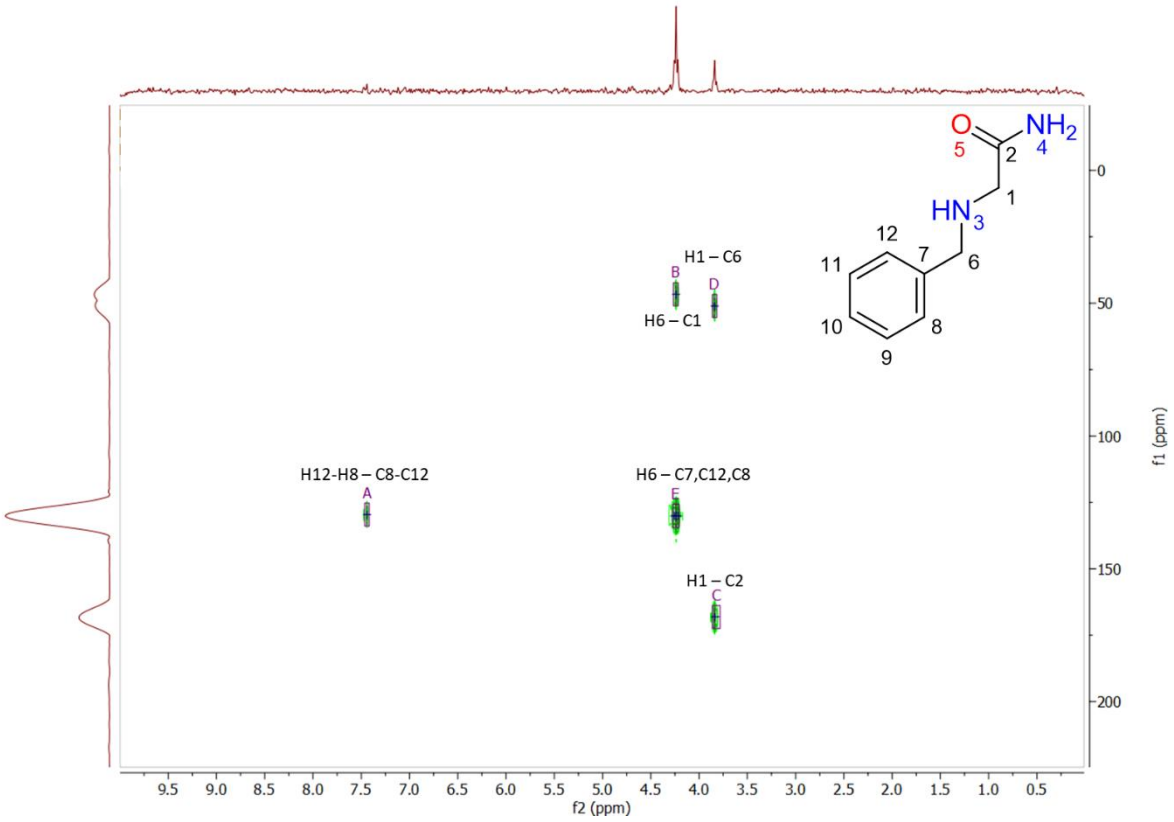

Figure S6 – Nf HMBC ($^{1}H - {}^{13}C$, 400 MHz, D_2O).

Table S4 – Nf HMBC cross peaks.

F1 Carbon Shift (ppm)	F2 Proton Shift (ppm)	Assigned Carbon
50.73	3.84	H1 – C6
168.12		H1 – C2
46.53	4.24	H6 – C1
129.68		H6 – C7,C8,C12
129.68	7.47 – 7.43	H8,H9,H10,H11,H12 – C8,C9,C10,C11,C12A

2.2. Nfe

^{1}H NMR

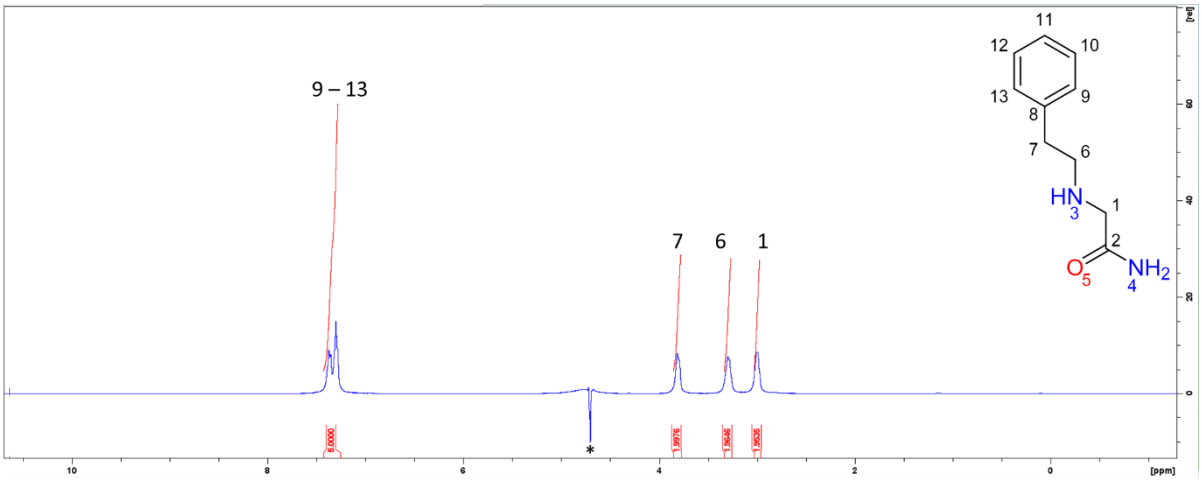

Figure S7 – Nfe ^{1}H NMR (400 MHz, D_2O) δ (ppm): 7.39 – 7.28 (m, 5H), 3.81 (t, 2H), 3.28 (s, 2H), 2.99 (t, 2H). * is H_2O

$^{1}H - {}^{13}C$ HSQC NMR

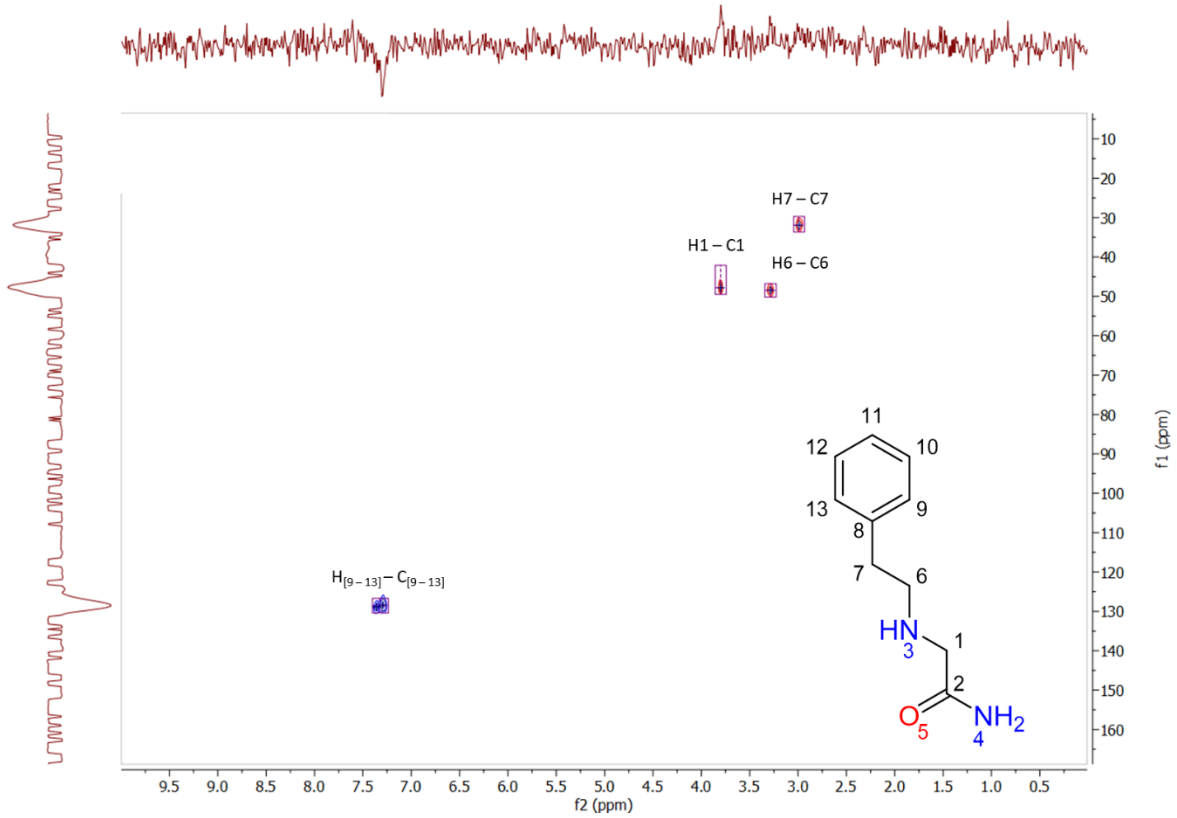

Figure S8 – Nfe HSQC ($^{1}H - {}^{13}C$, 400 MHz, D_2O).

Table S5 – Nfe HSQC cross peaks.

F1 Carbon Shift (ppm)	F2 Proton Shift (ppm)	Assigned Carbon
31.97	2.99	H7 – C7
48.47	3.28	H6 – C6
47.82	3.81	H1 – C1
128.64	7.39 – 7.28	9 – 13

$^{1}H - {}^{13}C$ HMBC NMR

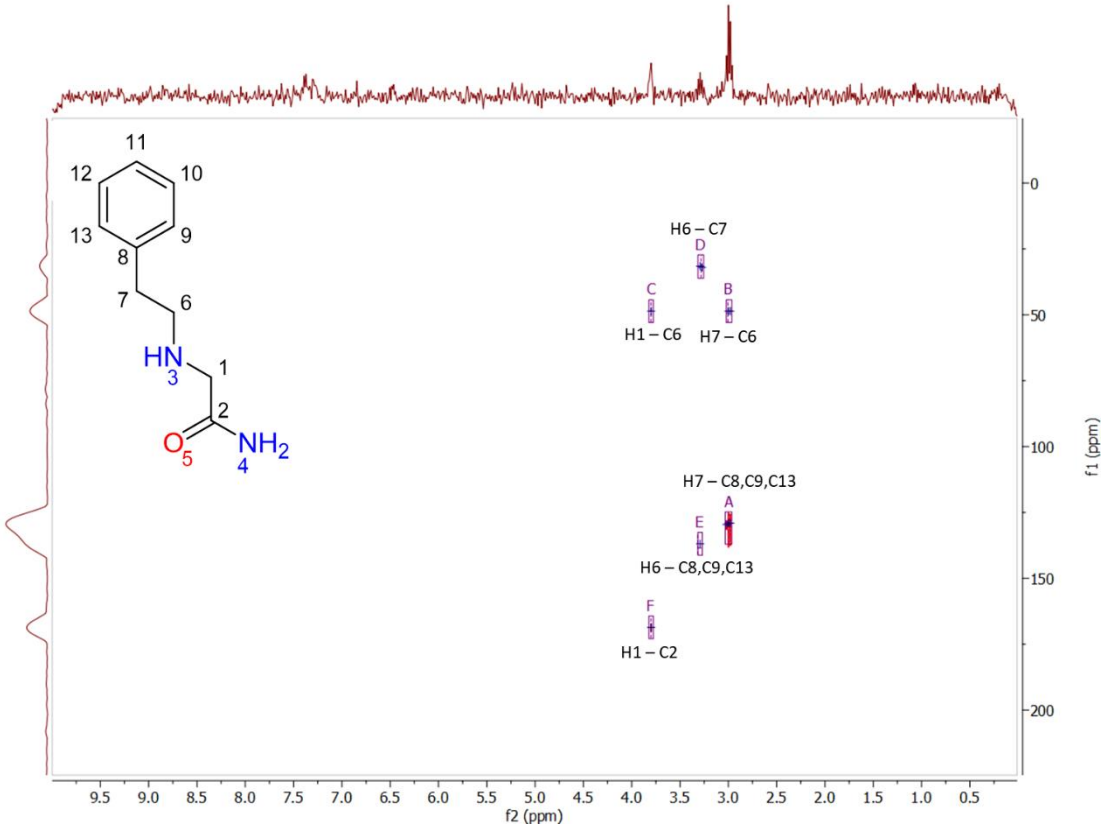

Figure S9 – Nfe HMBC ($^{1}H - {}^{13}C$, 400 MHz, D_2O).

Table S6 – Nfe HMBC cross peaks.

F1 Carbon Shift (ppm)	F2 Proton Shift (ppm)	Peak Inter-relation
48.47	2.99	H7 – C6
128.64		H7 – C8, C9, C13
31.97	3.28	H6 – C7
129.00		H6 – C8,C9,C13
48.47	3.81	H1 – C6
168.61		H1 – C2

2.3. Nfes

^{1}H NMR

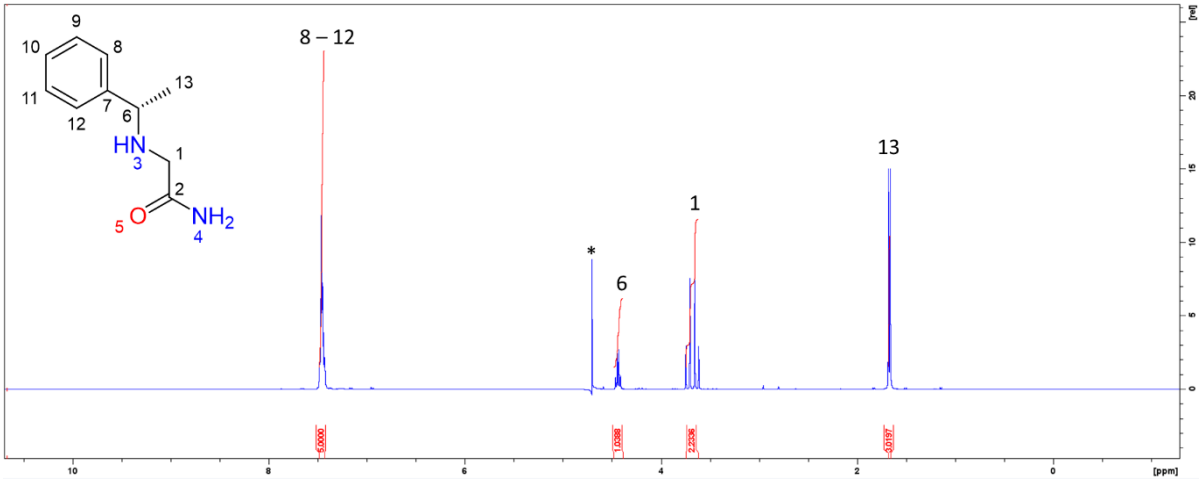

Figure S10 – Nfes ^{1}H NMR (400 MHz, D_2O) δ (ppm): 7.49 – 7.42 (m, 5H), 4.44 (s,1H), 3.63 (m*, 2H) 1.67 (s, 3H). (Note: doublet from $^{2}J_{HH}$ coupling on C_α which exhibit a strong roof effect giving the appearance of a quartet). * is H_2O. d

$^{1}H - {}^{13}C$ HSQC NMR

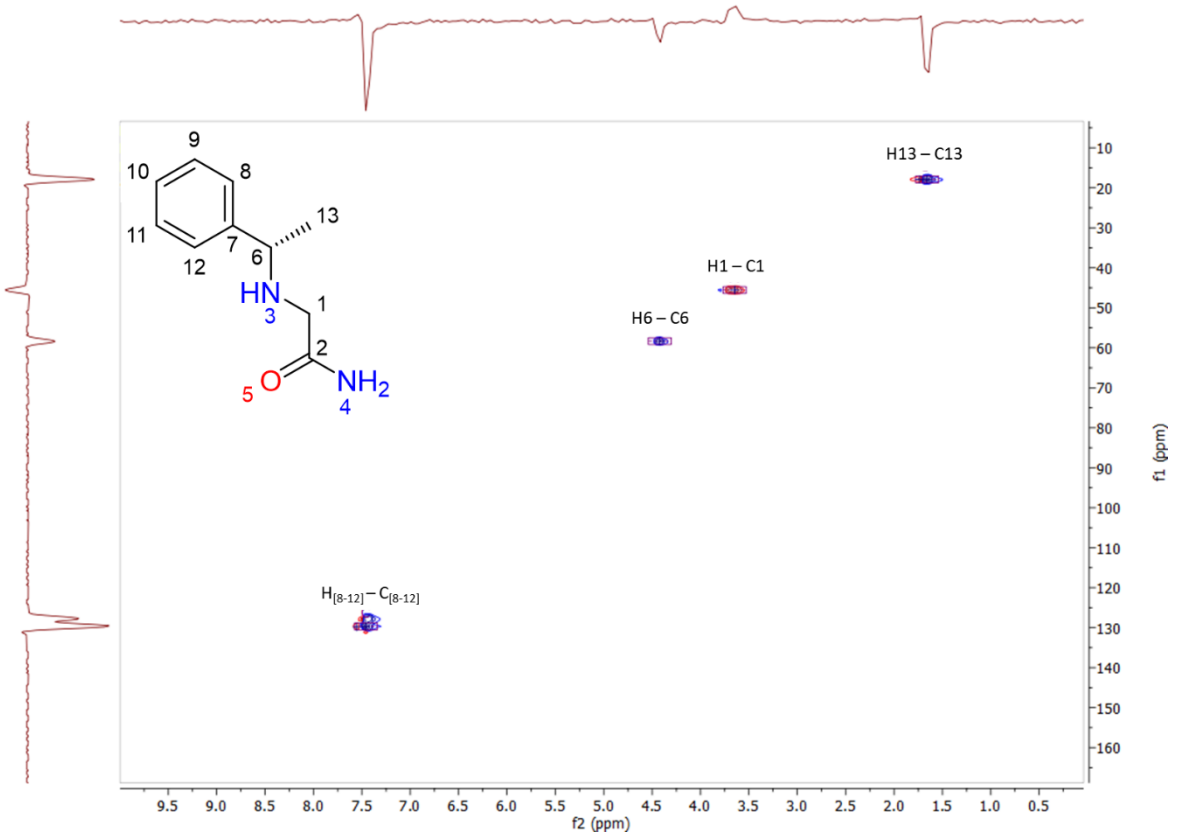

Figure S11 – Nfes HSQC ($^{1}H - {}^{13}C$, 400 MHz, D_2O).

Table S7 – Nfes HSQC cross peaks.

F1 Carbon Shift (ppm)	F2 Proton Shift (ppm)	Assigned Carbon
18.13	1.67	H13 – C13
17.85	3.63	H1 – C1
45.72	4.44	H6 – C6
129.24	7.49 – 7.42	$H_{[8-12]} - C_{[8-12]}$

$^{1}H - {}^{13}C$ HMBC NMR

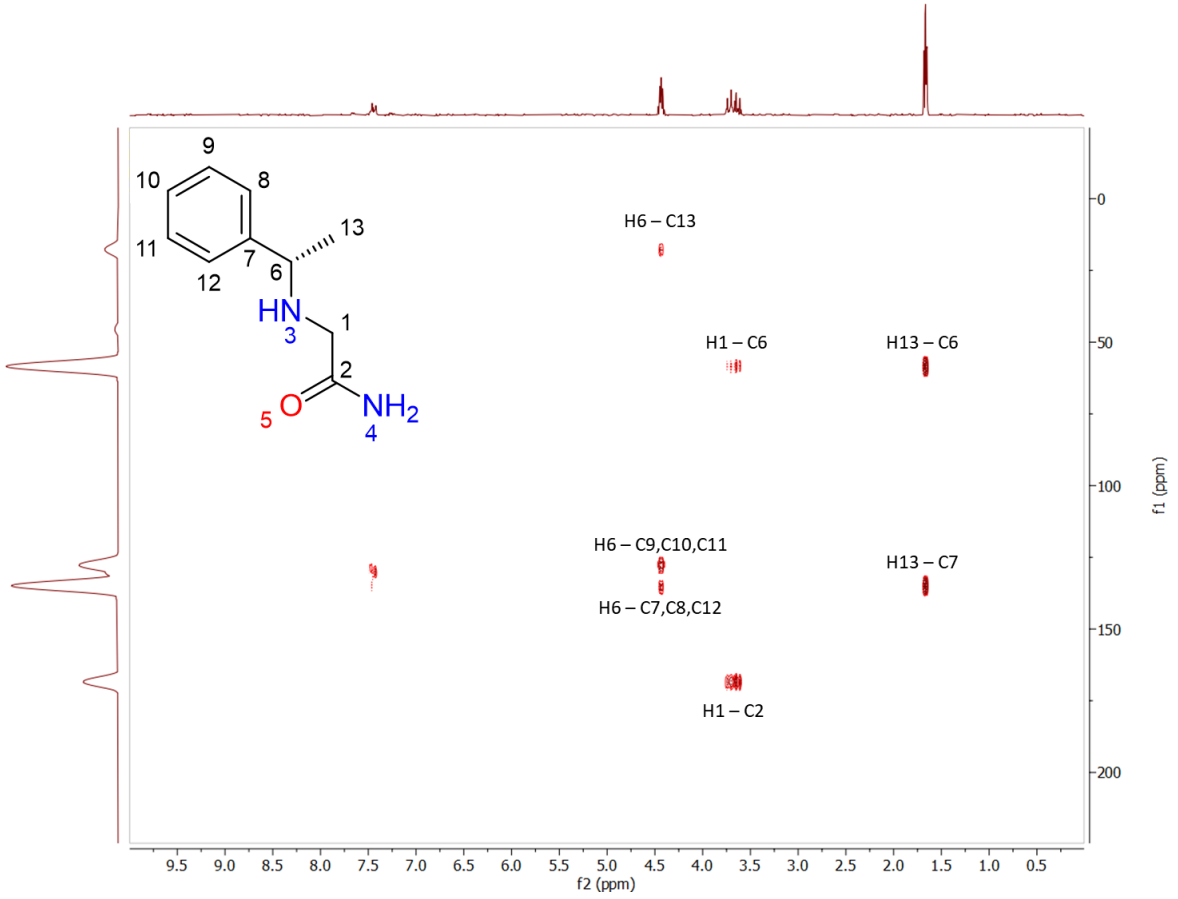

Figure S12 – Nfes HMBC ($^{1}H - {}^{13}C$, 400 MHz, D_2O).

Table S8 – Nfes HMBC cross peaks.

F1 Carbon Shift (ppm)	F2 Proton Shift (ppm)	F2 Proton Shift (ppm)
58.43	1.67	1.67
134.87		H13 – C6
58.43	3.63	3.63
168.85		H1 – C2
17.65	4.44	4.44
127.29		H6 – C9,C10,C11
135.25		H6 – C7,C8,C12

2.4. Nfe[4Cl]

^{1}H NMR

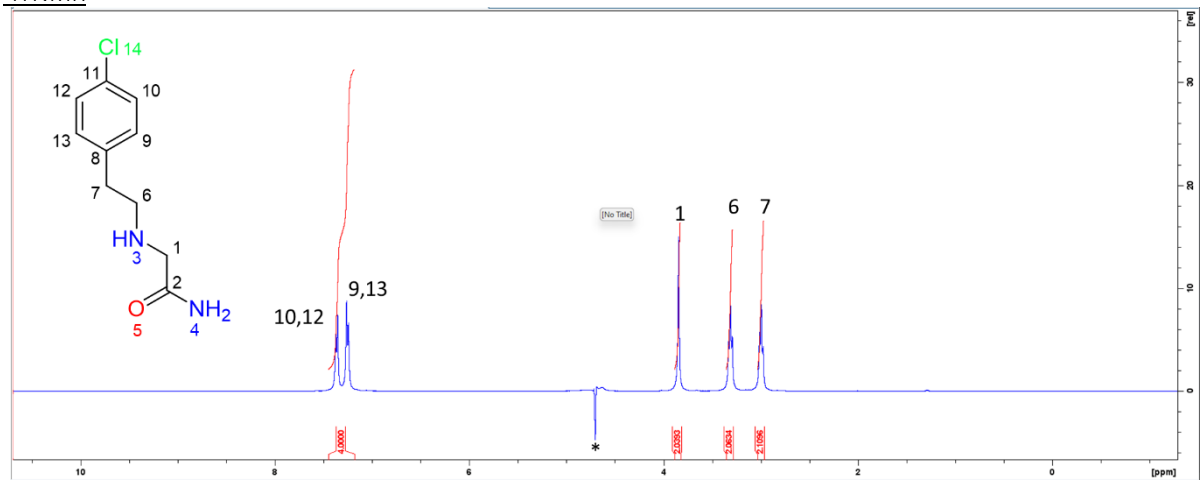

Figure S13 – Nfe[4Cl] ^{1}H NMR (400 MHz, D_2O) δ (ppm): 7.37 – 7.24 (dd, 4H), 3.84 (s,2H), 3.31 (t,2H), 2.99 (t,2H), * is H_2O.

$^{1}H - {}^{13}C$ HSQC NMR

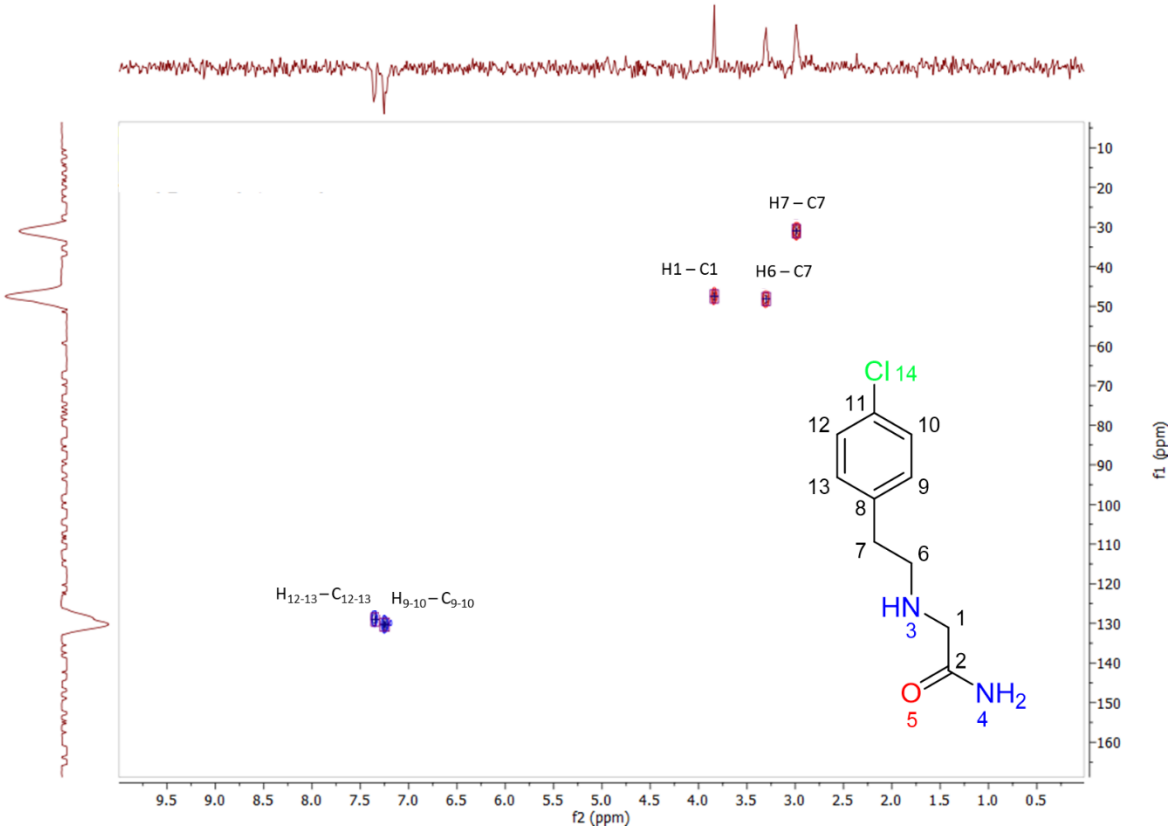

Figure S14 – Nfe[4Cl] HSQC ($^{1}H - {}^{13}C$, 400 MHz, D_2O).

Table S9 – Nfe[4Cl] HSQC cross peaks.

F1 Carbon Shift (ppm)	F2 Proton Shift (ppm)	Assigned Carbon
31.00	2.99	H7 – C7
48.15	3.31	H6 – C6
47.50	3.84	H1 – H1
130.32	7.26 – 7.24	$H_{9-10} - C_{9-10}$
129.03	7.37 – 7.35	$H_{12-13} - C_{12-13}$

$^{1}H - {}^{13}C$ HMBC NMR

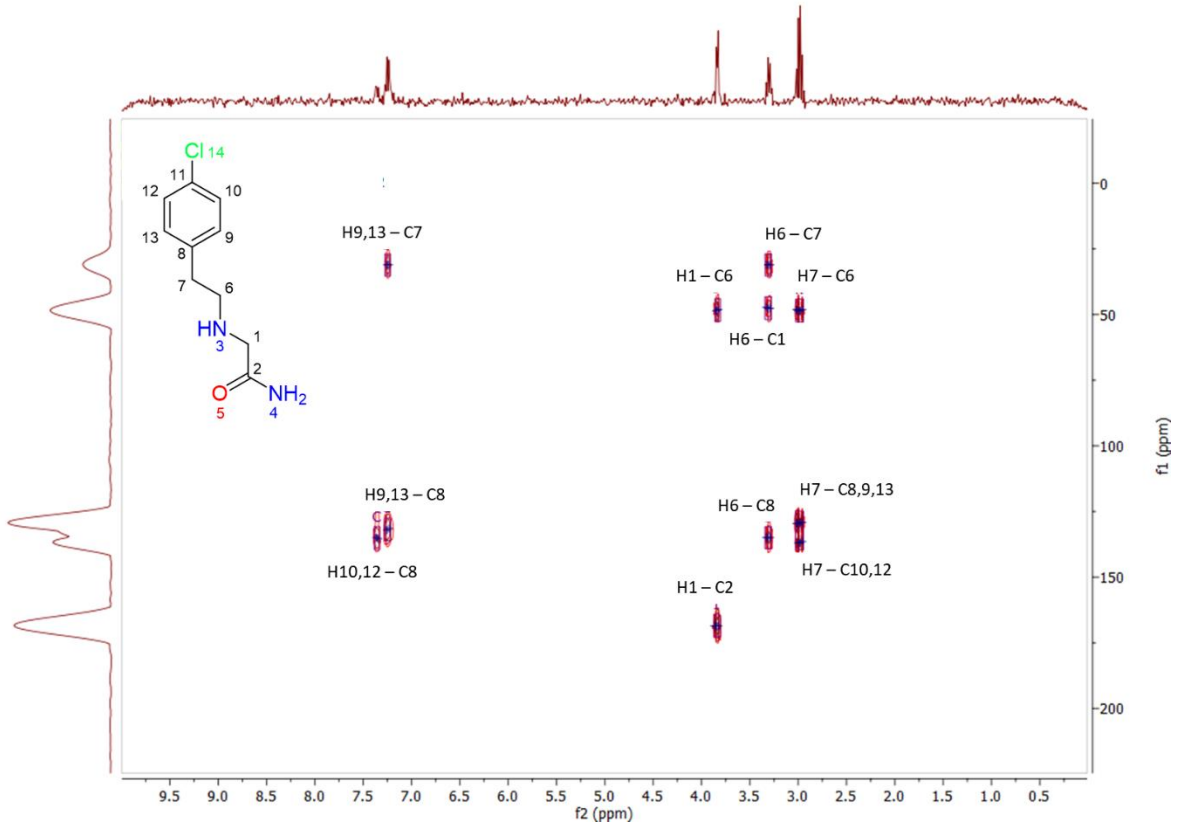

Figure S15 – Nfe[4Cl] HMBC ($^{1}H - {}^{13}C$, 400 MHz, D_2O).

Table S10 – Nfe[4Cl] HMBC cross peaks.

F1 Carbon Shift (ppm)	F2 Proton Shift (ppm)	Assigned Carbon
48.48	2.99	H7 – C6
131.82		H7 – C8,9,10,12,13
31.06	3.31	H6 – C7
47.54		H6 – C1
134.95		H6 – C8
48.34	3.84	H1 – C6
168.61		H1 – C2
31.06	7.25	H8,13 – C7
132.05		H8,13 – C8
134.22		H10,12 – C8

2.5. *boc*-Nk

^{1}H NMR

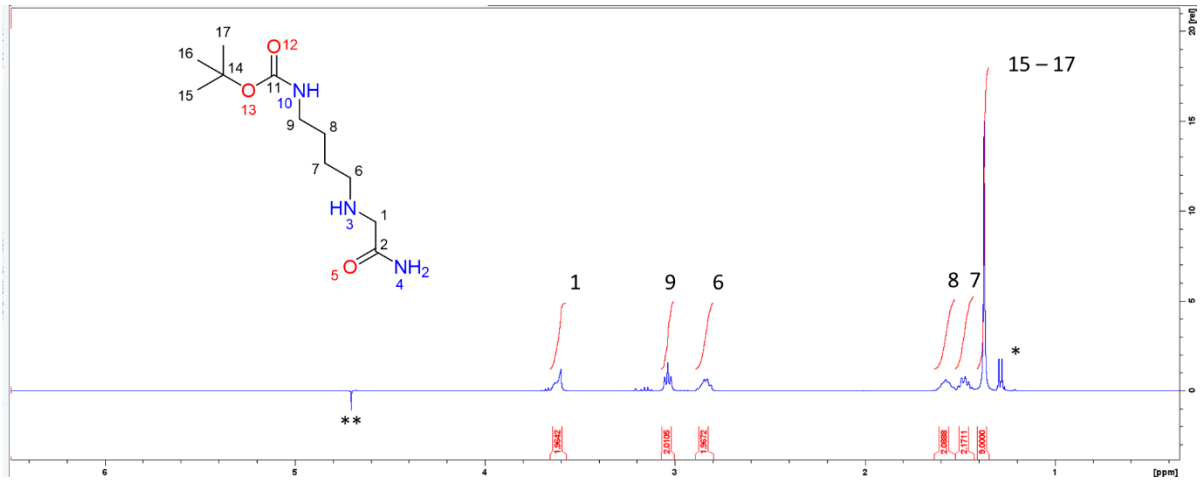

Figure S16 – *boc*-Nk ^{1}H NMR (400 MHz, D_2O) δ (ppm): 3.62 (s,2H), 3.04 (t,2H), 2.83 (t,2H), 1.58 (p, 2H), 1.48 (p,2H), 1.37 (s, 9H). * is thought to be due to the presence of IPA from spatula cleaning, ** is H_2O.

$^{1}H - {}^{13}C$ HSQC NMR

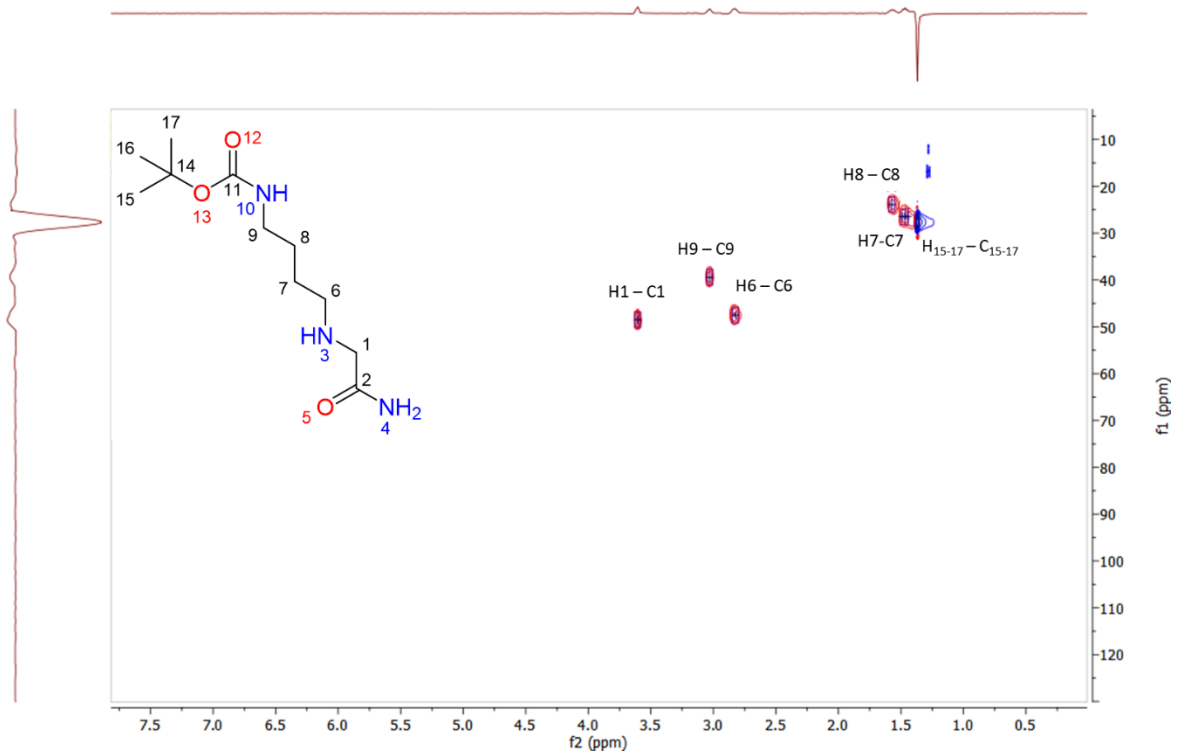

Figure S17 – *boc*-Nk HSQC ($^{1}H - {}^{13}C$, 400 MHz, D_2O).

Table S11 – *boc*-Nk HSQC cross peaks.

F1 Carbon Shift (ppm)	F2 Proton Shift (ppm)	Assigned Carbon
27.54	1.36	$H_{15-17} - C_{15-17}$
26.47	1.47	H7 – C7
23.88	1.57	H8 – C8
47.11	2.84	H6 – C6
39.41	3.03	H9 – C9
48.47	3.60	H1 – C1

$^{1}H - {}^{13}C$ HMBC NMR

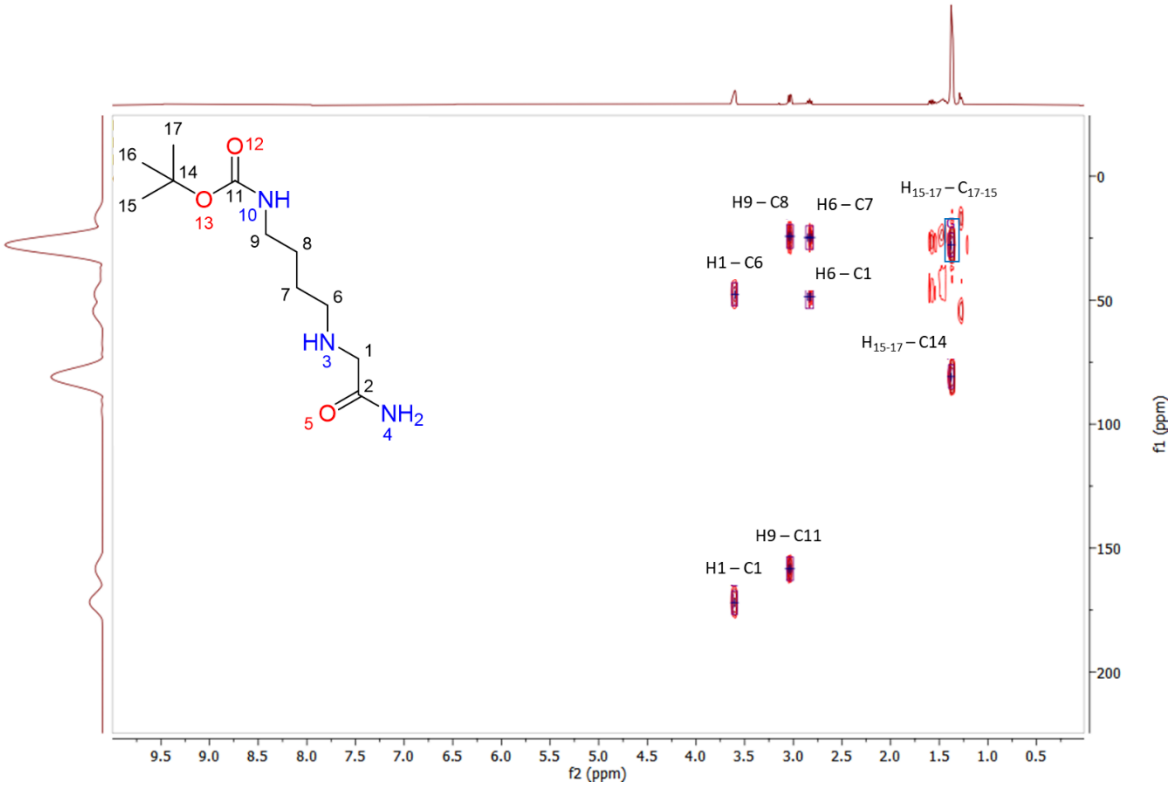

Figure S18 – *boc*-Nk HMBC ($^{1}H - {}^{13}C$, 400 MHz, D_2O).

Table S12 – *boc*-Nk HMBC cross peaks.

F1 Carbon Shift (ppm)	F2 Proton Shift (ppm)	Assigned Carbon
27.65	1.38	$H_{15-17} - C_{17-15}$
81.41		$H_{15-17} - C14$
24.72	2.83	H6 – C7
48.62		H6 – C1
24.4	3.04	H9 – C8
159.41		H9 – C11
47.65	3.60	H1 – C6
171.96	3.61	H1 – C2

2.6. *boc*-Nke

^{1}H NMR

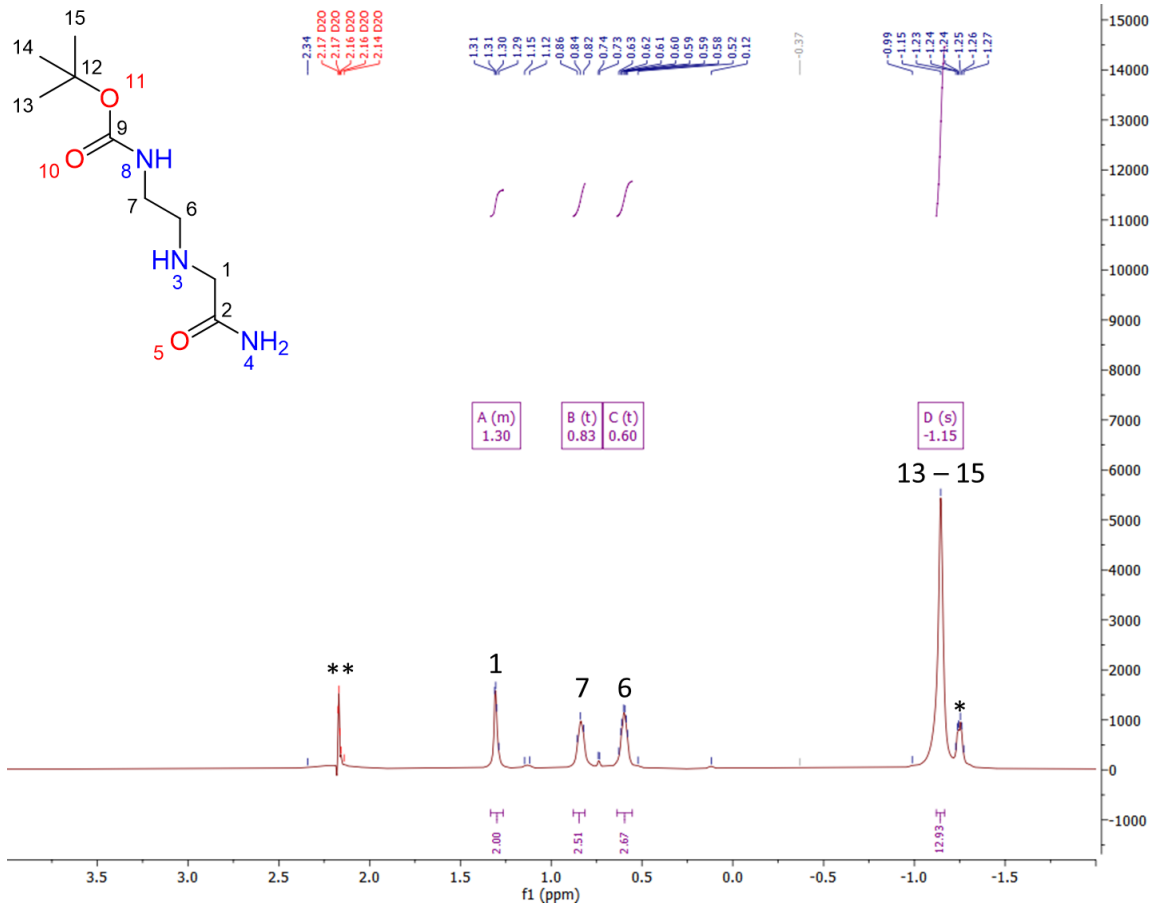

Figure S19 – *boc*-Nke ^{1}H NMR (400 MHz, D_2O) δ (ppm): 1.30 (s,2.00H), 0.83 (t, 2.51H), 0.6 (t,2.67H), -1.15(s, 12,93H). * Is thought to be IPA and ** is H_2O.

$^{1}H - {}^{13}C$ HSQC NMR

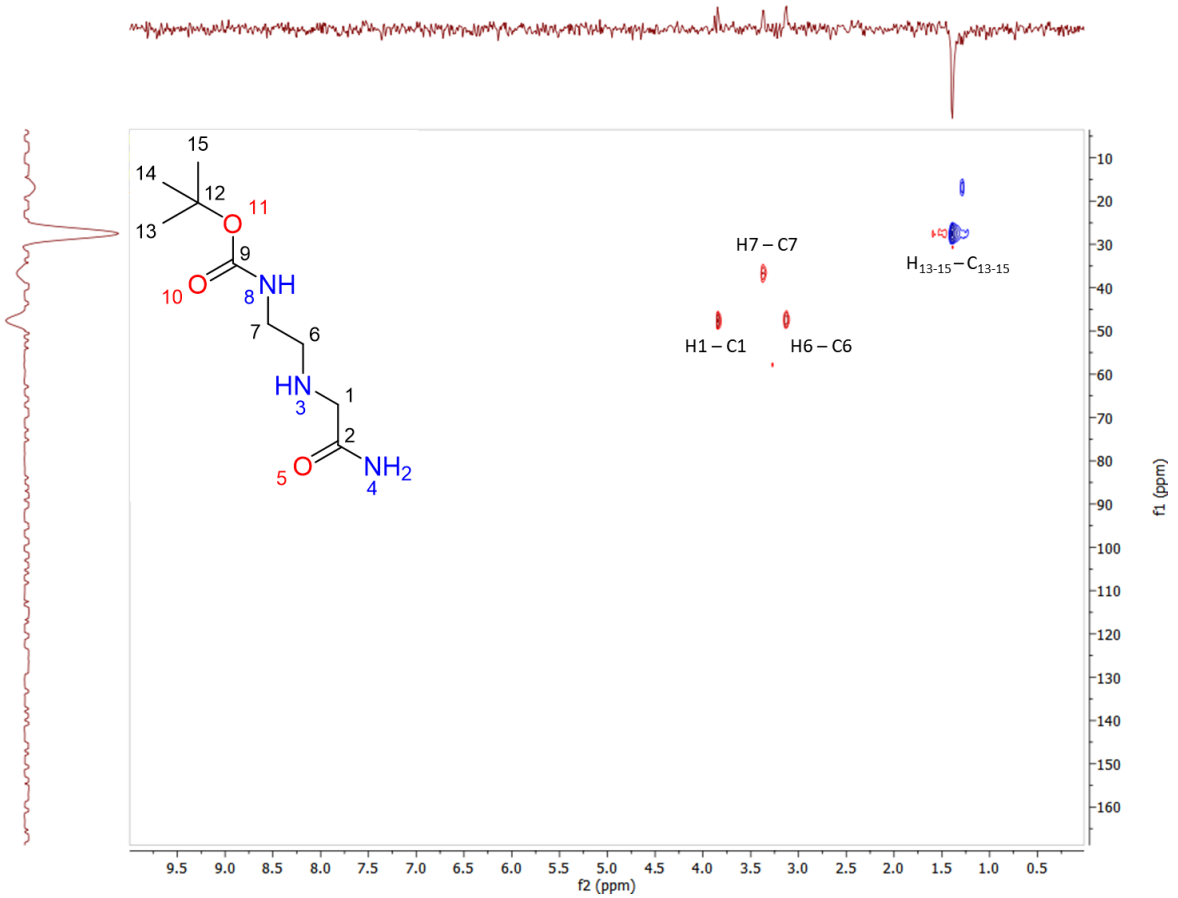

Figure S20 – *boc*-Nke HSQC ($^{1}H - {}^{13}C$, 400 MHz, D_2O).

Table S13 – *boc*-Nk HSQC cross peaks.

F1 Carbon Shift (ppm)	F2 Proton Shift (ppm)	Assigned Carbon
27.49	1.39	$H_{13-15} - C_{13-15}$
47.77	3.13	H6 – C6
36.55	3.38	H7 – C7
47.77	3.84	H1 – C1

$^{1}H - {}^{13}C$ HMBC NMR

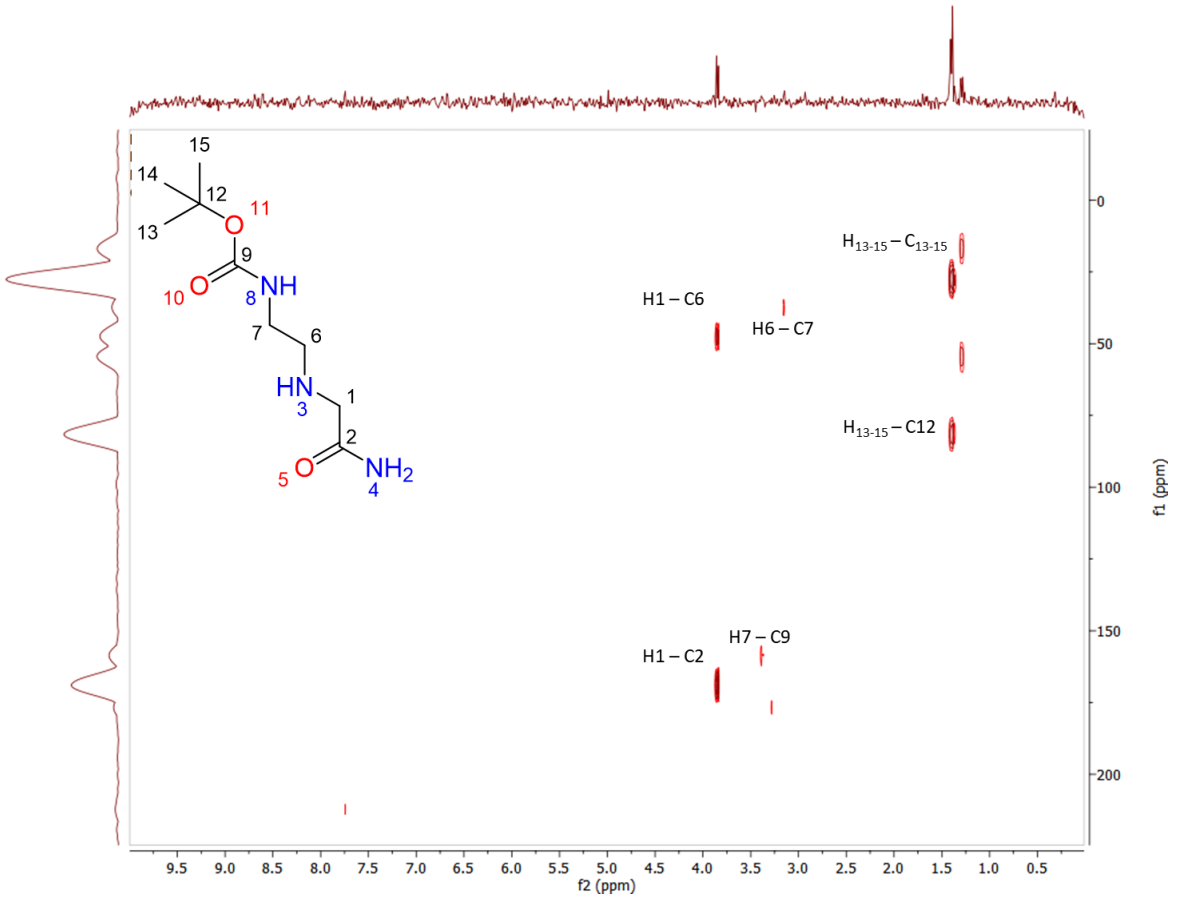

Figure S21 – *boc*-Nk HMBC ($^{1}H - {}^{13}C$, 400 MHz, D_2O).

Table S14 – *boc*-Nk HMBC cross peaks.

F1 Carbon Shift (ppm)	F2 Proton Shift (ppm)	Assigned Carbon
28.23	1.39	$H_{13-15} - C_{15-13}$
81.91		$H_{13-15} - C12$
37.46	3.14	H6 – C7
159.00	3.38	H7 – C9
48.47	3.85	H1 – C6
169.93		H1 – C2

2.7. Nab

^{1}H NMR

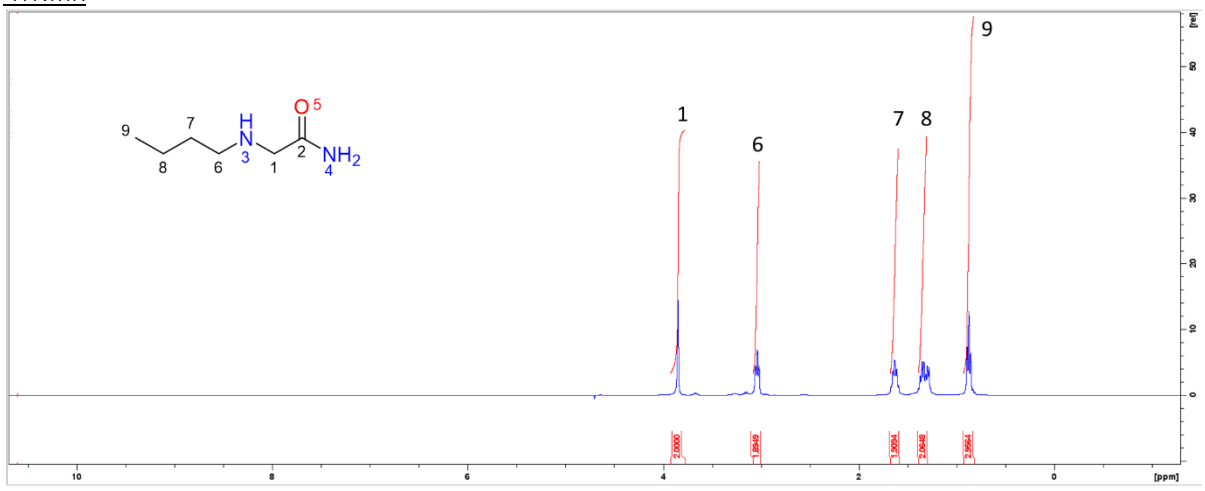

Figure S22 – Nab ^{1}H NMR (400 MHz, D_2O) δ (ppm): 3.85 (s,2H),3.04 (t,2 H), 1.63 (p,2H), 1.32 (m,2H), 0.85 (t, 3H).

$^{1}H - {}^{13}C$ HSQC NMR

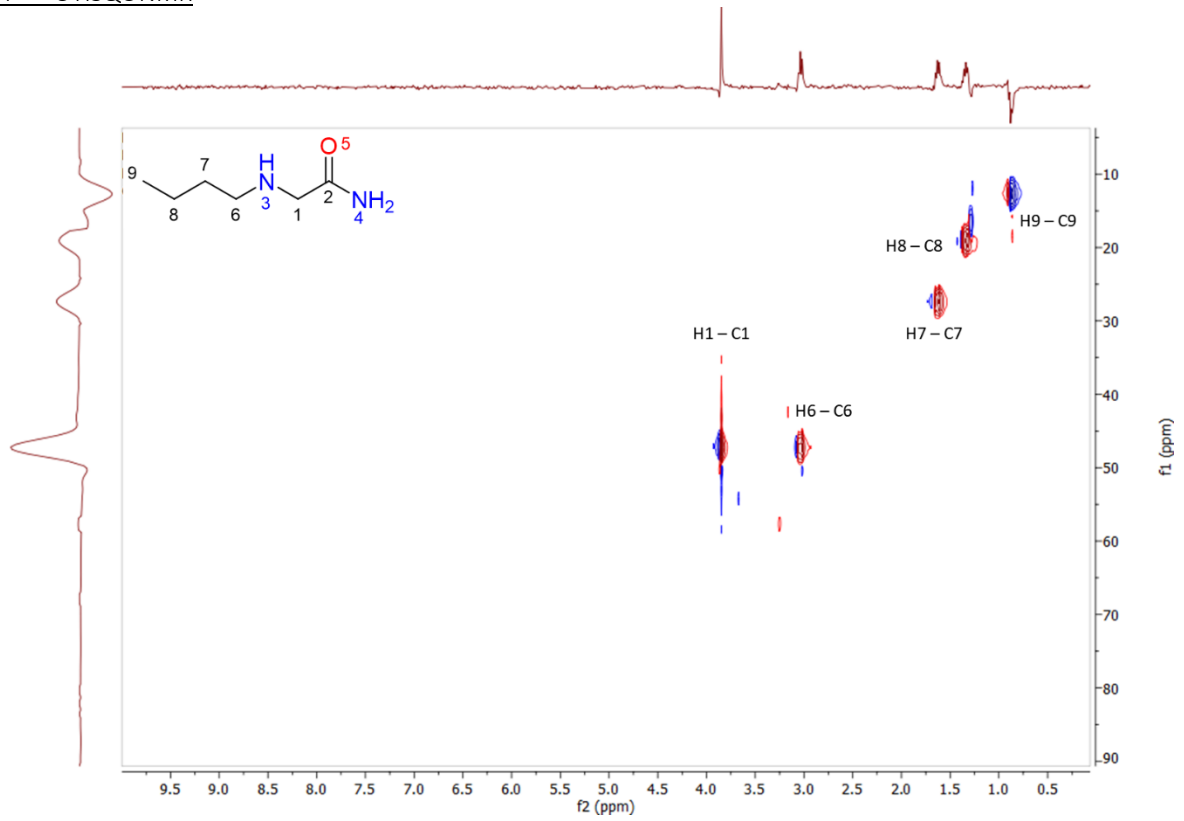

Figure S23 –Nab HSQC ($^{1}H - {}^{13}C$, 400 MHz, D_2O).

Table S15 – Nab HSQC cross peaks.

F2 Proton Shift (ppm)	F1 Carbon Shift (ppm)	Assigned Carbon
0.85	12.70	H9 – C9
1.32	19.12	H8 – C8
1.63	27.50	H7 – C7
3.04	47.31	H6 – C6
3.85	47.47	H1 – C1

$^{1}H - {}^{13}C$ HMBC NMR

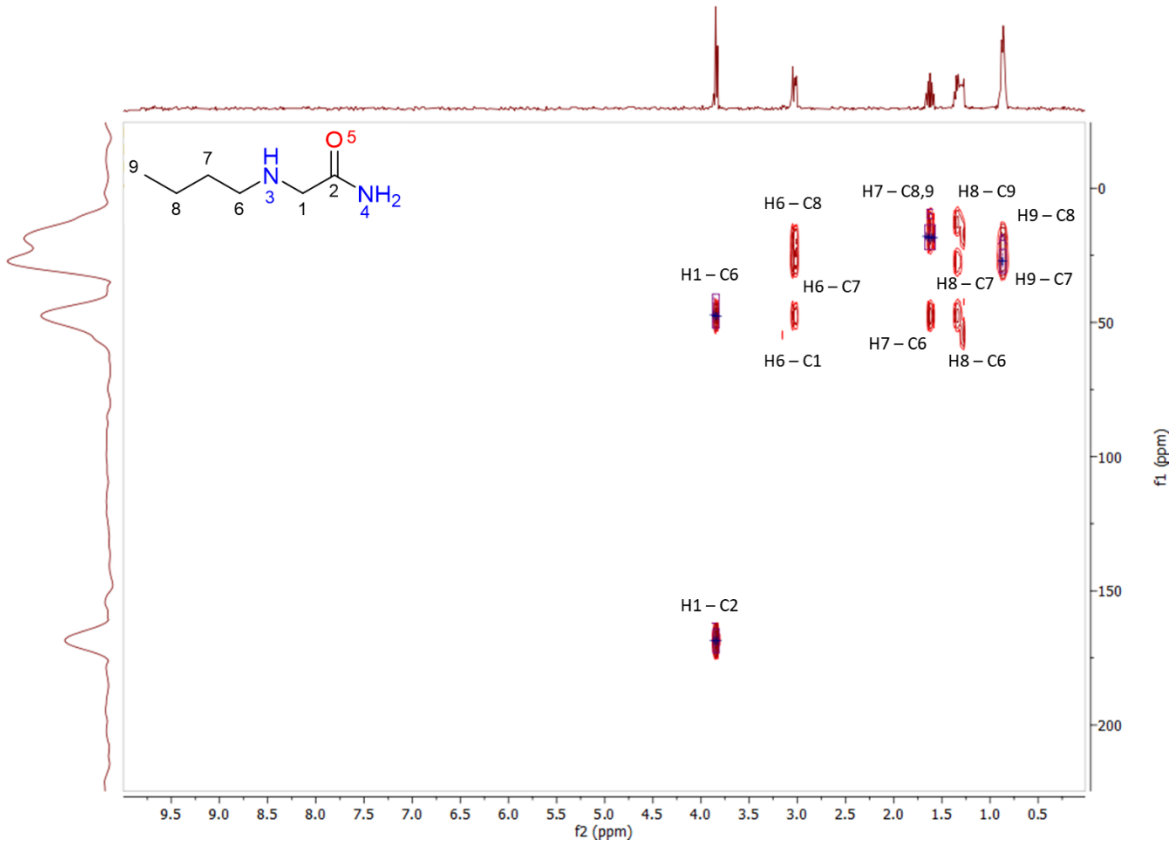

Figure S24 –Nab HMBC ($^{1}H - {}^{13}C$, 400 MHz, D_2O).

Table S16 – Nab HMBC cross peaks.

F1 Carbon Shift (ppm)	F2 Proton Shift (ppm)	Assigned Carbon
17.88	0.85	H9 – C8
27.22		H9 – C7
12.36	1.32	H8 – C9
27.79		H8 – C7
47.88		H8 – C6
18.87	1.63	H7 – C8
47.88		H7 – C6
17.88	3.04	H6 – C8
27.22		H6 – C7
47.88		H6 – C1
47.45	3.85	H1 – C6
169.45		H1 – C2

3. Experimental LogD Measurements

3.1 LogD Measurement Method

The method described by Cobb *et al.*[4] was broadly followed in this work. 500 µL of octanol (Sigma Aldrich) measured by weight was placed in an HPLC vial and to this 500 µL of PBS solution was added (Gibco 10X, diluted as required) containing the dissolved peptoid material over a concentration range of 0.3 – 5 mg/mL as required for a given species. More material was required for aliphatic monomers (*e.g.*, Nle, Nab or *boc*-Nk) as opposed to their aromatic counterparts (*e.g.*, Nf, Nfe, Nfes or Nfe[4Cl]). This vial was then sealed and agitated at 150 rpm for ~ 24h in an incubator to maintain a constant temperature of 25°C. Then a portion of both phases (~ 100 µL) were analysed using reversed-phase high performance liquid chromatography (HPLC) using a Luna 5 μm C18 column (Phenomenex, 100 Å, 100 x 4.6 mm) with a gradient of 2 to 45 % acetonitrile water over either 15 or 30 minutes with 0.1% trifluoroacetic acid as an additive. The resultant peak areas were integrated (peak area per minute) and compared between the two phases.

LogD Method Validation

3.2. Phe-OH

L-Phenylalanine from Sigma Aldrich (reagent grade).

Table S17 – Retention time, peak area/minute and peak height for 0.3 and 3 mg/mL Phe-OH.

	PBS Phase			Octanol Phase			LogD
Experiment	RT (min)	Area mAU*min	Height (mAU)	RT (min)	Area mAU*min	Height (mAU)	
1 (214 nm)	7.822	70.2561	528.685	7.807	2.3946	29.631	-1.445
	7.806	71.9372	533.671	7.772	2.8087	34.513	-1.502
	7.778	72.9688	540.613	7.775	2.9031	34.91	-1.482
2 (254 nm)	7.516	63.2309	223.089	7.782	2.3537	23.939	-1.467
	7.489	65.8692	227.06	7.821	2.1321	22.138	-1.408
	7.49	66.0093	228.642	7.791	2.3782	24.481	-1.400
						$\bar{x}$	-1.451
						σ	0.037

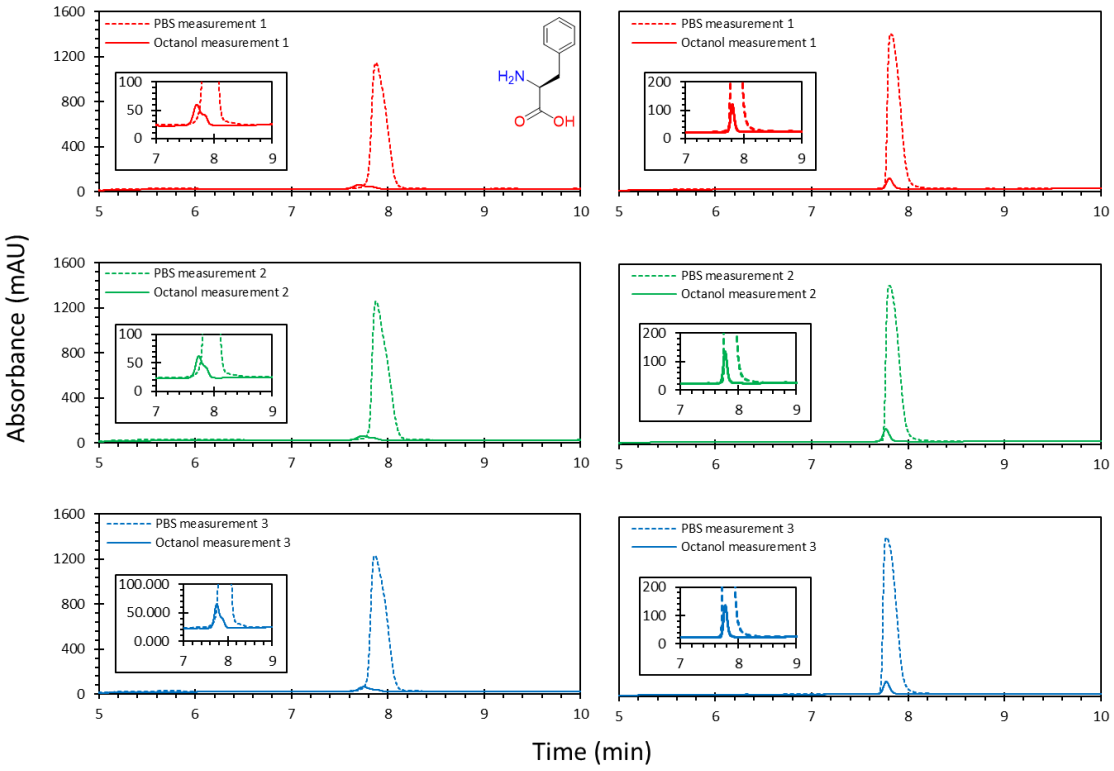

Figure S25 – LogD traces for Phe by two triplicate measurements; the cut-away included shows the absorbance of the *n*-octanol phase the absorbance for which is very small compared to the PBS phase.

3.3. Phe-NH_2

L-Phenylalanine Amidated from Bachem.

Table S18 – Retention time, peak area/minute and peak height for 0.3 mg/mL Phe-NH_2 at 214 nm.

	PBS Phase			Octanol Phase			LogD
Experiment	RT (min)	Area mAU*min	Height (mAU)	RT (min)	Area mAU*min	Height (mAU)	
1	6.868	122.3923	668.116	6.791	102.1841	937.537	-0.078
	6.848	124.8132	666.971	6.737	117.5884	1015.647	-0.026
	6.848	124.096	666.394	6.723	119.882	1026.751	-0.015
						$\overline{x}$	-0.040
						σ	0.028

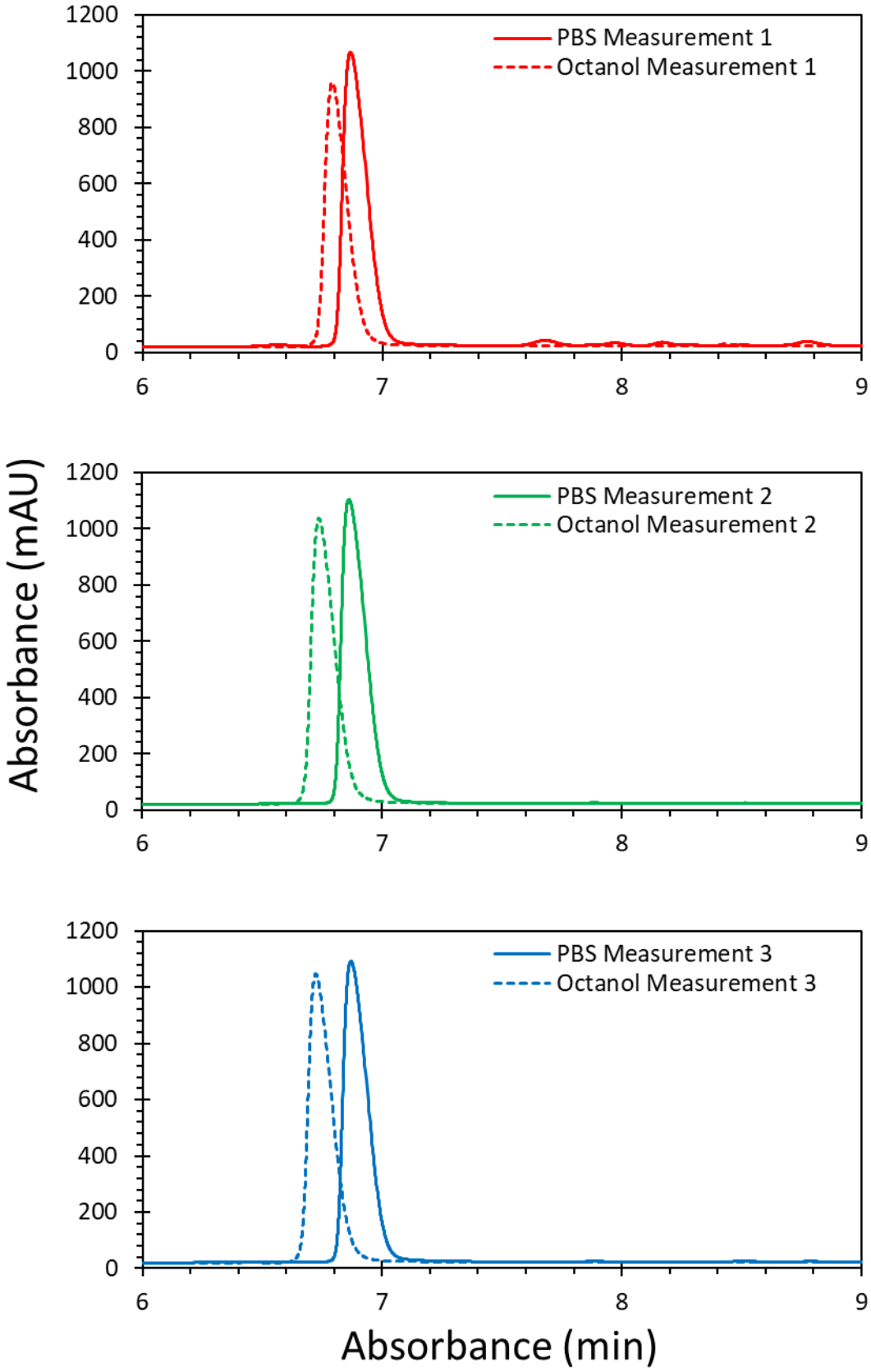

Figure S26 – LogD traces for Phe-NH_2 by triplicate measurements, like Phe in the apparently larger portion of material in the aqueous phase verses the *n*-octanol phase.

3.4. Nf-NH_2

Table S19 – Retention time, peak area/minute and peak height for 0.3 mg/mL Nf-NH_2 at 214 nm.

	PBS Phase			Octanol Phase			LogD
Experiment	**RT (min)**	**Area mAU*min**	**Height (mAU)**	**RT (min)**	**Area mAU*min**	**Height (mAU)**	
1	7.04	58.97	443.57	6.89	62.69	435.79	0.027
	7.01	68.65	501.01	6.89	71.18	482.73	0.016
	7.02	63.86	472.49	6.87	67.38	466.77	0.023
2	6.56	78.21	743.88	6.39	77.09	696.07	-0.006
	6.57	77.75	742.64	6.37	75.17	694.36	-0.015
	6.57	72.37	700.99	6.38	71.50	676.20	-0.005
						$\overline{x}$	0.007
						σ	0.016

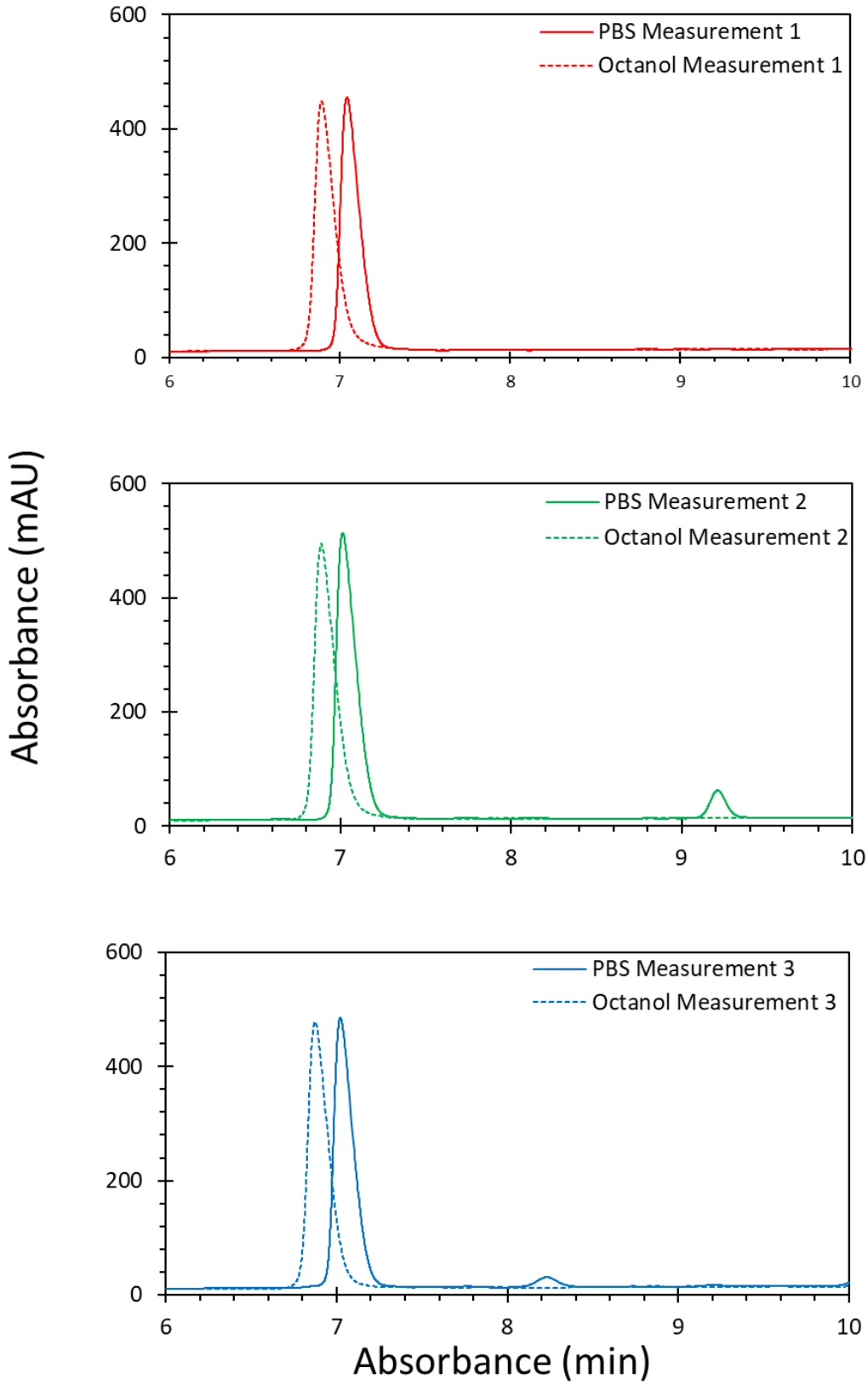

Figure S27 – LogD traces for Nf-NH_2 by triplicate measurements; there the PBS and *n*-octanol phases are roughly the same which is consistent with the calculated logD for this species of ~ 0.0.

3.5. Nfe-NH_2

Table S20 – Retention time, peak area/minute and peak height for 0.3 mg/mL Nfe-NH_2 at 214 nm.

	PBS Phase			Octanol Phase			LogD
Experiment	RT (min)	Area mAU*min	Height (mAU)	RT (min)	Area mAU*min	Height (mAU)	
1	8.564	51.170	449.020	8.363	71.749	672.906	0.147
	8.564	51.691	442.385	8.376	72.458	683.324	0.147
	8.545	52.236	458.700	8.379	73.007	682.070	0.145
2	8.428	54.774	563.263	8.279	75.094	705.311	0.137
	8.422	59.360	600.988	8.278	73.307	698.970	0.092
	8.416	60.101	613.289	8.273	74.785	701.231	0.095
						$\bar{x}$	0.127
						σ	0.024

3.6. Nfes-NH_2

Table S21 – Retention time, peak area/minute and peak height for 0.3 mg/mL Nfes-NH_2 at 214 nm.

	PBS Phase			Octanol Phase			LogD
Experiment	RT (min)	Area mAU*min	Height (mAU)	RT (min)	Area mAU*min	Height (mAU)	
1	8.160	28.002	257.332	8.032	73.726	770.291	0.420
	8.157	27.837	254.908	8.038	70.956	738.780	0.406
	8.096	25.631	211.643	8.014	74.099	779.652	0.461
2	8.069	32.083	400.821	7.962	81.961	855.469	0.407
	8.097	30.985	392.645	7.932	76.601	790.709	0.393
	8.084	32.407	409.168	7.937	78.491	816.791	0.384
						$\bar{x}$	0.412
						σ	0.025

3.7. Nfe[4Cl]-NH_2

Table S22 – Retention time, peak area/minute and peak height for 0.3 mg/mL Nfe[Cl]-NH_2 at 25d4 nm.

	PBS Phase			Octanol Phase			LogD
Experiment	RT (min)	Area mAU*min	Height (mAU)	RT (min)	Area mAU*min	Height (mAU)	
1	11.366	0.440	5.002	11.231	3.718	27.466	0.927
	11.372	0.481	5.564	11.229	3.540	29.144	0.867
	11.375	0.476	5.482	11.201	3.893	30.824	0.912
2	11.426	0.427	4.985	11.216	3.773	29.874	0.947
	11.444	0.454	5.204	11.236	3.165	26.783	0.844
	11.427	0.458	5.196	11.201	3.901	30.742	0.930
						$\bar{x}$	0.904
						σ	0.037

3.8. *boc*-Nk-NH_2

Table S23 – Retention time, peak area/minute and peak height for 0.3 and 3 mg/mL Nk-NH_2 at 214 nm.

	PBS Phase			Octanol Phase			LogD
Experiment	RT (minu)	Area mAU*min	Height (mAU)	RT (min)	Area mAU*min	Height (mAU)	
1 (0.3 mg/mL)	9.879	2.01	18.982	9.747	1.9003	18.228	-0.028
	9.871	1.7212	18.303	9.747	1.9135	18.592	-0.135
	9.862	1.8131	18.837	9.762	1.9483	18.349	-0.050
2 (3 mg/mL)	9.684	18.3723	93.121	9.507	18.1676	89.911	-0.024
	9.605	19.0887	94.907	9.507	18.2537	90.632	0.046
	9.615	18.7249	95.06	9.493	18.5871	91.751	0.031
						$\bar{x}$	0.004
						σ	0.026

3.9. *boc*-Nke-NH_2

Table S24 – Retention time, peak area/minute and peak height for 3 mg/mL Nke-NH_2 at 214 nm.

	PBS Phase			Octanol Phase			LogD
Experiment	RT (minu)	Area mAU*min	Height (mAU)	RT (min)	Area mAU*min	Height (mAU)	
1	8.064	31.2289	123.94	8.182	5.8504	44.741	-0.727
	8.06	31.3381	123.519	8.173	5.7686	44.586	-0.735
	8.074	30.5535	122.4	8.178	5.6239	43.763	-0.735
2	8.061	33.4668	127.624	8.191	6.0177	45.579	-0.745
	8.066	31.7201	124.134	8.182	6.1794	45.497	-0.710
	8.079	30.6581	120.947	8.198	5.9123	44.451	-0.715
						$\bar{x}$	-0.728
						σ	0.012

3.10 Nab-NH_2

Table S25 – Retention time, peak area/minute and peak height for 3 and 5 mg/mL of Nab-NH_2 at 214 nm.

		PBS Phase			Octanol Phase			LogD
Experiment	Conc (mg/mL)	RT (min)	Area mAU*min	Height (mAU)	RT (min)	Area mAU*min	Height (mAU)	
1	3	3.130	29.870	124.185	3.234	1.916	16.583	-1.193
	3	3.144	31.491	106.600	3.229	1.939	16.013	-1.211
	3	3.128	29.808	122.223	3.218	1.874	15.841	-1.202
2	5	3.044	50.018	171.128	3.149	2.620	22.595	-1.281
	5	3.015	49.848	176.143	3.142	2.747	24.285	-1.259
	5	3.015	52.605	183.445	3.133	2.932	25.126	-1.254
							$\bar{x}$	-1.233
							σ	0.033

5. Computational Details

5.1. Swarm-CG Optimisations

5.1.1 Atomistic MD

In all cases the starting structure for the simulation was the lowest energy conformer in the gas phase which was obtained using the GFN-FF metadynamics Conformer/Rotameter Ensemble Sampling Tool (CREST).[5] The structure was then solvated with TIP3P in a box of dimensions 3.8 x 3.8 x 3.8 nm. To generate a Gromacs readable topology file from the CGenFF peptoid parameters the TopoTools VMD plugin was used (command line: topo writegmxtop).[6] Following this the structure was minimised using the steep integrator for 100,000 steps (emtol = 100 kJ mol^{-1} nm^{-1}). A Verlet cutoff-scheme was used. Van der Waals interactions were calculated below a cut-off of 1.2 nm with a force-switch as the vdw-modifier beginning at 1.0 nm. Electrostatic interactions were calculated below a cutoff of 1.2 nm, beyond which particle-mesh Ewald (PME) summation was used to calculate long-range interactions, using a grid spacing of 0.12 nm. Additional setting for CHARMM simulations within Gromacs details can be found on the Gromacs website.[7] Hydrogen bonds were constrained using the LINCS algorithm.[8] These core settings were used in all subsequent steps.

The system was then simulated in the NVT ensemble with a leap-frog algorithm (1,000,000 steps, ts = 1 fs, 1ns). A velocity rescaling algorithm was used to maintain a temperature of 298.15 K with a time constant of 1.0 ps. Velocities were generated according to a Maxwell distribution at the given temperature using a random seed. Following this a short NPT ensemble treatment of the system was done with isotropic pressure coupling using a Parrinello-Rahman barostat (200,000 steps, ts = 1 fs, 0.2 ns). A reference pressure of 1.01325 bar, time constant of 1.0 ps and compressibility of 4.5×10^{-5} bar^{-1} with velocity rescaling were used. The production simulation, from which atomistic position data was obtained, was also in the NPT ensemble (5,000,000 steps, ts = 2 fs, 10 ns) here Nose-Hoover temperature coupling was used with a 1.0 ps time constant additionally the time constant for pressure coupling was 2.0 ps. To ensure adequate coupling of velocities the molecule, solvent and ions were treated as separate coupling groups. This method follows that adopted by Zhao *et al*. in the simulation of peptoid nanosheets.[9]

5.1.2 Coarse-Grained MD Optimisations

A peptoid was solvated in 5 x 5 x 5 nm box with Martini water and minimised using the steep integrator for 100,000 steps (emtol = 10 kJ mol^{-1} nm^{-1}). The Martini straight cut-off scheme of 1.1 nm was used for both electrostatic and VdW interactions, for the latter reaction-field electrostatics were used and a dielectric screening constant of 15 was used. A Potential-shift-verlet vdw-modifier was used. Constraints were handled using the LINCS algorithm.[8] Following the minimisation, a short NPT ensemble equilibration followed (40,000 steps, ts = 25 fs, 1ns). Velocity rescaling (v-rescale) was used to maintain a temperature of 298.15 K (tau-t = 1.0 ps). For pressure control Berendsen pressure coupling was used with semiisotropic pressure coupling, a 12.0 ps time constant was used. In all dimensions a compressibility of 3.0×10^{-4} bar^{-1} was used with a reference pressure

of 1.0 bar and time constant of 12.0 ps. To ensure adequate coupling of velocities the molecule, solvent and ions were treated as separate coupling groups. These same simulation settings were also used in the subsequent production run also for the SWARM-CG optimisation.

5.1.3 Coarse-Grained MD Evaluations

Simulations were performed to utilise SWARM-CG in evaluate mode (`scg_evaluate`) to generate the plots = in Section 6.0. The same treatment of VdW and electrostatics as in section 5.1.2 was used for each step of these simulations. Some small differences exist in the ensemble treatment in the NPT production simulation. Specifically, Parrinello-Rahman pressure coupling was used with isotropic pressure coupling and the same time-constant, compressibility and reference pressure. Note these evaluations were also undertaken yielding the same number of frames as the reference atomistic trajectory (1,000,000, ts = 25 fs, 25 ns).

5.2. Umbrella Sampling and WHAM

To evaluate the Umbrella Sampling (US) method used to fit non-bonded parameters for the peptoid monomers we applied it to evaluating the LogD of the amino acids modelled in the Martini 2.1 protein forcefield (Note: we started with the files from the Martini tutorial on free-energy techniques.[10] The only significant difference being use of a target temperature of 298.15 K and reference pressure of 1.01325 bar to reflect the laboratory experiments. An additional minimisation step of the starting system done prior to the system preparation outlined in the tutorial. Also, in the production run a 1100 kJ mol^{-1} harmonic potential in the production step, where a force constant of 1000 kJ mol^{-1} was used in window set-up and equilibration). The number of bins used was 200 and 100 Bootstraps were used.

5.3. Backbone Angle Parameterisation

5.3.1 Multimolecular Systems

Atomistic MD: Each system was composed of 25 molecules that were solvated with TIP3P water to a concentration of ~ 0.65 M (mg/mL), chlorine ions were added to ensure system neutrality as required for use of Particle Mesh Ewald (PME) electrostatics. A PME grid spacing of 0.1 Å was used throughout to treat long range electrostatic interactions. Lennard Jones interactions were smoothly shifted to zero at a cutoff of 1.2 nm. All systems were built using Gromacs[11] and visualized using visual molecular dynamics (VMD).[12] All systems were initially minimized for 10,000 steps; this was followed by heating to 298.15 K from 0 K in 10-degree increments increasing every 1,000 steps (80,000 steps total). Then the systems were equilibrated for (2,000,000 steps, ts = 2 fs, 4 ns) with a Langevin thermostat, employing a damping factor of 5 and a Langevin barostat with a reference pressure of 1.01325 bar. Following this, a production simulation using the same conditions was carried out for 50 ns. NAMD version 2.15 was used for all MD simulations.[13] A 2fs timestep was used throughout. Mapping data is shown in Figures S28 – S31.

CG-MD: The same treatment of VdW and electrostatics as in section 5.1.2 was used for each step of these simulations. After minimisation using the steep integrator for 100,000 steps. A short equilibration was done (500,000 steps, ts = 20 fs, 10 ns) with velocity rescaling to maintain a temperature of 298.15 K and with a time constant of 0.1 ps to improve stability. To ensure adequate coupling of velocities the molecule, solvent and ions were treated as separate coupling groups. A Berendsen barostat was used with isotropic pressure coupling and with 12 ps time constant. A compressibility of 3.0×10^{-4} bar^{-1} was used with a reference pressure of 1.01325 bar. Temperatures were generated using according to a Maxwell distribution at the given temperature using a random seed. In the production simulation (1,000,000 steps, ts = 25 fs, 50 ns), from which angle measurements were made, the temperature coupling time was increased to 1.0 ps and a Parrinello-Rahman barostat was used with the same time constant, compressibility and reference pressure as the equilibration step.

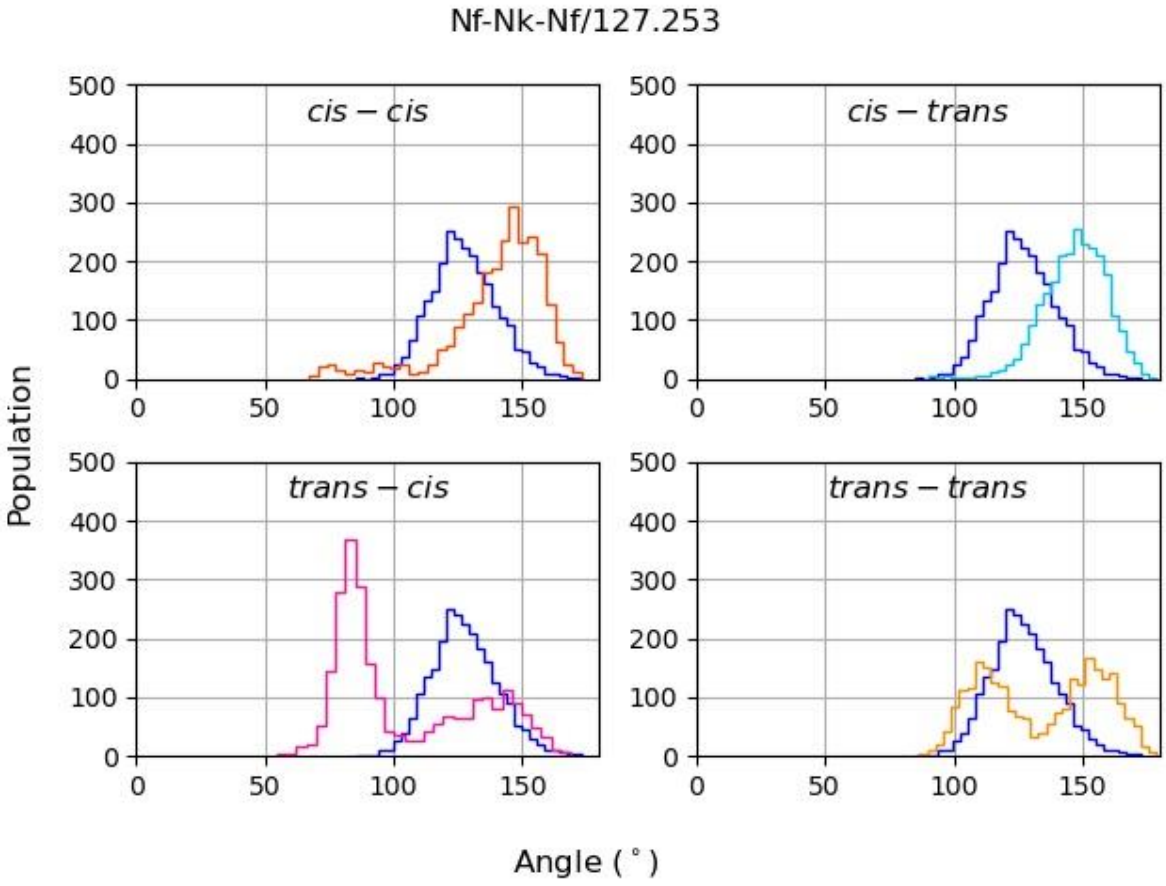

Figure S28. Overlay of BB – BB – BB angle distribution for Nf-Nk-Nf where the coloured distribution corresponds to that backbone conformation while the blue is the CG estimate, angles from 25 molecules molecule for 50 ns. Good agreement is obtained for all sequence states considered.

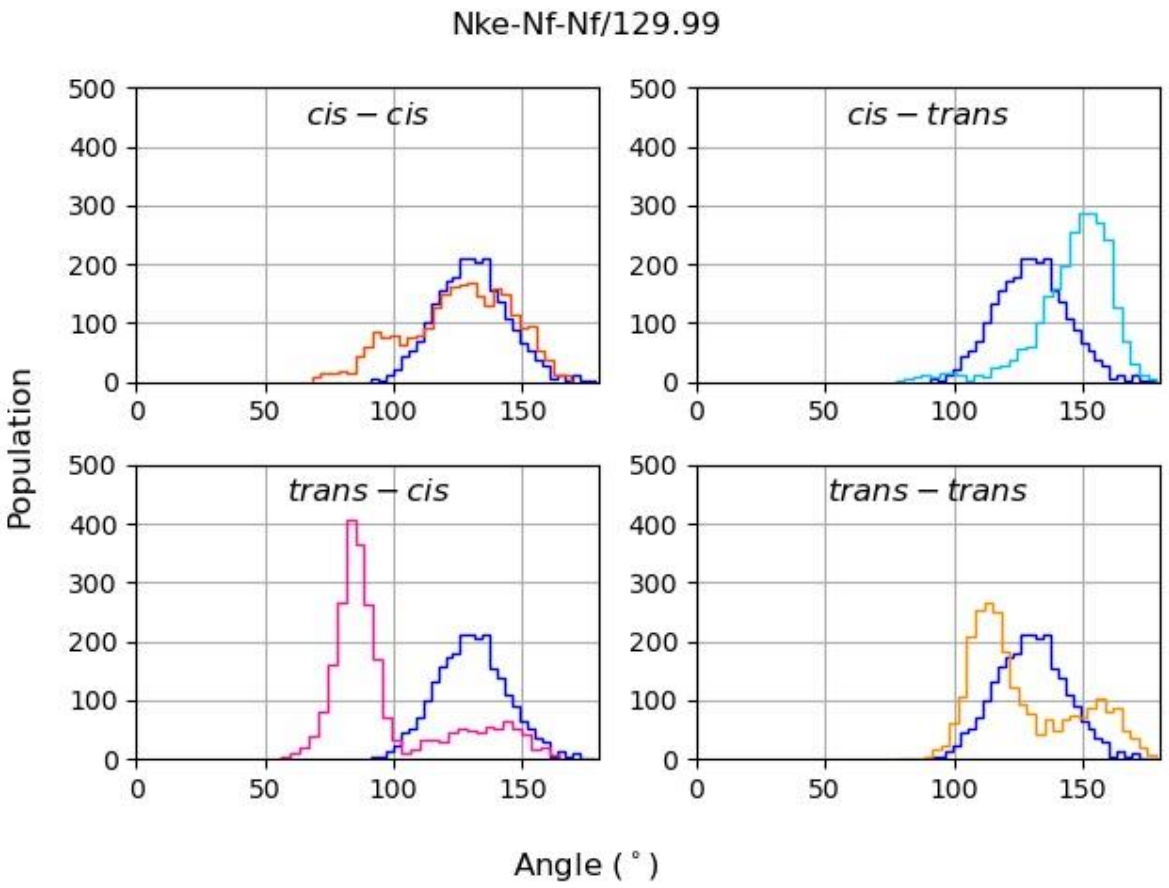

Figure S29. Overlay of BB – BB – BB angle distribution for Nke-Nf-Nf where the coloured distribution corresponds to that backbone conformation while the blue is the CG estimate, angles from 25 molecules molecule for 50 ns. Good agreement is obtained for all sequence states considered.

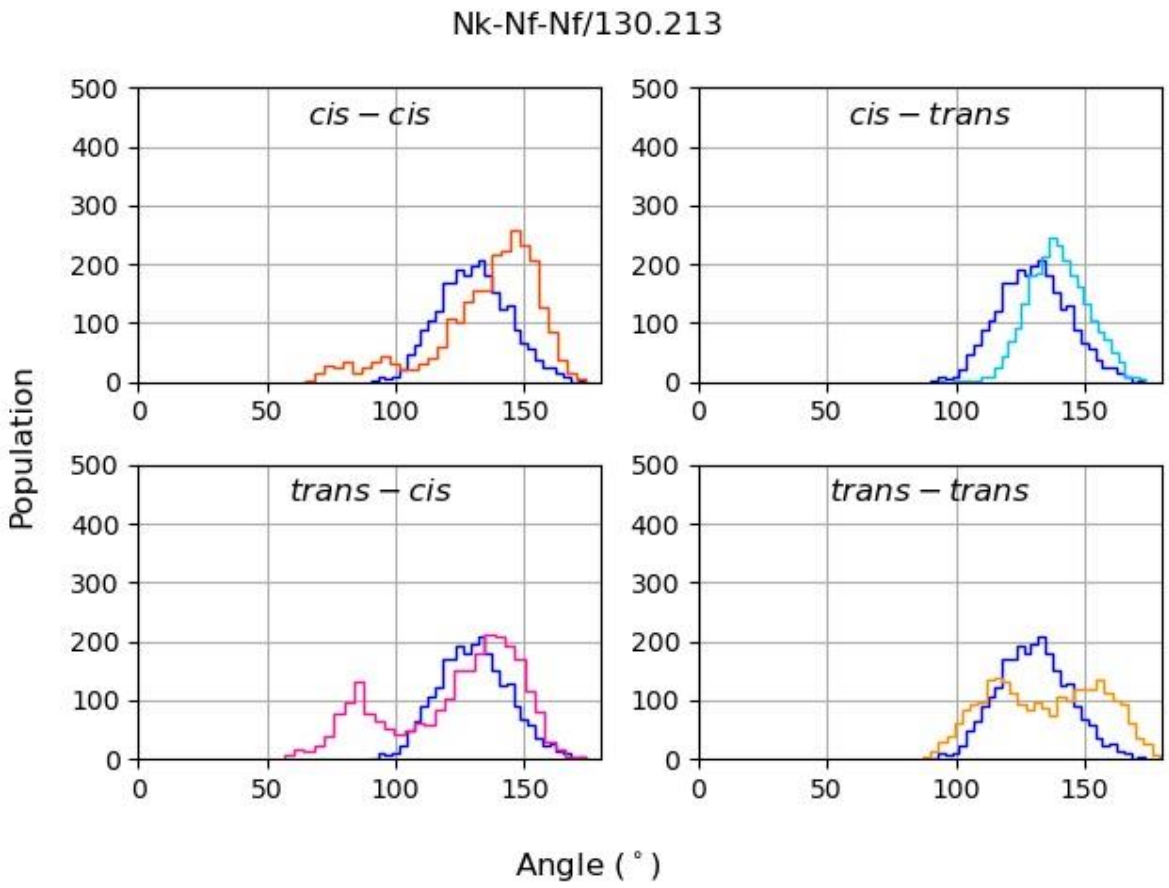

Figure S30. Overlay of BB – BB – BB angle distribution for Nk-Nf-Nf where the coloured distribution corresponds to that backbone conformation while the blue is the CG estimate, angles from 25 molecules molecule for 50 ns. Good agreement is obtained for all sequence states considered.

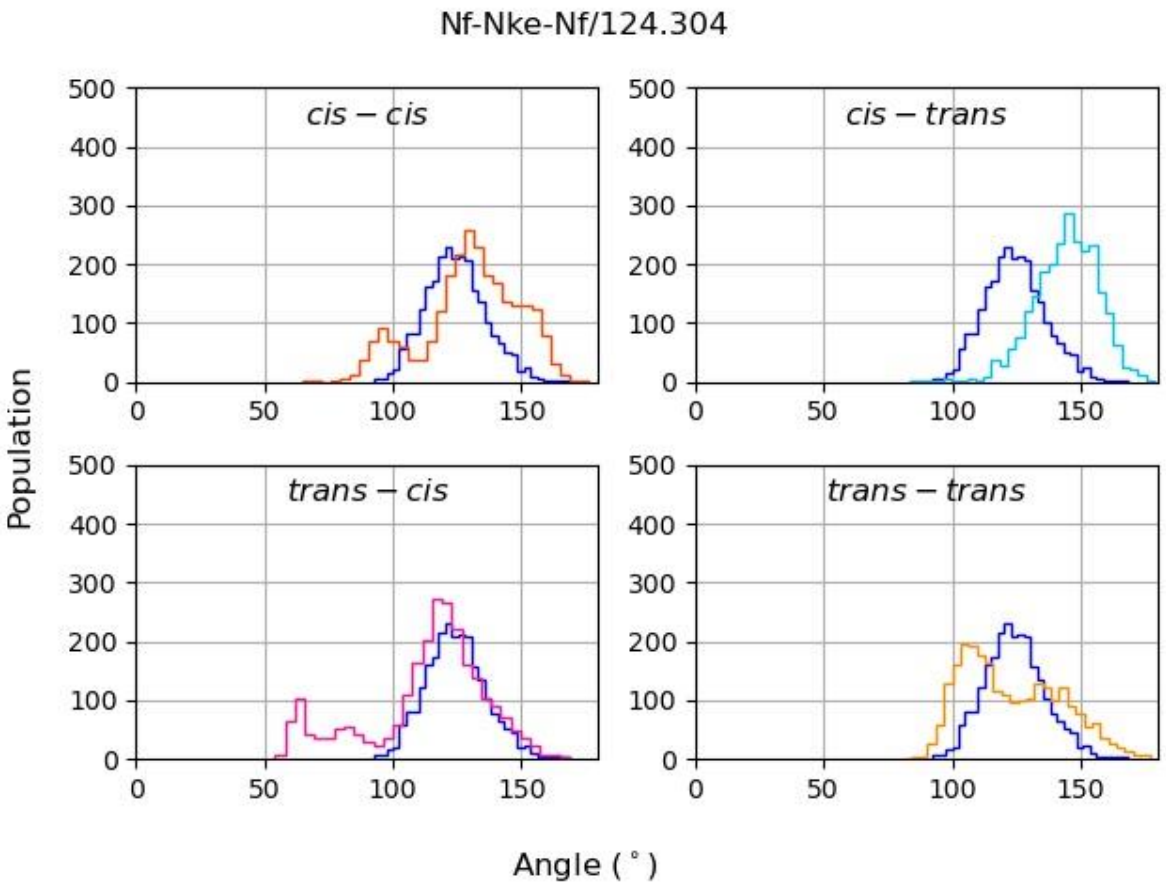

Figure S31. Overlay of BB – BB – BB angle distribution for Nf-Nke-Nf where the coloured distribution corresponds to that backbone conformation while the blue is the CG estimate, angles from 25 molecules molecule for 50 ns. Good agreement is obtained for all sequence states considered.

5.3.2 Single Molecule Systems

Atomistic MD: In this work the same parameters and set-up as described in 5.1.1 was done. The system was minimized initially for 10,000,000 steps (emtol = 100 kJ mol^{-1} nm^{-1}). The equilibration step was then done in the NPT ensemble with the Berendsen barostat (tau-p = 1.0 ps) for (3,000,000 steps, ts=2fs, 6 ns) with velocity generation to a Maxwell distribution which was maintained by the v-rescale method (tau-t = 1.0 ps) and the 100 ns production simulation (50,000,000 steps, ts=2fs, 100ns) employed a Parrinello-Rahman barostat and (tau-p = 2.0 ps) Nose-hoover thermostat (tau-t = 1.0 ps).

Comparison of backbone angle (as, $BB_1 – BB_2 – BB_3$) for single molecules give generally good agreement between CG angle distributions and all amide states at the AA level of detail (Figures S32 – S38). ω distributions for each residue of the trimers are included to highlight how in Nfes-X-Nfes sequences that a transition from *trans* to *cis* occurs over the 100 ns simulation (Figures S39 – S41). This is in line with chemical expectations, where the Nfes residue is a *cis* amide promoting monomer. Despite this good agreement between the CG and AA levels of detail are preserved.

CG-MD: The same treatment of VdW and electrostatics as in section 5.1.2 was used for each step of these simulations. The system was minimized initially for 100,000 steps (emtol = 1 kJ mol^{-1} nm^{-1}). Followed by an equilibration (4,000,000 steps, ts = 25 fs, 100 ns) with an isotropic Berendsen barostat and v-rescale thermostat,

pressure coupling 5.0 ps and a temperature coupling time of 1.0 ps. The target pressure was 1.0135 bar, compressibility of 3x10-4 bar^{-1}, and temperature was 298.15 K.

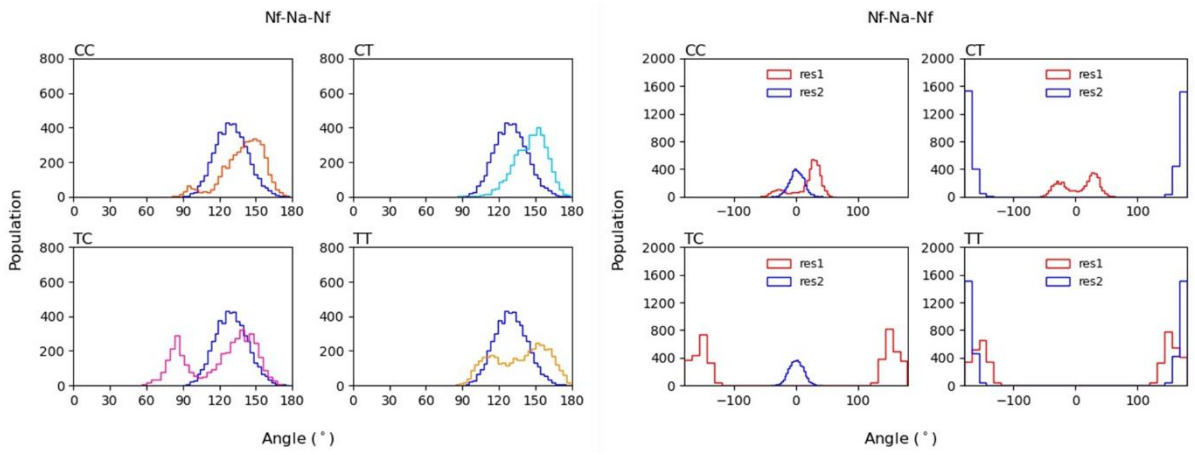

Figure S32. Overlay of BB – BB – BB angle distribution for Nf-Na-Nf where the coloured distribution corresponds to specific amide backbone conformation while the blue is the CG estimate, single molecule for 100 ns. Amide ω torsions are provided and conform to the expected sequence state.

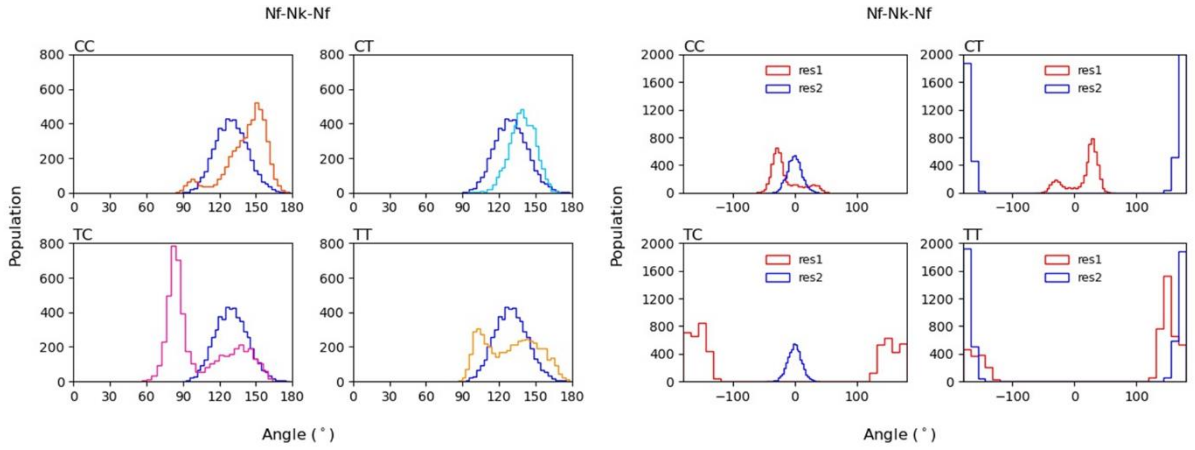

Figure S33. Overlay of BB – BB – BB angle distribution for Nf-Nk-Nf where the coloured distribution corresponds to specific amide backbone conformation while the blue is the CG estimate, single molecule for 100 ns. Amide ω torsions are provided and conform to the expected sequence state.

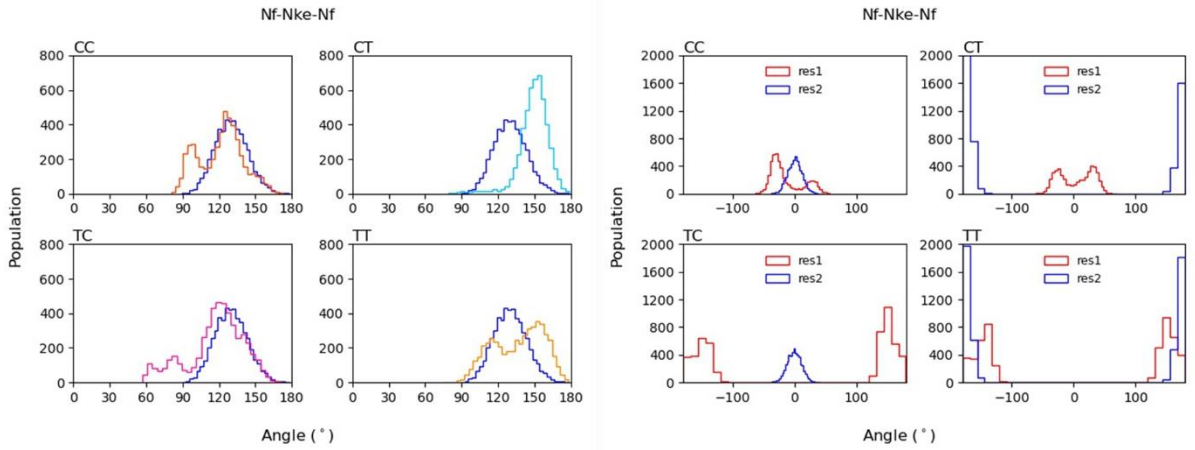

Figure S34. Overlay of BB – BB – BB angle distribution for Nf-Nke-Nf where the coloured distribution corresponds to specific amide backbone conformation while the blue is the CG estimate, single molecule for 100 ns. Amide ω torsions are provided and conform to the expected sequence state.

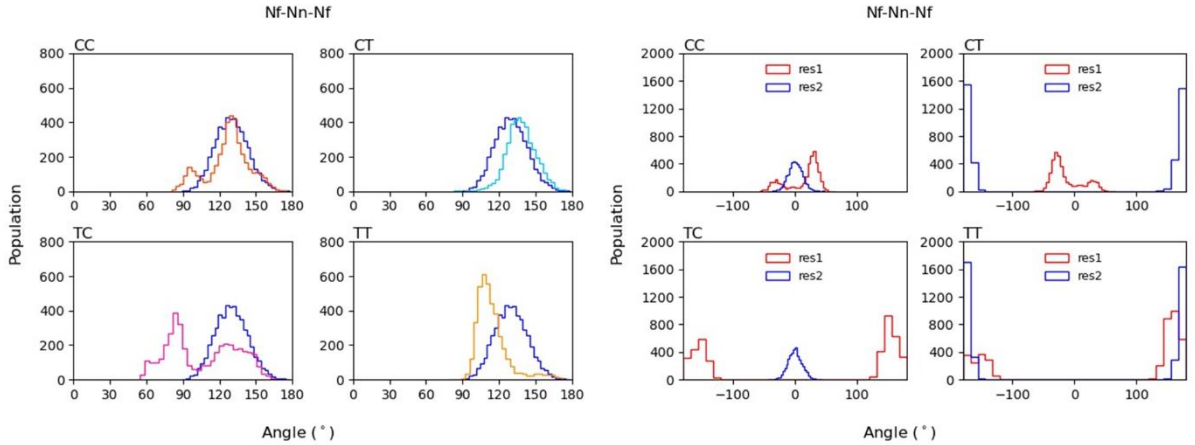

Figure S35. Overlay of BB – BB – BB angle distribution for Nf-Nn-Nf where the coloured distribution corresponds to specific amide backbone conformation while the blue is the CG estimate, single molecule for 100 ns. Amide ω torsions are provided and conform to the expected sequence state.

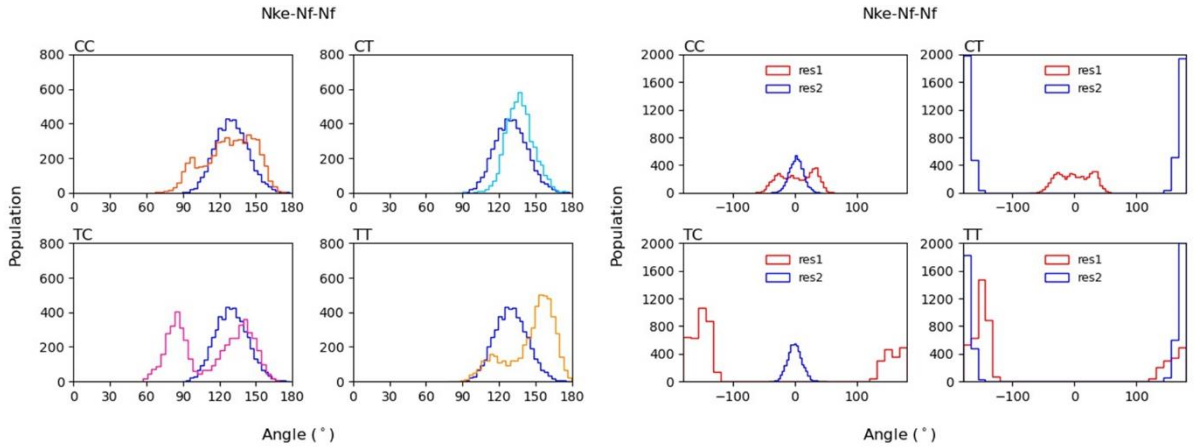

Figure S36. Overlay of BB – BB – BB angle distribution for Nke-Nf-Nf where the coloured distribution corresponds to specific amide backbone conformation while the blue is the CG estimate, single molecule for 100 ns. Amide ω torsions are provided and conform to the expected sequence state.

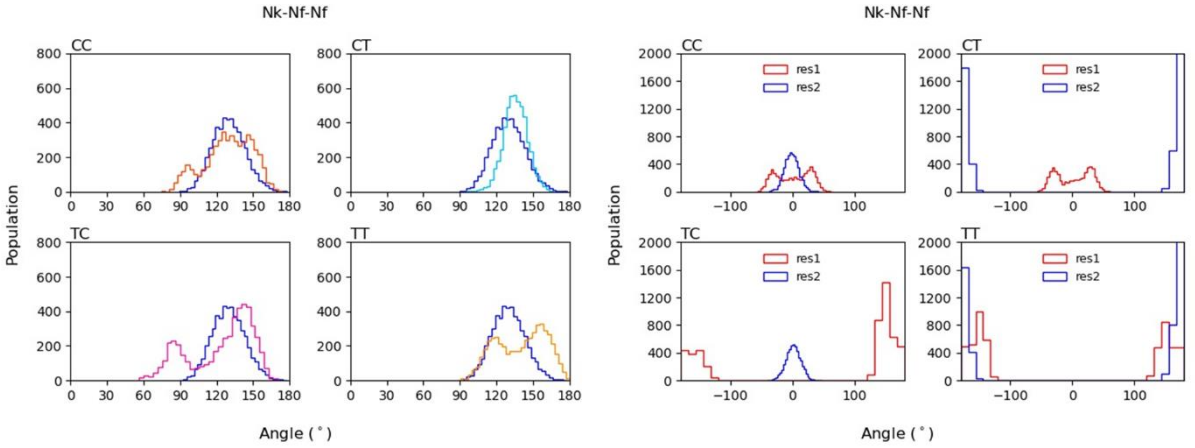

Figure S37. Overlay of BB – BB – BB angle distribution for Nk-Nf-Nf where the coloured distribution corresponds to specific amide backbone conformation while the blue is the CG estimate, single molecule for 100 ns Amide ω torsions are provided and conform to the expected sequence state.

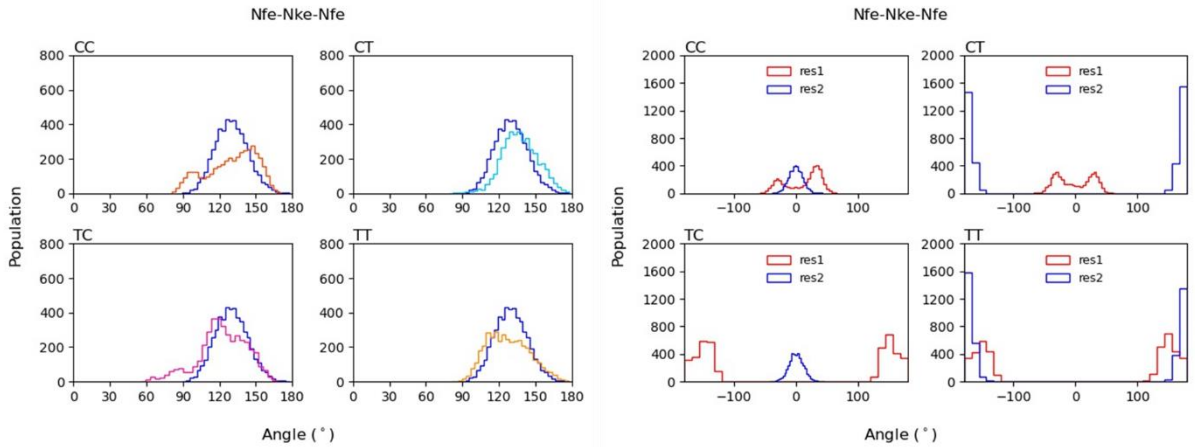

Figure S38. Overlay of BB – BB – BB angle distribution for Nfe-Nke-Nfe where the coloured distribution corresponds to specific amide backbone conformation while the blue is the CG estimate, single molecule for 100 ns Amide ω torsions are provided and conform to the expected sequence state.

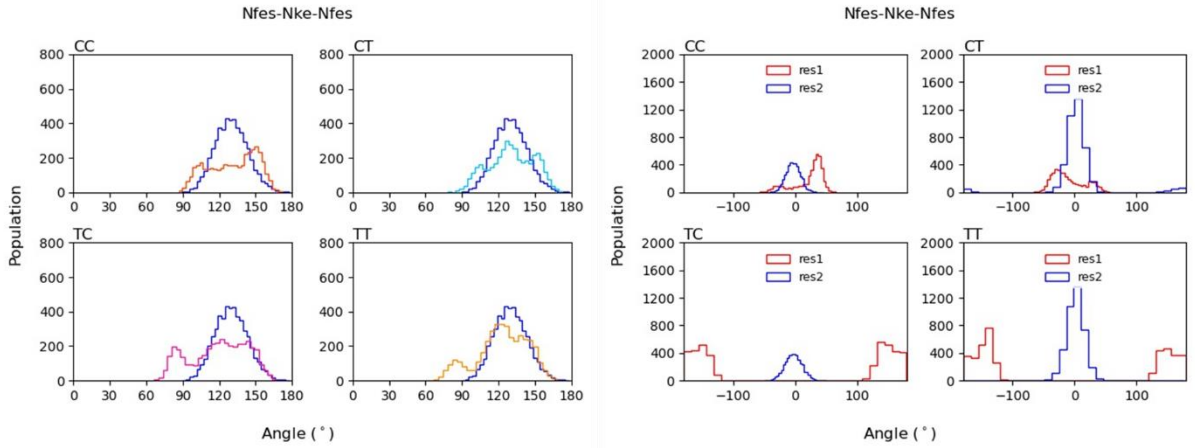

Figure S39. Overlay of BB – BB – BB angle distribution for Nfes-Nke-Nfes where the coloured distribution corresponds to specific amide backbone conformation while the blue is the CG estimate, single molecule for 100 ns. Amide ω torsions exhibit a switch where the second residue is *trans*, following expectations that Nfes residues promote this confromation.

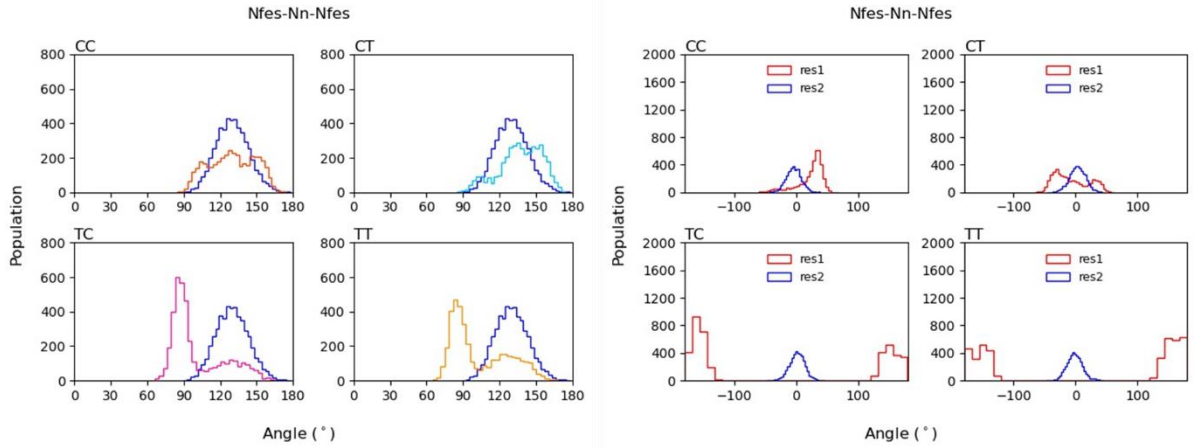

Figure S40. Overlay of BB – BB – BB angle distribution for Nfes-Nn-Nfes where the coloured distribution corresponds to specific amide backbone conformation while the blue is the CG estimate, single molecule for 100 ns. Amide ω torsions exhibit a switch where the second residue is *trans*, following expectations that Nfes residues promote this confromation.

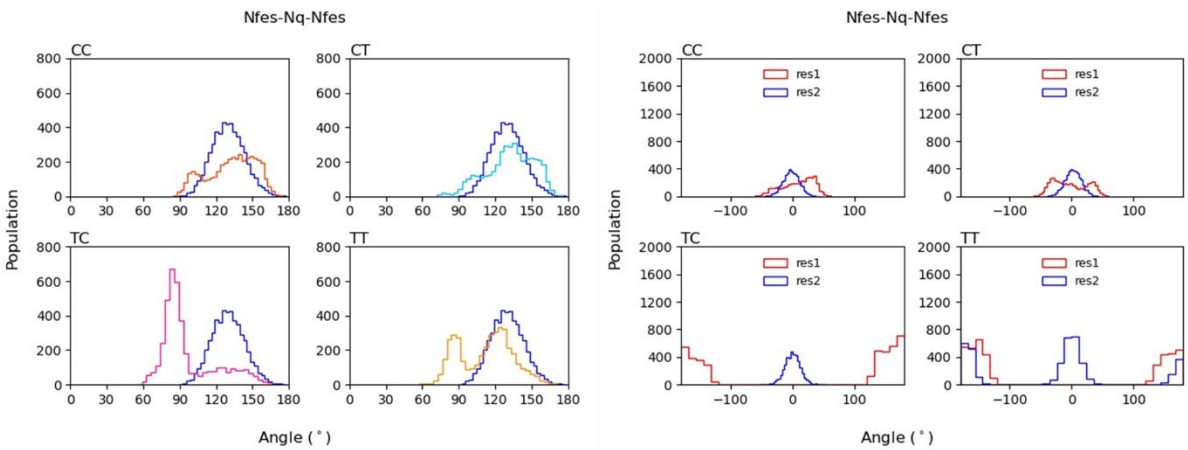

Figure S41. Overlay of BB – BB – BB angle distribution for Nfes-Nq-Nfes where the coloured distribution corresponds to specific amide backbone conformation while the blue is the CG estimate. Amide ω torsions exhibit a switch where the second residue is *trans*, following expectations that Nfes residues promote this conformation.

5.4. Peptoid Helix Simulations

5.4.1 Atomistic MD

A hexameric peptoid $(Nk\text{-}Nfes\text{-}Nfes)_2$ was solvated with TIP3P water and chloride ions in 4 x 4 x 4 nm after minimisation using the system settings described in Section 5.1.1. The following treatment was performed, firstly an NVT ensemble was applied to the system with velocity generation; velocity rescaling was to a reference temperature of 298.15 K with a time constant of 1.0 ps (3,000,000 steps, ts = 1 fs, 3 ns). Following this an NPT ensemble was applied using the same temperature coupling and isotropic Berendsen pressure coupling, with a time constant of 1.0 ps, compressibility of 4.5×10^{-5} bar^{-1}, target pressure of 1.01325 bar (3,000,000 steps, ts = 2 fs, 6 ns). The production run employed the NPT ensemble with Nose-Hoover temperature coupling, isotropic Parrinello-Rahman pressure coupling for which a time constant of 2.0 ps was used (50,000,000 steps, ts = 2 fs, 100 ns).

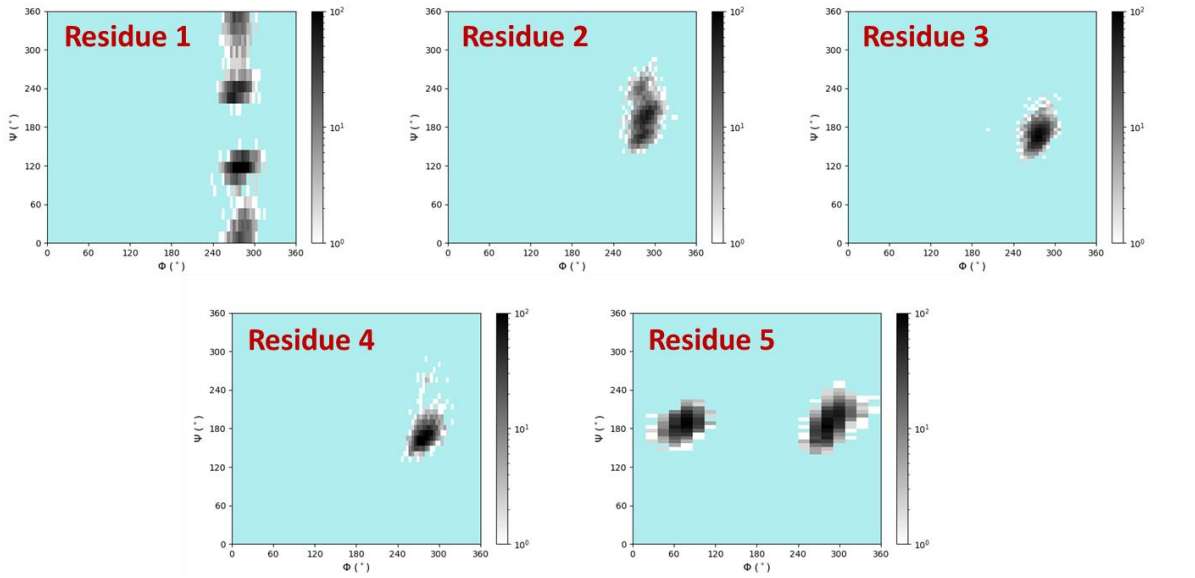

Figure S42. ϕ/ψ sampling for helical peptoid fragement (Nk-Nfes-Nfes)$_2$ on a per torsion pair basis. Sampling of the α_D^- region is an indicator that our representation of the Nfes residue, within a helical structure, adopts the correct backbone torsions. The increased degrees of freedom at residue 1 and 5 are thought to be due to the absence of helix enforcing residues at one flank of either torsion. (number of bins = 30).

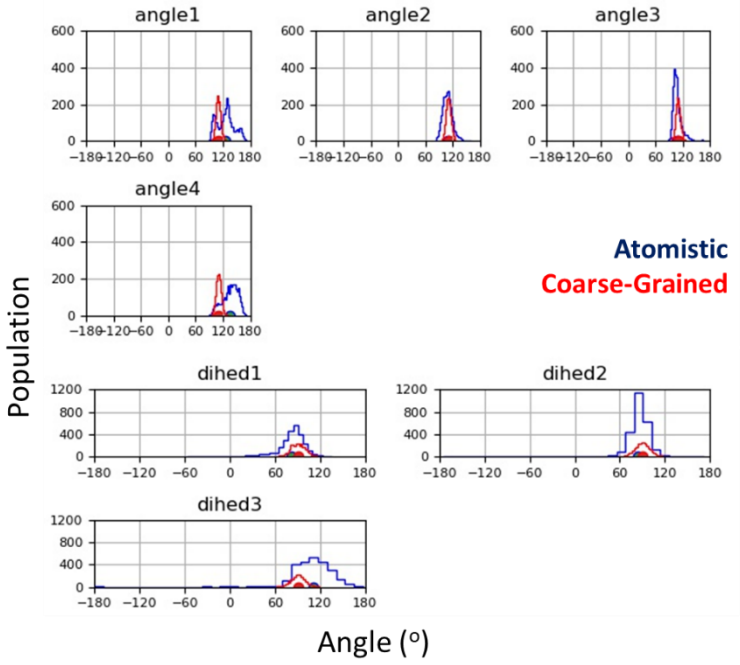

Figure S43. Comparison of atomistic and coarse-grained angle and dihedral distributions for 100 ns of simulation, using a Centre of Geometry (COG) mapping scheme; good agreement in the magnitude and locations of both terms are found in this duplicate experiment to that in the main text indicating that the selected parameters accurately reproduce the higher theory level sampling.

5.4.2 Coarse-Grained MD

A hexameric CG peptoid (Nk-Nfex-Nfex)$_2$ was solvated in a 5 x 5 x 5 nm box with Martini water and chloride ions. The same treatment of VdW and electrostatics as in section 5.1.2 was used for each step of these simulations. Minimisation was for 10,000 steps (emtol = 100 kJ mol^{-1} nm^{-1}). For the equilibration (500,000, ts = 10fs, 5 ns) and production (5,000,000, ts = 20fs, 100 ns) steps velocity rescaling was used to maintain a constant temperature of 298.15 K (tau-t = 1.0 ps). Isotropic pressure coupling was done using Berendsen and Parrinello-Rahman barostat for the equilibration and production stages respectively (tau-p = 12.0 ps). The reference pressure was 1.01325 bar with a compressibility of 3.0x10^{-4} bar^{-1}. Temperatures were generated according to a Maxwell distribution using a pseudo random seed (`gen_seed = -1`). To ensure adequate coupling of velocities the molecule, solvent and ions were treated as separate coupling groups.

5.5. Self-Assembly Screening

5.5.1 Assembly of dipeptoid Nf-Nf

For this experiment 300 molecules were inserted into a 12.5 x 12.5 x 12.5 nm equilibrated water box with a minimum separation radius of 0.3 nm. The same treatment of VdW and electrostatics as in section 5.1.2 was used for each step of these simulations. Minimisation was for 100,000 steps (emtol = 1 kJ mol^{-1} nm^{-1}). For the equilibration (400,000 steps, ts = 25 fs, 10 ns) and production (10,000,000 steps, ts = 25 fs, 250 ns) steps velocity rescaling was used to maintain a constant temperature of 298.15 K (tau-t = 1.0 ps). To ensure adequate coupling of velocities the molecules and solvent were treated as separate coupling groups. Isotropic pressure coupling was done using Berendsen and Parrinello-Rahman barostat for the equilibration and production stages respectively (tau-p = 12.0 ps). The reference pressure was 1.01325 bar with a compressibility of 3.0x10^{-4} bar^{-1}. Temperatures were generated according to a Maxwell distribution using a pseudo random seed (`gen_seed = -1`).

5.5.2 Single Monomer Assembly Screening

For this experiment 600 molecules were inserted into a 12.5 x 12.5 x 12.5 nm equilibrated water box with a minimum radius of separation of 0.3 nm and neutralised as required. The same treatment of VdW and electrostatics as in section 5.1.2 was used for each step of these simulations. Minimisation was for 100,000 steps (emtol = 1 kJ mol^{-1} nm^{-1}). The treatment of the NPT ensemble in equilibration and production followed that of outlined in 5.5.1. The equilibration duration was (40,000 steps, ts = 25 fs, 1 ns) and production duration was (8,000,000 steps, ts = 25 fs, 200 ns).

5.6. Peptoid Nanosheet Simulations

The same treatment of VdW and electrostatics as in section 5.1.2 was used for each step of these simulations. Minimisation was for 100,000 steps (emtol = 1 kJ mol^{-1} nm^{-1}). The treatment of the NPT ensemble in equilibration and production followed that of outlined in 5.5.1. Here a 10 fs timestep was used. The equilibration duration was (100,000 steps, ts = 10 fs, 10 ns) and production duration was (25,000,000 steps, ts = 10 fs, 250 ns).

5.7. Peptoid Tape Simulations

Minimisation was for 10,000 steps (emtol = 100 kJ mol^{-1} nm^{-1}). The same treatment of VdW and electrostatics as in section 5.1.2 was used for each step of these simulations and the treatment of the NPT ensemble in equilibration and production followed that of outlined in 5.5.1. The equilibration duration was (100, 000 steps, ts = 25 fs, 10 ns) and production duration was (6,000,000 steps, ts = 25 fs, 150 ns).

5.8. Free Assembly of Nf-Nke-Nf

300 tripeptoids were solvated in the same manner as outlined in 5.5.2 and run as outlined in 5.3.2. Minimisation was for 100,000 steps (emtol = 1 kJ mol^{-1} nm^{-1}). The production simulation (6,250,000 steps, ts= 40ns, 250ns) employed a Berendsen barostat (tau-p = 8.0), results for these duplicate experiments shown in Figure S94.

6. Bead Mapping

Blue distributions correspond to the *mid* parameter for a given residue and **pink** the specific amide state.

6.1 Nab

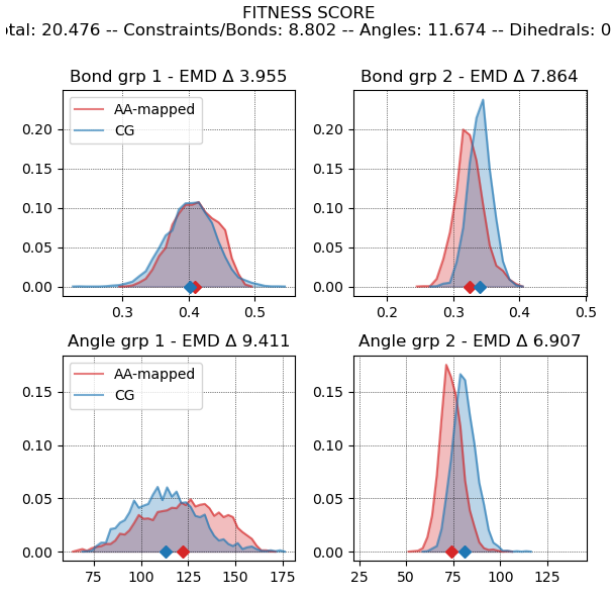

Figure S44. Nab in the cis amide conformation.

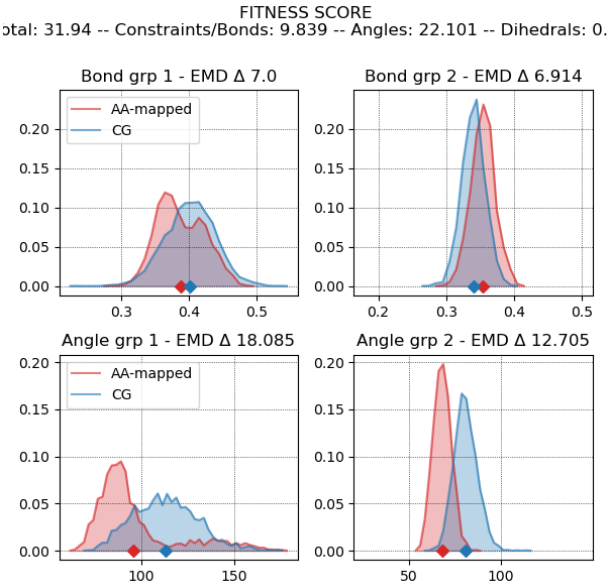

Figure S45. Nab in the trans amide conformation.

<u>Bond 1:</u> {BB_n, BB_{n+1}} – SC1

<u>Bond 2:</u> BB_n – BB_{n+1}

<u>Angle 1</u>: SC1 – BB_n – BB_{n+1}

<u>Angle 2:</u> SC1 – BB_{n+1} – BB_n

6.2 Nd

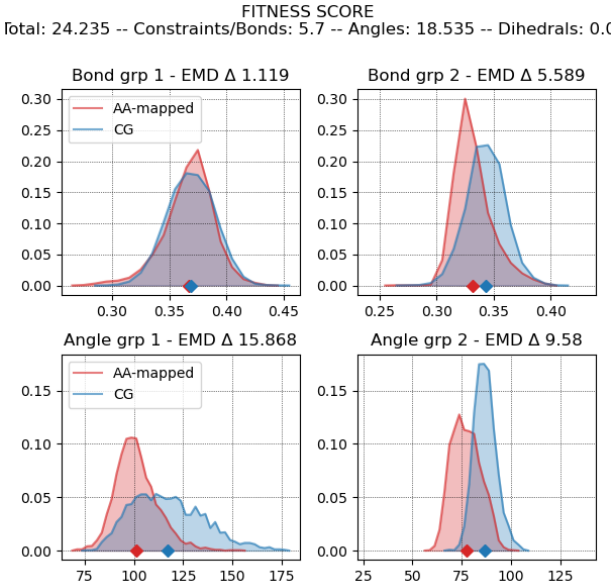

Figure S46. Nd in the cis amide conformation.

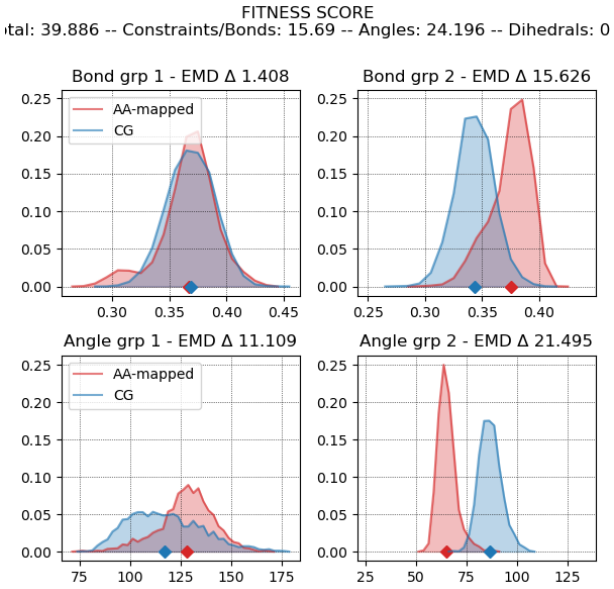

Figure S47. Nd in the trans amide conformation.

Bond 1: {BB_n, BB_{n+1}} – SC1

Bond 2: BB_n – BB_{n+1}

Angle 1: SC1 – BB_n – BB_{n+1}

Angle 2: SC1 – BB_{n+1} – BB_n

6.3 Ne

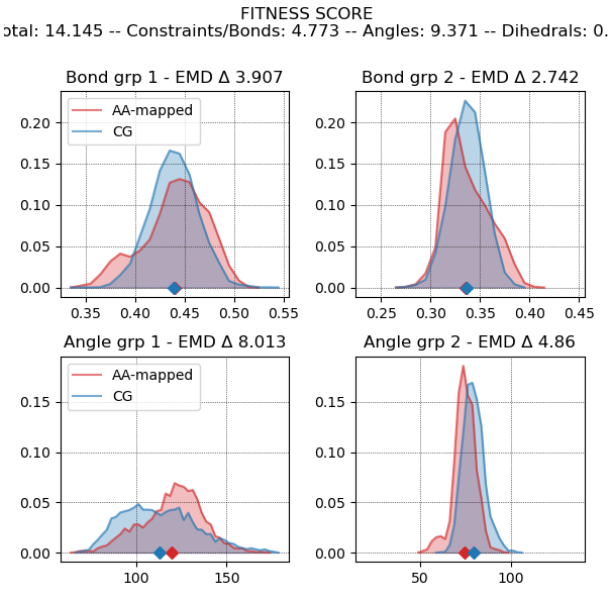

Figure S48. Ne in the *cis* amide conformation.

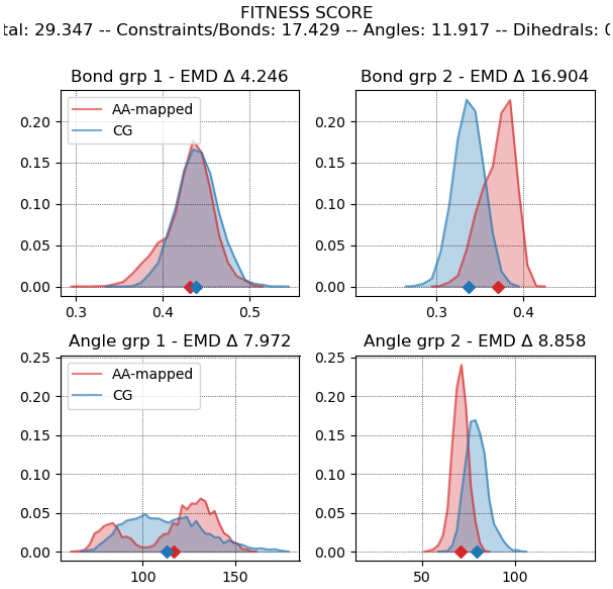

Figure S49. Ne in the *trans* amide conformation.

Bond 1: {BB_n, BB_{n+1}} – SC1

Bond 2: BB_n – BB_{n+1}

Angle 1: SC1 – BB_n – BB_{n+1}

Angle 2: SC1 – BB_{n+1} – BB_n

6.4 Nf

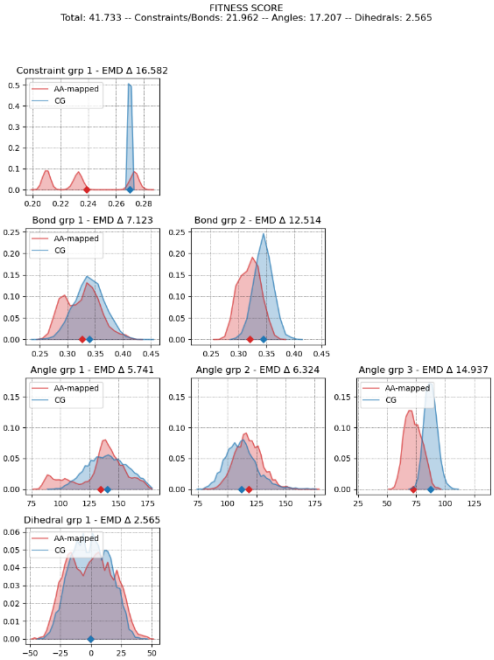

Figure S50. Nf in the cis amide conformation.

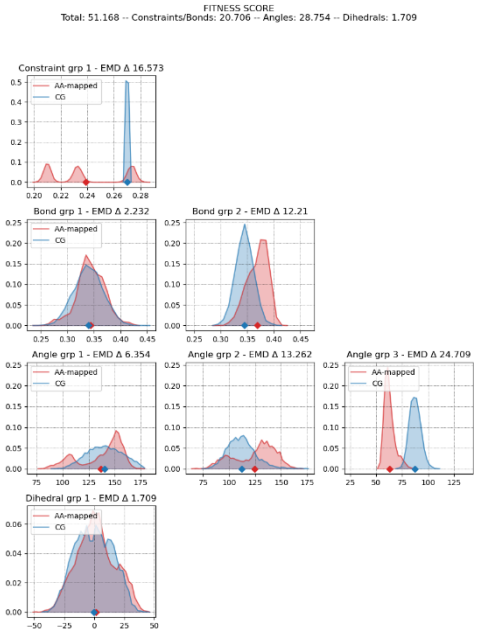

Figure S51. Nf in the trans amide conformation.

Constraint 1: SC1-SC2/SC2-SC3/SC3-SC1

Bond 1: {BB_n, BB_{n+1}} – SC1

Bond 2: BB_n – BB_{n+1}

Angle 1: {BB_n, BB_{n+1}} – SC1 – SC2

Angle 2: SC1 – BB_n – BB_{n+1}

Angle 3: SC1 – BB_{n+1} – BB_n

Improper Dihedral 1: {BB_n, BB_{n+1}}– SC2 – SC3 –SC1

6.5 Nf[naph]

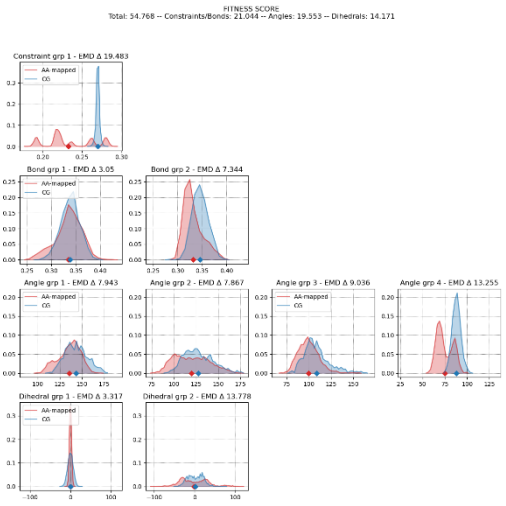

Figure S52. Nf[naph] in the cis amide conformation.

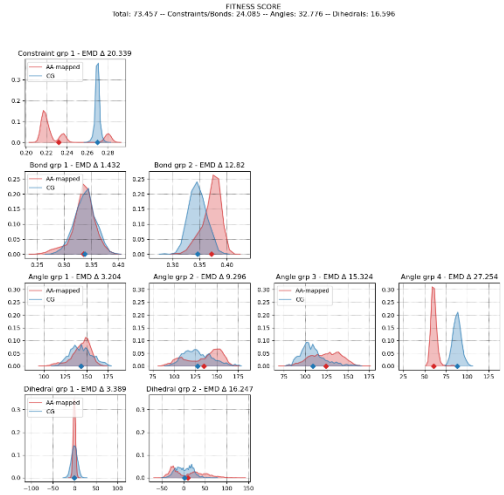

Figure S53. Nf[naph] in the trans amide conformation.

Constraint 1: SC1-SC2/SC2-SC3/SC3-SC1/etc.

Bond 1: {BB_n, BB_{n+1}} – SC1

Bond 2: BB_n – BB_{n+1}

Angle 1: {BB_n, BB_{n+1}} – SC1 – SC2

Angle 1: {BB_n, BB_{n+1}} – SC1 – SC3

Angle 2: SC1 – BB_n – BB_{n+1}

Angle 3: SC1 – BB_{n+1} – BB_n

Improper Dihedral 1: SC1– SC3 –SC4–SC2

6.6 Nfe

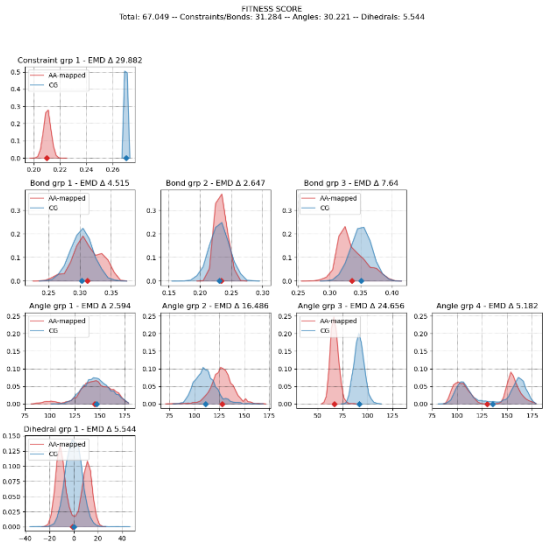

Figure S54. Nfe in the cis amide conformation.

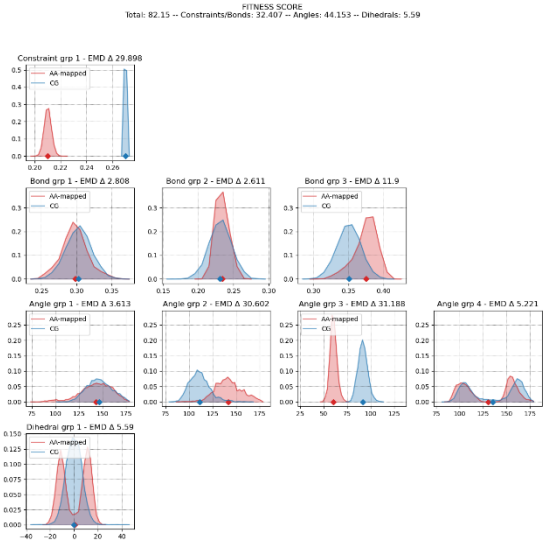

Figure S55. Nfe in the trans amide conformation.

Constraint 1: SC1-SC2/SC2-SC3/SC3-SC1

Bond 1: {BB_n, BB_{n+1}} – SC1

Bond 2: SC1 – SC2

Bond 3: BB_n – BB_{n+1}

Angle 1: BB_n – SC1 – SC2

Angle 2: SC1 – BB_n – BB_{n+1}

Angle 3: SC1 – BB_{n+1} – $BB1_n$

Angle 4: SC1 – SC2 – {SC3, SC4

Improper Dihedral 1: SC1 – SC3 – SC4 – SC2

6.7 Nfe[4Br]

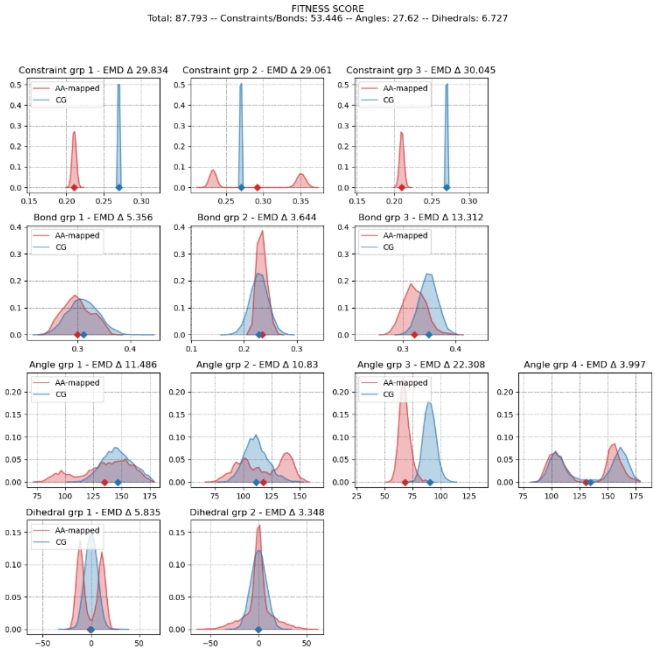

Figure S56. Nfe[4Br] in the cis amide conformation.

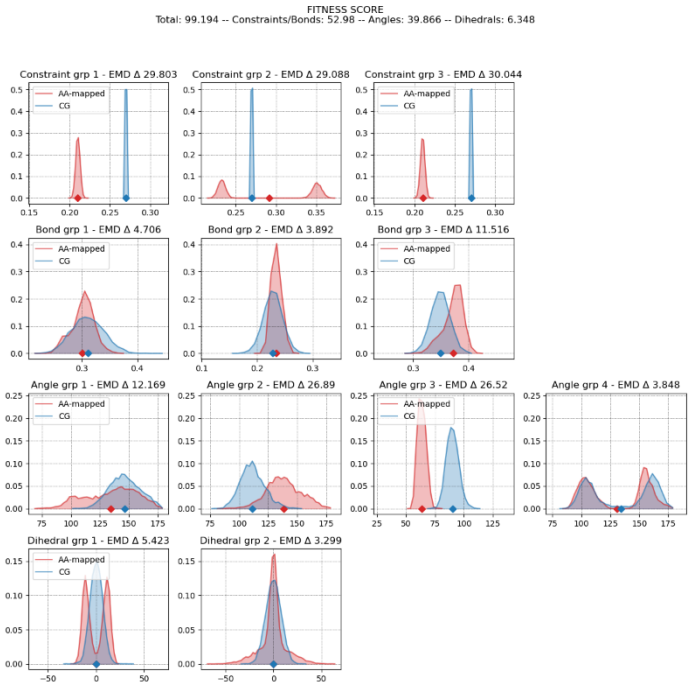

Figure S57. Nfe[4Br] in the trans amide conformation.

Constraint 1: SC2-SC3/SC2-SC4

Constraint 2: SC5-SC3/SC5-SC4

Constraint 3: SC4-SC5

Bond 1: {BB_n, BB_{n+1}} – SC1

Bond 2: SC1 – SC2

Bond 3: BB_n – BB_{n+1}

Angle 1: {BB_n, BB_{n+1}} – SC1 – SC2

Angle 2: SC1 – BB_n – BB_{n+1}

Angle 3: SC1 – BB_{n+1} – BB_n

Angle 4: SC1 – SC2 – {SC3, SC4}

Improper Dihedral 1: SC1 – SC3 – SC4 – SC2

6.8 Nfex

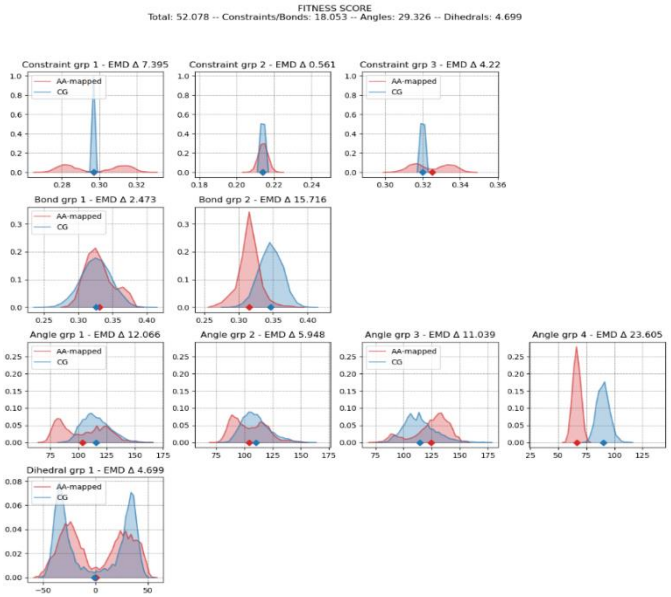

Figure S58. Nfer in the cis amide conformation.

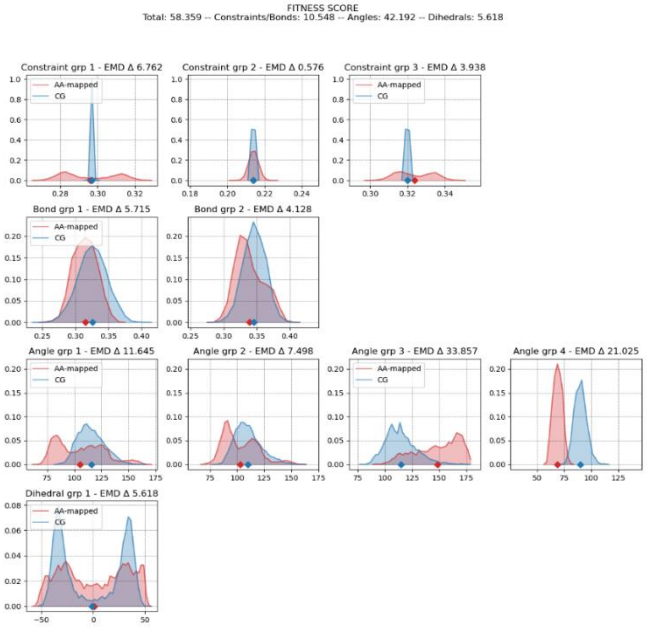

Figure S59. Nfer in the trans amide conformation.

Constraint 1: SC1-SC2

Constraint 2: SC2-SC3

Constraint 3: SC3-SC1

Bond 1: {BB_n, BB_{n+1}} – SC1

Bond 2: BB_n – BB_{n+1}

Angle 1: {BB_n, BB_{n+1}} – SC1 – SC2

Angle 2: {BB_n, BB_{n+1}} – SC1 – SC3

Angle 3: SC1 – BB_{n+1} – BB_n

Angle 4: SC1 – BB_n – BB_{n+1}

Improper Dihedral 1: SC1 – SC3 – SC4 – SC2

6.9 Nfn

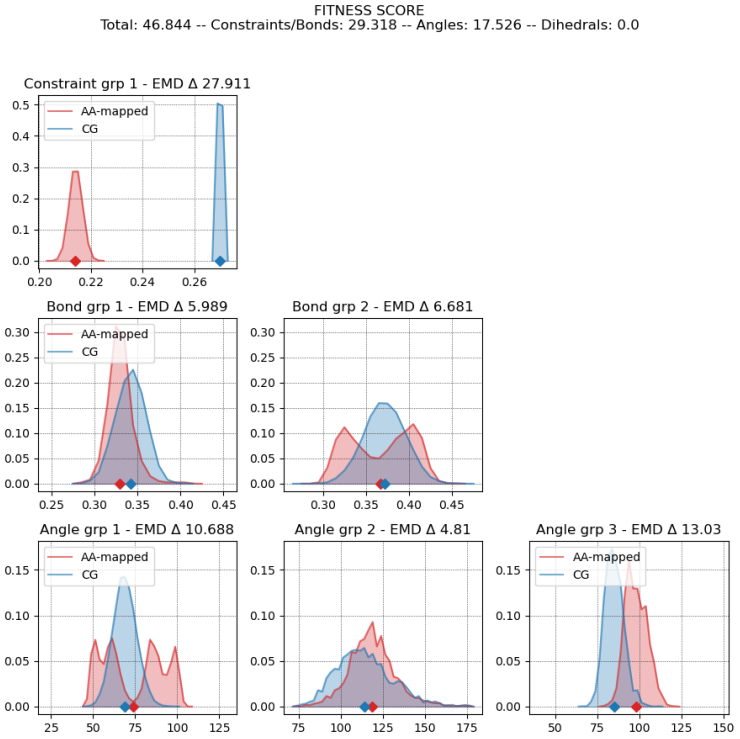

Figure S60. Nfn in the trans amide conformation.

Constraint: SC1 – SC2

Bond 1: $BB_n - BB_{n+1}$

Bond 2: $\{BB_n, BB_{n+1}\}$ – SC1

Angle 1: $\{BB_n, BB_{n+1}\}$ – {SC1 – SC2, SC2 – SC1}

Angle 2: SC1 – BB_n – BB_{n+1}

Angle 3: SC1 – BB_{n+1} – BB_n

6.10 Ni

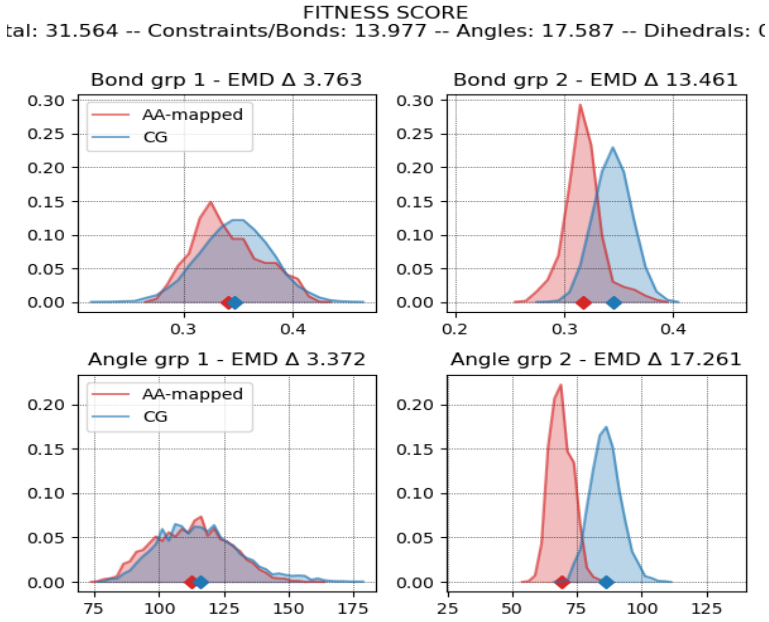

Figure S61. Ni in the cis amide conformation.

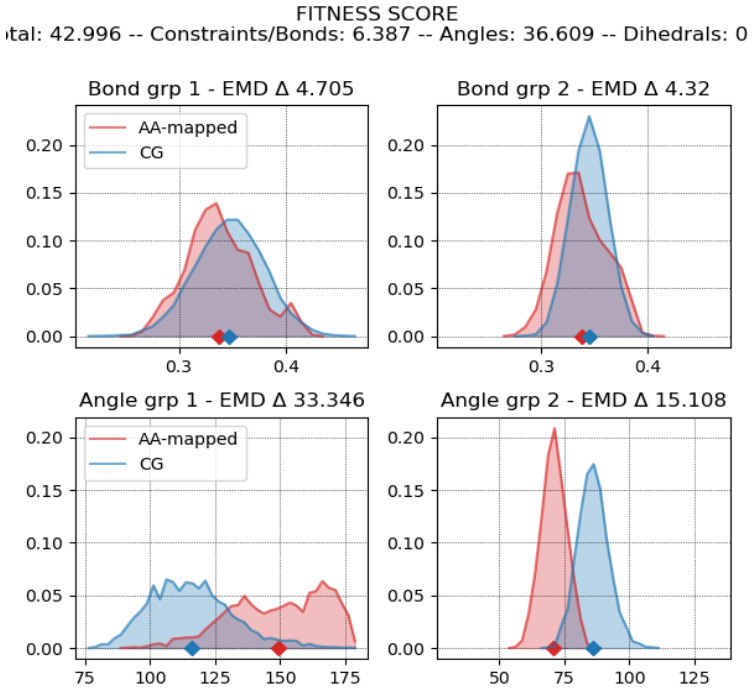

Figure S62. Ni in the trans amide conformation.

Bond 1: {BB_n, BB_{n+1}} – SC1

Bond 2: BB_n – BB_{n+1}

Angle 1: SC1 – BB_n – BB_{n+1}

Angle 2: SC1 – BB_{n+1} – BB_n

6.12 Nk

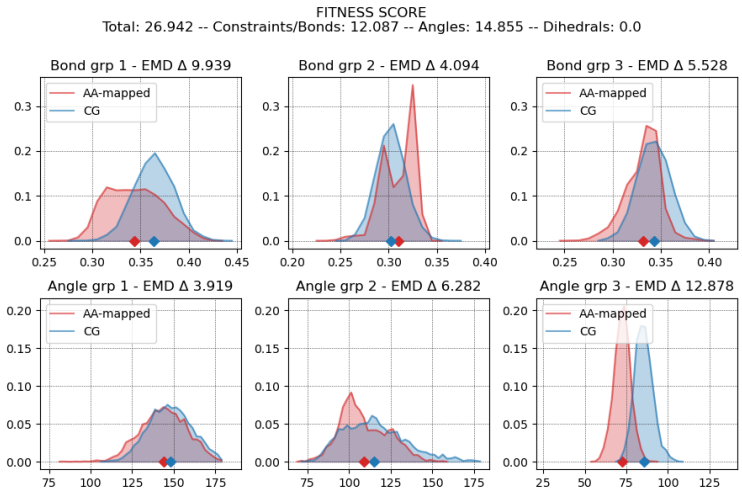

Figure S63. Nk in the cis amide conformation.

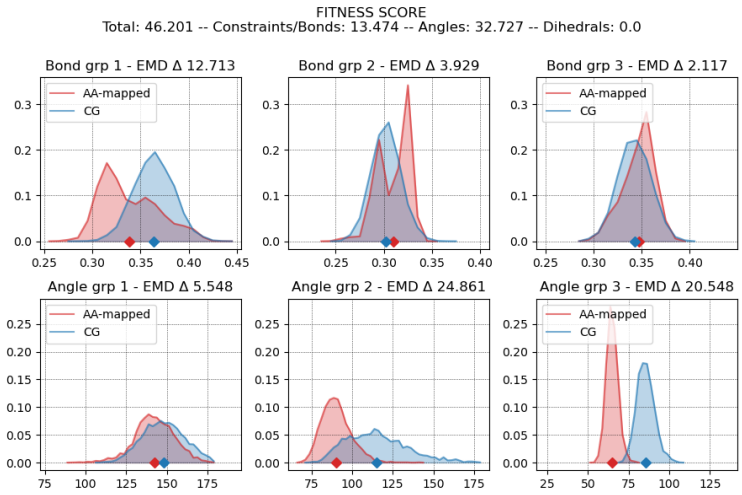

Figure S64. Nk in the trans amide conformation.

Bond 1: {BB_n, BB_{n+1}} – SC1

Bond 1: SC1 – SC2 & SC1 – SC2

Bond 3: BB_n – BB_{n+1}

Angle 1: {BB_n, BB_{n+1}} – SC1 – SC2

Angle 2: SC1 – BB_n – BB_{n+1}

Angle 2: SC1 – BB_{n+1} – BB_n

6.13 Nke

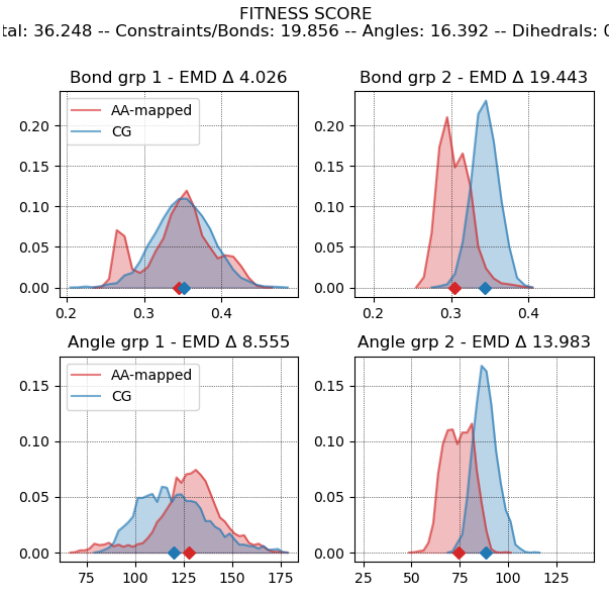

Figure S65. Nke in the cis amide conformation.

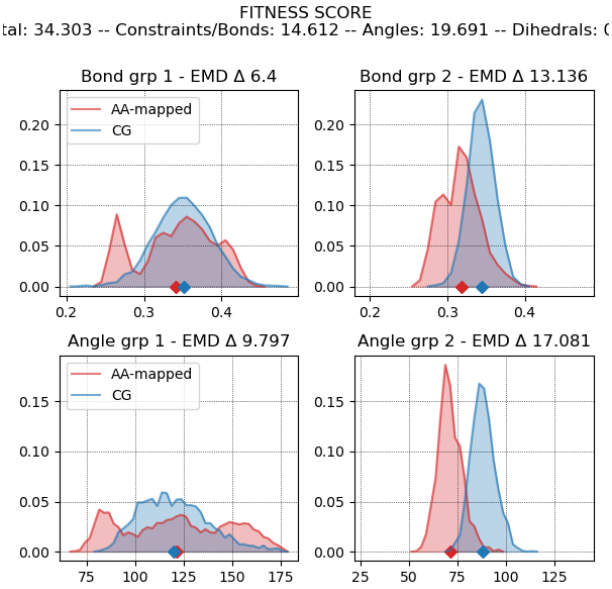

Figure S66. Nke in the trans amide conformation.

Bond 1: BB_n – SC1 & BB_{n+1} – SC1

Bond 2: BB_n – BB_{n+1}

Angle 1: SC1 – BB_n – BB_{n+1}

Angle 2: SC1 – BB_{n+1} – BB_n

6.14 Nl

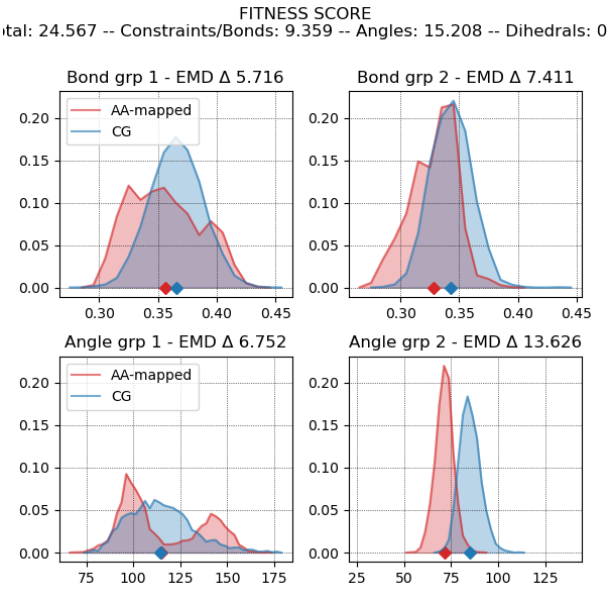

Figure S67. Nl in the cis amide conformation.

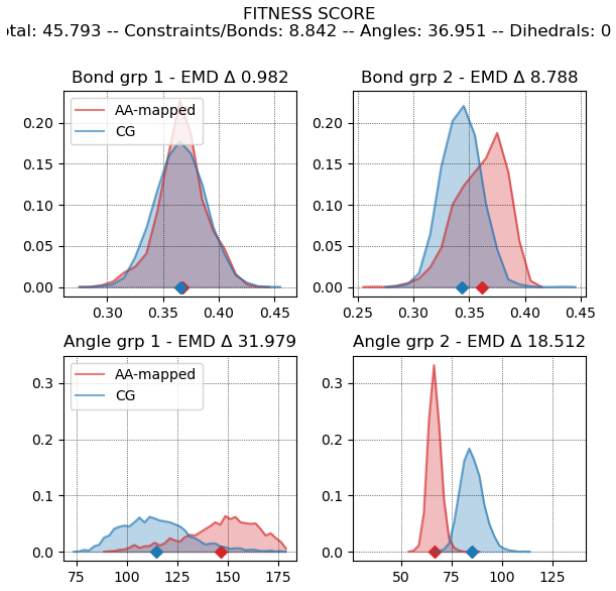

Figure S68. Nl in the trans amide conformation.

Bond 1: {BB_n, BB_{n+1}} – SC1

Bond 2: BB_n – BB_{n+1}

Angle 1: SC1 – BB_n – BB_{n+1}

Angle 2: SC1 – BB_{n+1} – BB_n

6.15 Nm

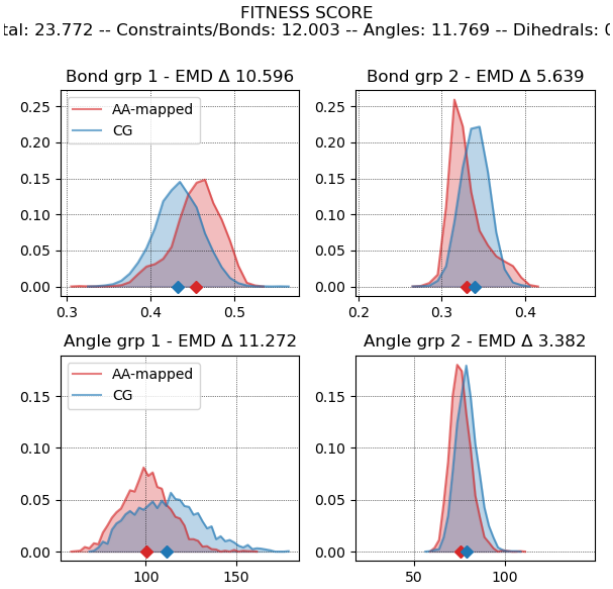

Figure S69. Nm in the cis amide conformation.

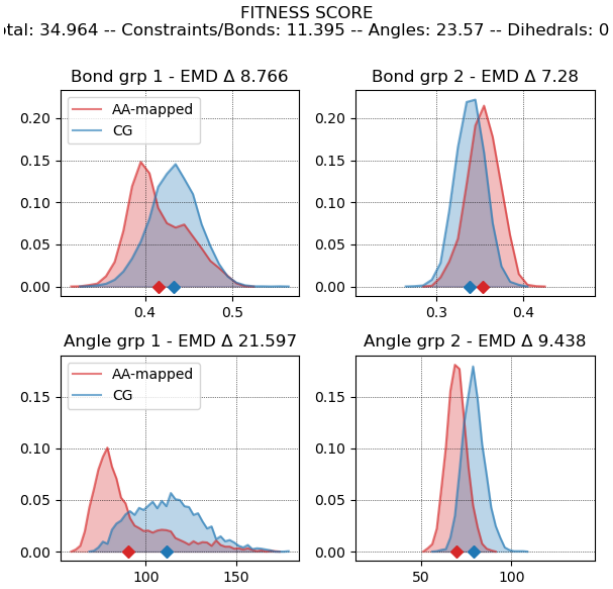

Figure S70. Nm in the trans amide conformation.

Bond 1: {BB_n, BB_{n+1}} – SC1

Bond 2: BB_n – BB_{n+1}

Angle 1: SC1 – BB_n – BB_{n+1}

Angle 2: SC1 – BB_{n+1} – BB_n

6.16 NmO

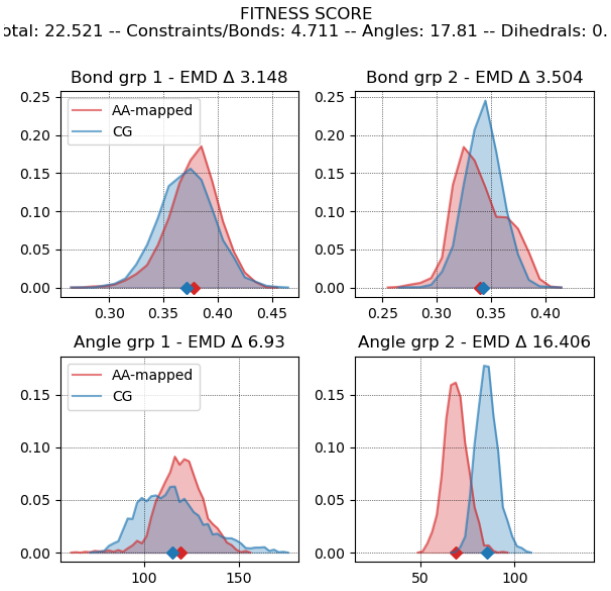

Figure S71. NmO in the cis amide conformation.

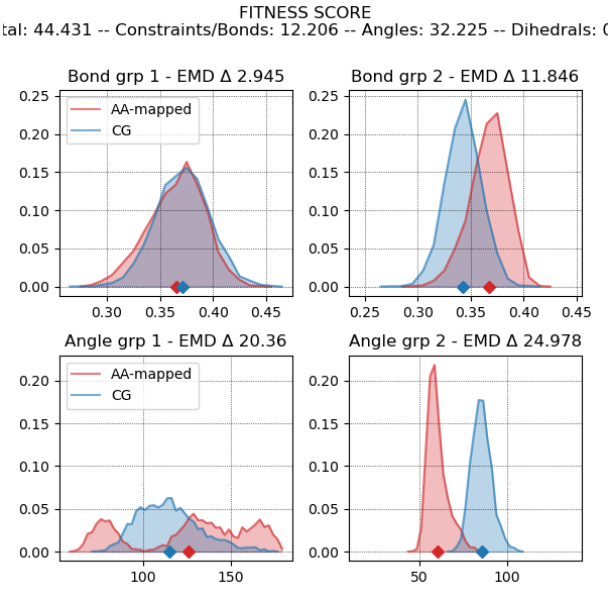

Figure S72. NmO in the trans amide conformation.

Bond 1: {BB_n, BB_{n+1}} – SC1

Bond 2: BB_n – BB_{n+1}

Angle 1: SC1 – BB_n – BB_{n+1}

Angle 2: SC1 – BB_{n+1} – BB_n

6.17 Nn

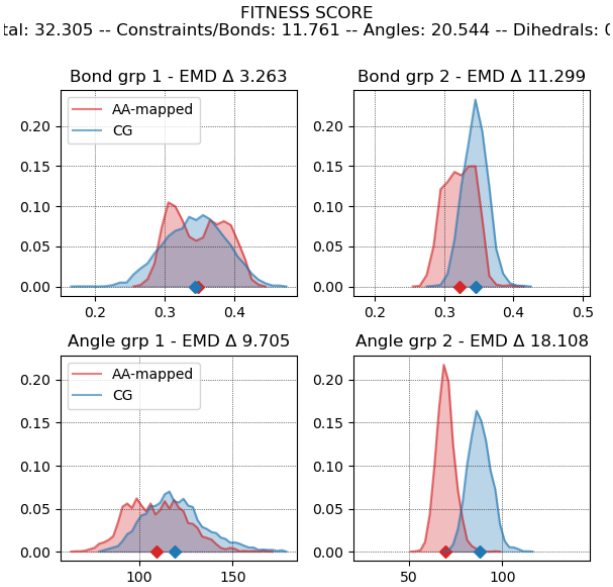

Figure S73. Nn in the cis amide conformation.

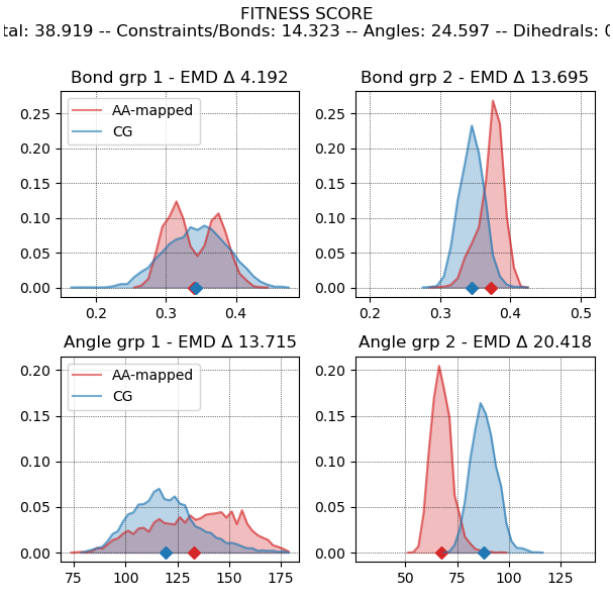

Figure S74. Nn in the trans amide conformation.

Bond 1: {BB_n, BB_{n+1}} – SC1

Bond 2: BB_n – BB_{n+1}

Angle 1: SC1 – BB_n – BB_{n+1}

Angle 2: SC1 – BB_{n+1} – BB_n

6.18 Nq

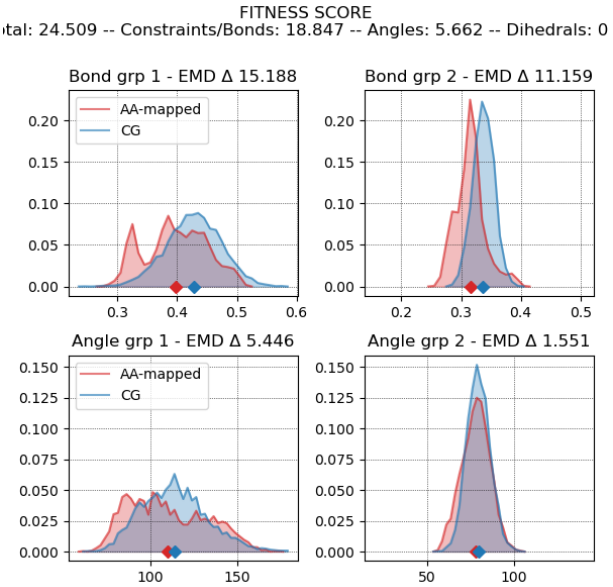

Figure S75. Nq in the cis amide conformation.

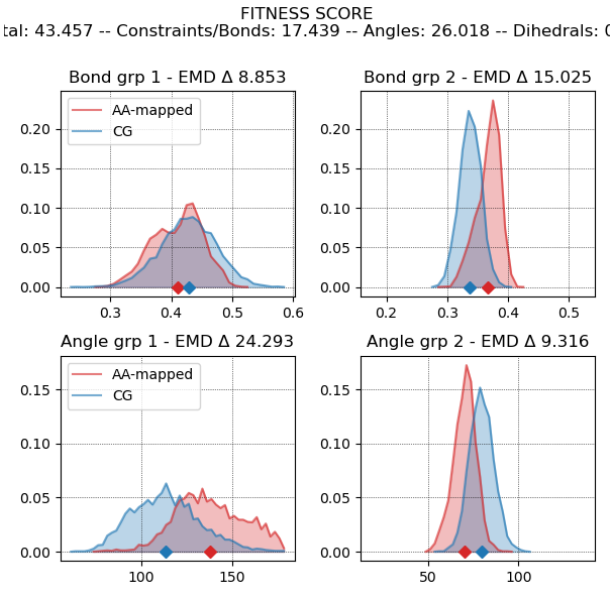

Figure S76. Nq in the trans amide conformation.

Bond 1: {BB_n, BB_{n+1}} – SC1

Bond 2: BB_n – BB_{n+1}

Angle 1: SC1 – BB_n – BB_{n+1}

Angle 2: SC1 – BB_{n+1} – BB_n

6.19 Nr

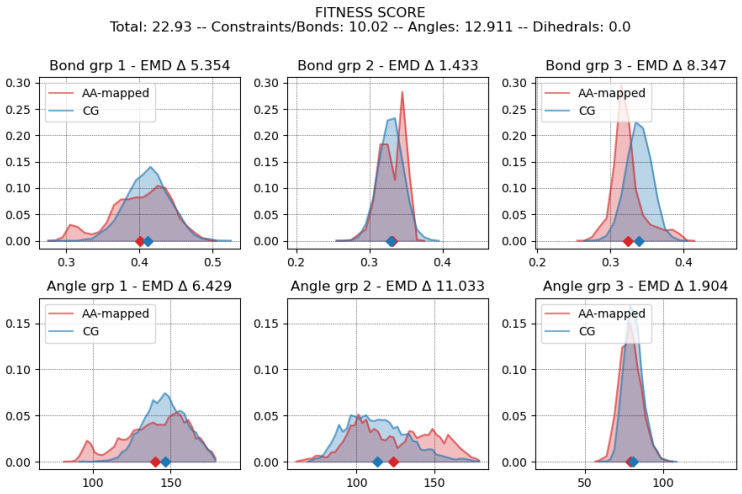

Figure S77. Nr in the cis amide conformation.

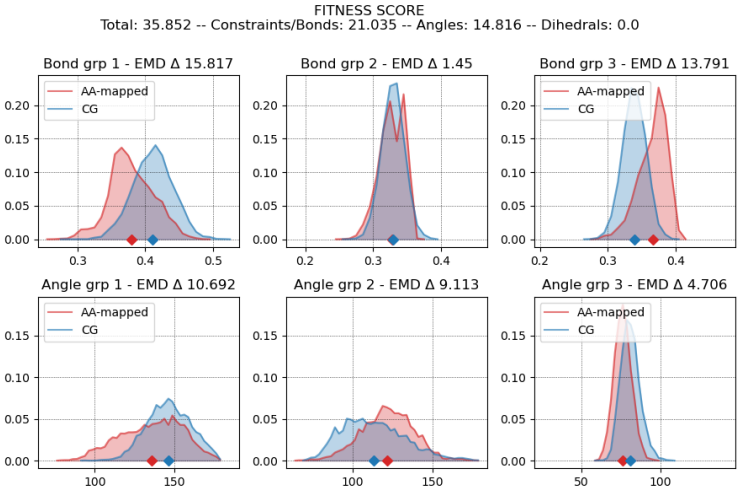

Figure S78. Nr in the trans amide conformation.

Bond 1: $\{BB_n, BB_{n+1}\}$ – SC1

Bond 1: SC1 – SC2 & SC1 – SC2

Bond 3: BB_n – BB_{n+1}

Angle 1: $\{BB_n, BB_{n+1}\}$ – SC1 – SC2

Angle 2: SC1 – BB_n – BB_{n+1}

Angle 2: SC2 – BB_{n+1} – BB_n

6.20 Ns

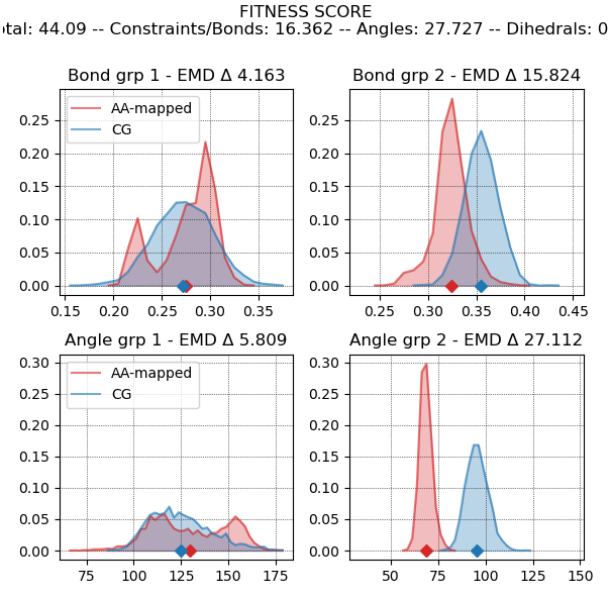

Figure S79. Ns in the cis amide conformation.

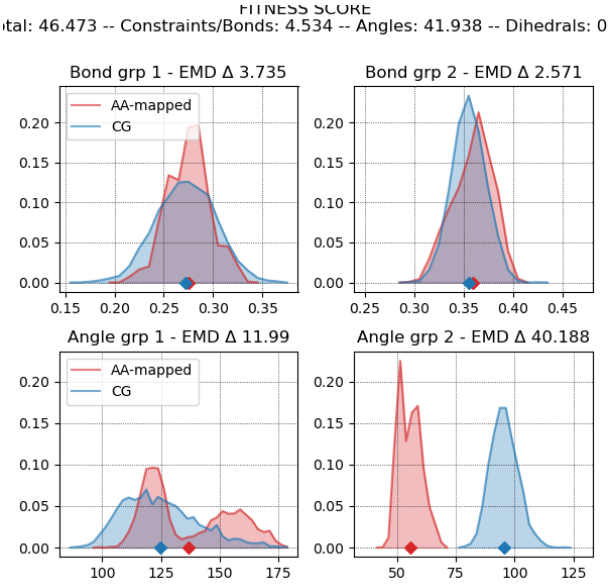

Figure S80. Ns in the trans amide conformation.

Bond 1: {BB_n, BB_{n+1}} – SC1

Bond 2: BB_n – BB_{n+1}

Angle 1: SC1 – BB_n – BB_{n+1}

Angle 2: SC1 – BB_{n+1} – BB_n

6.21 Nse

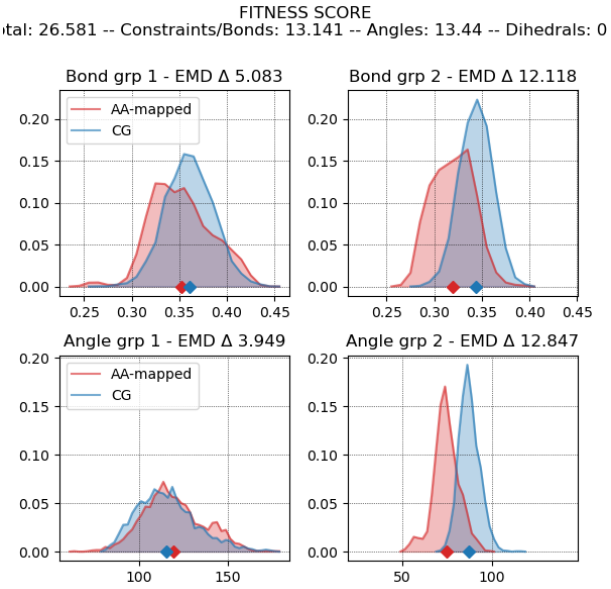

Figure S81. Nse in the cis amide conformation.

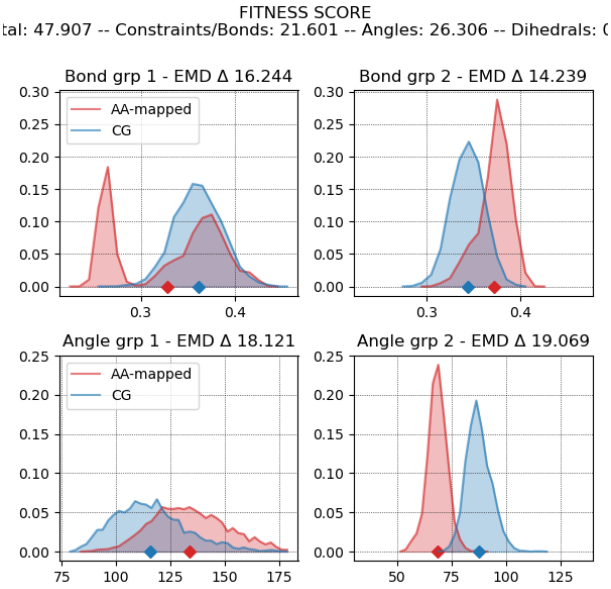

Figure S82. Nse in the trans amide conformation.

Bond 1: {BB_n, BB_{n+1}} – SC1

Bond 2: BB_n – BB_{n+1}

Angle 1: SC1 – BB_n – BB_{n+1}

Angle 2: SC1 – BB_{n+1} – BB_n

6.22 Nt

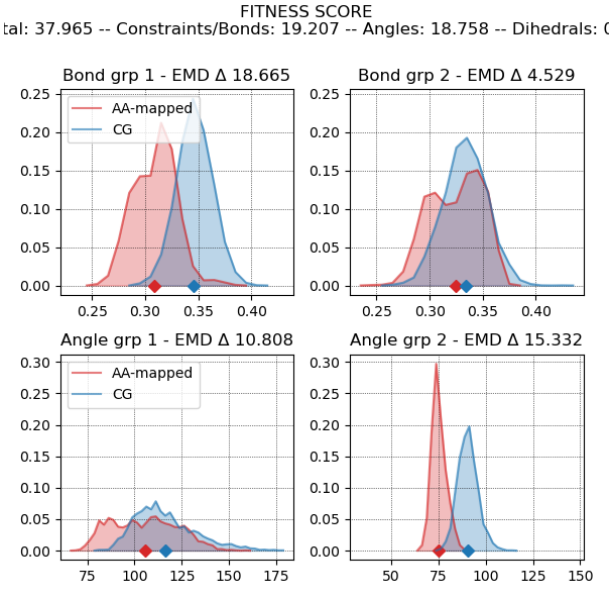

Figure S83. Nt in the cis amide conformation.

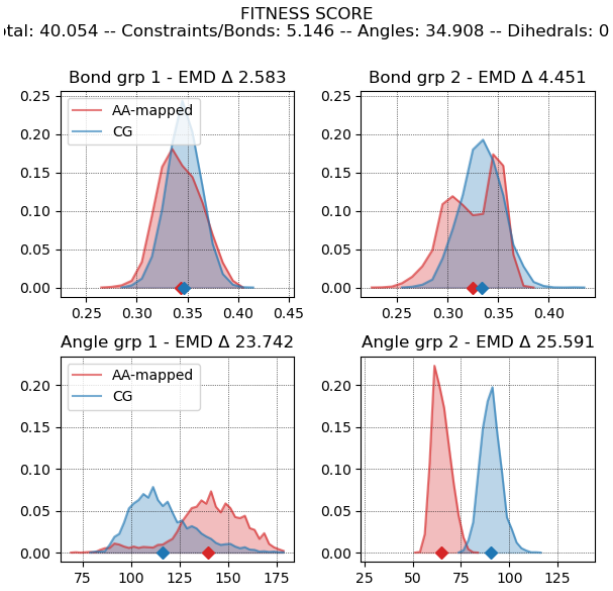

Figure S84. Nt in the trans amide conformation.

<u>Bond 1:</u> {BB_n, BB_{n+1}} – SC1

<u>Bond 2:</u> BB_n – BB_{n+1}

<u>Angle 1</u>: SC1 – BB_n – BB_{n+1}

<u>Angle 2:</u> SC1 – BB_{n+1} – BB_n

6.23 Nv

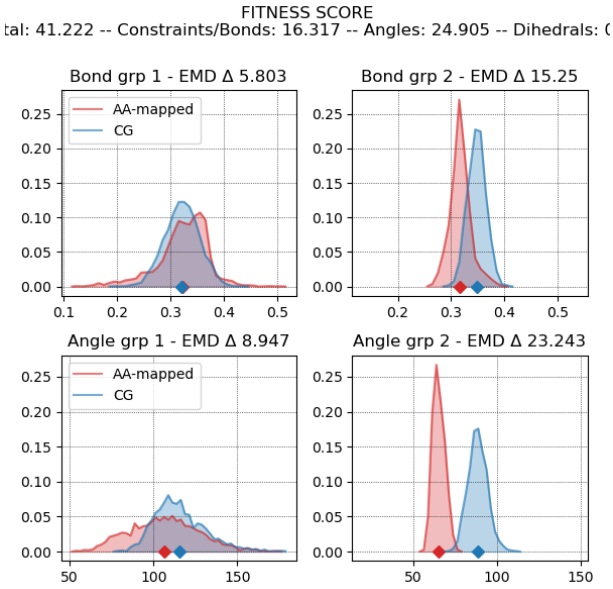

Figure S85. Nv in the cis amide conformation.

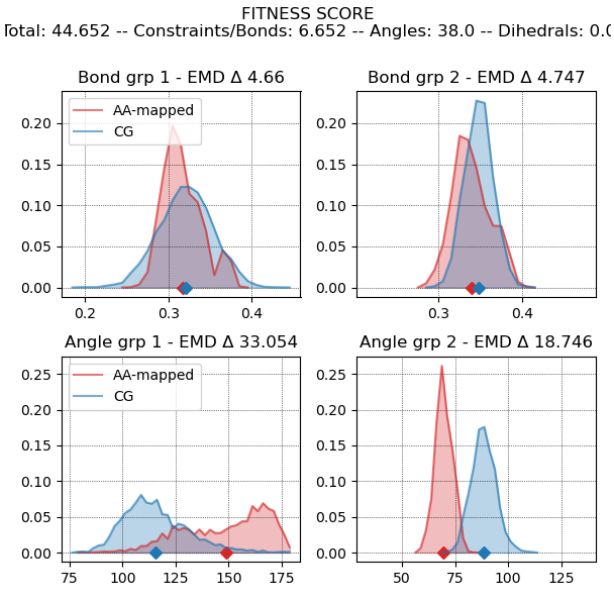

Figure S86. Nv in the trans amide conformation.

Bond 1: {BB_n, BB_{n+1}} – SC1

Bond 2: BB_n – BB_{n+1}

Angle 1: SC1 – BB_n – BB_{n+1}

Angle 2: SC1 – BB_{n+1} – BB_n

6.24 Nw

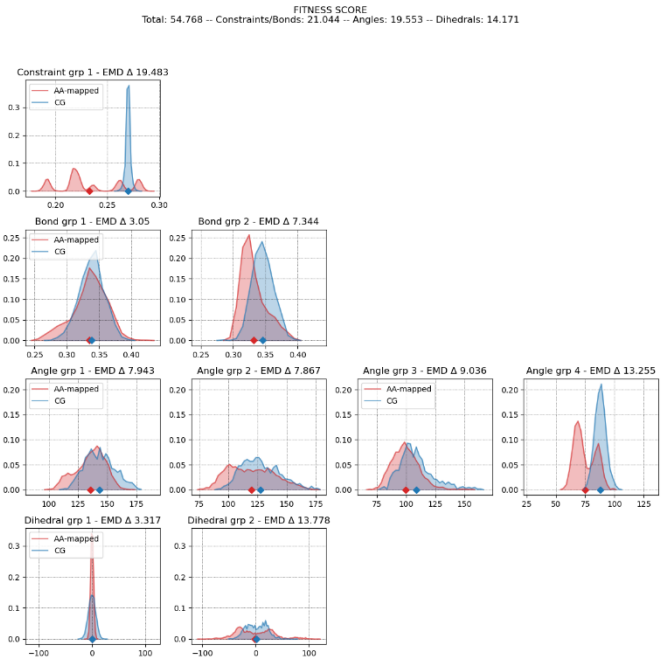

Figure S87. Nw in the cis amide conformation.

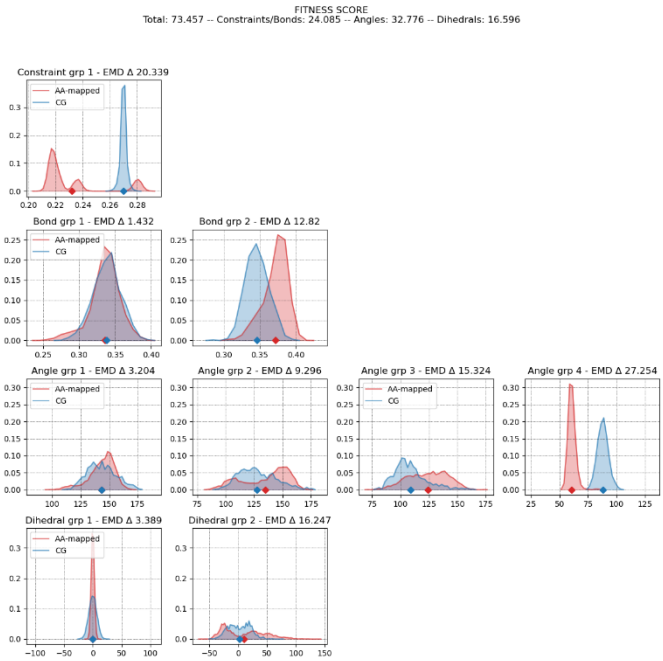

Figure S88. Nw in the trans amide conformation.

Constraint 1: SC1 – SC2 / SC2 – SC3 / etc.

Bond 1: {BB_n, BB_{n+1}} – SC1

Bond 2: BB_n – BB_{n+1}

Angle 1: {BB_n, BB_{n+1}} – SC1 – SC2

Angle 2: {BB_n, BB_{n+1}} – SC1 – SC3

Angle 3: SC1 – BB_n – BB_{n+1}

Angle 4: SC1 – BB_{n+1} – BB_n

Improper dihedral 1: SC1 – SC3 – SC4 – SC2

6.25 Nwe

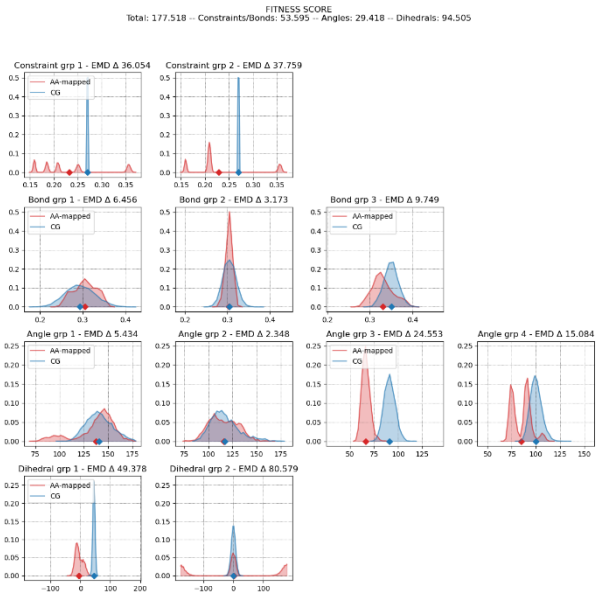

Figure S89. Nwe in the cis amide conformation.

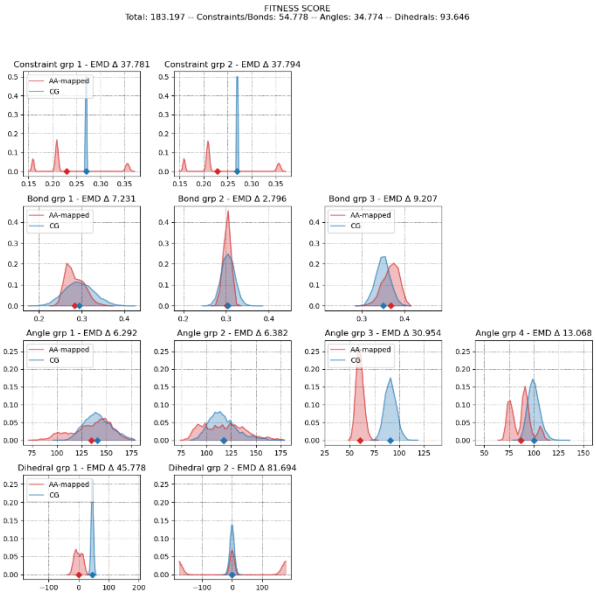

Figure S90. Nwe in the trans amide conformation.

Constraint 1: SC1 – SC2 / SC2 – SC3 / etc.

Bond 1: {BB_n, BB_{n+1}} – SC1

Bond 2: SC1 – SC2

Bond 3: BB_n – BB_{n+1}

Angle 1: {BB_n, BB_{n+1}} – SC1 – SC2

Angle 2: SC1 – BB_n – BB_{n+1}

Angle 3: SC1 – BB_{n+1} – BB_n

Angle 4: SC1 – {SC2-SC3, SC2-SC4}

Improper dihedral 1: SC1 – SC3 – SC4 – SC2

Improper dihedral 1: SC5 – SC2 – SC3 – SC4

6.26 Ny

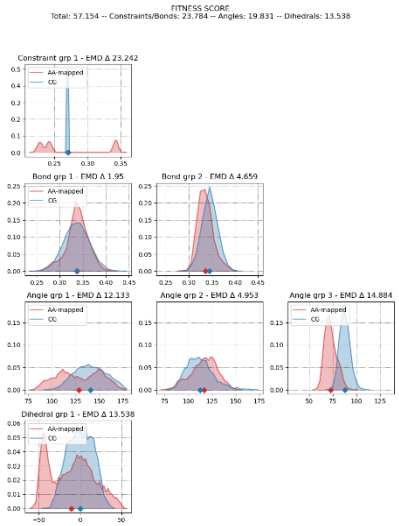

Figure S91. Ny in the cis amide conformation.

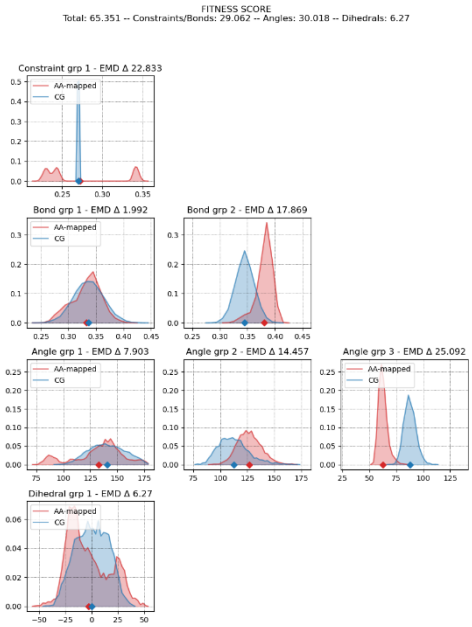

Figure S92. Ny in the trans amide conformation.

Constraint 1: SC1-SC2/SC2-SC3/SC3-SC1

Bond 1: {BB_n, BB_{n+1}} – SC1

Bond 2: BB_n – BB_{n+1}

Angle 1: {BB_n, BB_{n+1}} – SC1 – SC2

Angle 2: SC1 – BB_n – BB_{n+1}

Angle 3: SC1 – BB_{n+1} – BB_n

Improper Dihedral 1: {BB_n, BB_{n+1}}– SC2 – SC3 –SC1

7. Computational LogD Estimation

7.1. Single Amino Acids

We compared the LogD values evaluated for the Martini 2.1 amino acids to the measurements made by Fauchere and Pilska for the N-acetyl amino acid amides.[14] Partitioning between *n*-octanol and water was done at pH 7.0 to 7.2 (maintained by addition of either NaOH or HCl) and concentrations in the respective phases were evaluated using spectroscopic methods. To reflect the fact that termini were capped and that no charge was present, we set the amino acid backbone to a P5 bead in all cases. Generally, there is good agreement between the values obtained as an average of triplicate measurements with those obtained experimentally and that standard deviations within computational measurements were in all cases less than 0.2 logD units (Table S27). For Phe, Pro, Trp and Tyr were generally too hydrophobic with the biggest deviation from experimentally obtained values, this shortfall being among the motivation for the development of the Martini 2.2. amino acid model and beyond in which Phe, Pro and Trp are reparametrized. Evaluations done according to Eq.8.1.

$$\Delta G = 2.303RTlogP \qquad (7.1)$$

Where, $\Delta G = \Delta H_{oco} - \Delta H_{H2O}$, R = 0.008314 kJ/mol/K and T = 298.15 K. ΔH_{H2O} and ΔH_{oco} were taken as the maximum energy in both 0 – 0.5 nm and 3.5 – 4.0 nm in the resultant PMF. All results are in Tables S28 – S47.

Table S27 – Combined calculated amino acid LogPs compared to experimental values.

Amino Acid	$\bar{x}$ LogP	σ LogP	Fauchere and Pilska LogP
Ala	-1.673	0.076	-1.52
Cys	-0.484	0.137	-0.29
Gly	-1.564	0.121	-1.83
Hse	-2.002	0.233	-1.7
Ile	1.069	0.033	-0.03
Leu	0.936	0.070	-0.13
Met	-0.346	0.157	-0.6
Asn	-3.138	0.172	-2.41
Pro	2.922	0.164	-1.34
Gln	-2.883	0.200	-2.05
Ser	-2.228	0.074	-1.87
Thr	-2.191	0.030	-1.57
Val	0.529	0.124	-0.61
Asp	-3.026	0.059	-2.6
Glu	-3.133	0.170	-2.47
Lys	-1.989	0.167	-2.84
Arg	-2.627	0.086	-2.84
Phe	2.946	0.193	-0.04
Trp	2.159	0.047	0.42
Tyr	0.713	0.164	-0.87

Table S28 – Alanine

Simulation	Water energy [kj/mol]	Octanol energy [kj/mol]	ΔG [kj/mol]	LogD
1	-1.275	8.810	10.085	-1.767
2	-0.637	8.386	9.023	-1.580
3	-0.766	8.775	9.541	-1.671
			$\bar{x}$	-1.673
			σ	0.076
			Experiment	-1.52

Table S29 – Cysteine

Simulation	Water energy [kj/mol]	Octanol energy [kj/mol]	ΔG [kj/mol]	LogD
1	1.925	5.533	3.608	-0.632
2	3.940	5.657	1.718	-0.301
3	3.836	6.805	2.969	-0.520
			$\bar{x}$	-0.484
			σ	0.137
			Experiment	-0.29

Table S30 – Glycine

Simulation	Water energy [kj/mol]	Octanol energy [kj/mol]	ΔG [kj/mol]	LogD
1	-1.138	7.818	8.957	-1.569
2	-0.237	7.828	8.065	-1.413
3	-0.720	9.037	9.757	-1.709
			$\bar{x}$	-1.564
			σ	0.121
			Experiment	-1.83

Table S31 – Histidine

Simulation	Water energy [kj/mol]	Octanol energy [kj/mol]	ΔG [kj/mol]	LogD
1	2.346	12.047	9.701	-1.699
2	0.187	13.123	12.936	-2.266
3	1.585	13.231	11.645	-2.040
			$\bar{x}$	-2.002
			σ	0.233
			Experiment	-1.7

Table S32 – Isoleucine

Simulation	Water energy [kj/mol]	Octanol energy [kj/mol]	ΔG [kj/mol]	LogD
1	8.127	1.801	-6.325	1.108
2	7.819	1.701	-6.118	1.072
3	7.626	1.761	-5.865	1.027
			$\bar{x}$	1.069
			σ	0.033
			Experiment	-0.03

Table S33 – Leucine

Simulation	Water energy [kj/mol]	Octanol energy [kj/mol]	ΔG [kj/mol]	LogD
1	7.422	2.573	-4.849	0.849
2	8.262	2.907	-5.356	0.938
3	8.356	2.530	-5.826	1.021
			$\bar{x}$	0.936
			σ	0.070
			Experiment	-0.13

Table S34 – Methionine

Simulation	Water energy [kj/mol]	Octanol energy [kj/mol]	ΔG [kj/mol]	LogD
1	3.096	5.722	2.625	-0.460
2	4.783	5.489	0.706	-0.124
3	4.155	6.739	2.585	-0.453
			$\bar{x}$	-0.346
			σ	0.157
			Experiment	-0.6

Table S35 – Asparagine

Simulation	Water energy [kj/mol]	Octanol energy [kj/mol]	ΔG [kj/mol]	LogD
1	-3.629	13.829	17.458	-3.058
2	-2.476	14.531	17.007	-2.979
3	-2.731	16.545	19.276	-3.376
			$\bar{x}$	-3.138
			σ	0.172
			Experiment	-2.41

Table S36 – Proline

Simulation	Water energy [kj/mol]	Octanol energy [kj/mol]	ΔG [kj/mol]	LogD
1	13.483	-2.777	-16.260	2.848
2	13.659	-4.318	-17.977	3.149
3	12.616	-3.187	-15.803	2.768
			$\bar{x}$	2.922
			σ	0.164
			Experiment	-1.34

Table S37 – Glutamine

Simulation	Water energy [kj/mol]	Octanol energy [kj/mol]	ΔG [kj/mol]	LogD
1	-1.227	14.107	15.334	-2.686
2	-2.105	15.919	18.024	-3.157
3	-2.366	13.647	16.013	-2.805
			$\bar{x}$	-2.883
			σ	0.200
			Experiment	-2.05

Table S38 – Serine

Simulation	Water energy [kj/mol]	Octanol energy [kj/mol]	ΔG [kj/mol]	LogD
1	-0.688	12.237	12.926	-2.264
2	-0.829	12.281	13.110	-2.296
3	-0.974	11.160	12.134	-2.125
			$\bar{x}$	-2.883
			σ	0.200
			Experiment	-1.87

Table S39 – Threonine

Simulation	Water energy [kj/mol]	Octanol energy [kj/mol]	ΔG [kj/mol]	LogD
1	-1.096	11.655	12.751	-2.233
2	-1.099	11.292	12.391	-2.170
3	-1.028	11.356	12.385	-2.169
			$\bar{x}$	-2.191
			σ	0.030
			Experiment	-1.57

Table S40 – Valine

Simulation	Water energy [kj/mol]	Octanol energy [kj/mol]	ΔG [kj/mol]	LogD
1	4.478	2.356	-2.122	0.372
2	6.676	2.830	-3.846	0.674
3	6.335	3.243	-3.092	0.542
			$\bar{x}$	0.529
			σ	0.124
			Experiment	-0.61

Table S41 – Aspartic Acid

Simulation	Water energy [kj/mol]	Octanol energy [kj/mol]	ΔG [kj/mol]	LogD
1	-1.274	16.342	17.616	-3.086
2	-2.617	14.774	17.391	-3.046
3	-1.456	15.356	16.812	-2.945
			$\bar{x}$	-3.026
			σ	0.059
			Experiment	-2.6

Table S42 – Glutamic Acid

Simulation	Water energy [kj/mol]	Octanol energy [kj/mol]	ΔG [kj/mol]	LogD
1	-2.841	14.702	17.543	-3.073
2	-2.596	16.612	19.208	-3.365
3	-1.078	15.824	16.902	-2.961
			$\bar{x}$	-3.133
			σ	0.170
			Experiment	-2.47

Table S43 – Lysine

Simulation	Water energy [kj/mol]	Octanol energy [kj/mol]	ΔG [kj/mol]	LogD
1	0.429	13.132	12.703	-2.225
2	0.322	10.933	10.612	-1.859
3	0.413	11.158	10.745	-1.882
			$\bar{x}$	-1.989
			σ	0.167
			Experiment	-2.84

Table S44 – Arginine

Simulation	Water energy [kj/mol]	Octanol energy [kj/mol]	ΔG [kj/mol]	LogD
1	-1.292	14.398	15.690	-2.748
2	0.238	14.830	14.591	-2.556
3	-0.394	14.324	14.718	-2.578
			$\bar{x}$	-2.627
			σ	0.086
			Experiment	-2.84

Table S45 – Phenylalanine

Simulation	Water energy [kj/mol]	Octanol energy [kj/mol]	ΔG [kj/mol]	LogD
1	15.728	-0.037	-15.765	2.761
2	16.917	-1.424	-18.341	3.213
3	16.593	0.236	-16.357	2.865
			$\bar{x}$	2.946
			σ	0.193
			Experiment	-0.04

Table S46 – Tryptophan

Simulation	Water energy [kj/mol]	Octanol energy [kj/mol]	ΔG [kj/mol]	LogD
1	13.473	1.226	-12.247	2.145
2	13.803	1.759	-12.044	2.110
3	14.007	1.318	-12.690	2.223
			$\bar{x}$	2.159
			σ	0.047
			Experiment	0.42

Table S47 – Tyrosine

Simulation	Water energy [kj/mol]	Octanol energy [kj/mol]	ΔG [kj/mol]	LogD
1	9.149	4.651	-4.499	0.788
2	9.167	4.224	-4.943	0.866
3	7.249	4.475	-2.774	0.486
			$\bar{x}$	0.713
			σ	0.164
			Experiment	-0.87

7.2. Single Peptoid Residues

Table S48 – Nf

Simulation	Water energy [kj/mol]	Octanol energy [kj/mol]	ΔG [kj/mol]	LogD
1	21.15964	-6.62587	-27.78551	4.867
2	20.98874	-5.874386	-26.863126	4.705
3	20.85884	-5.646056	-26.504896	4.643
			$\bar{x}$	4.738
			σ	0.094

Table S49 – Nfe

Simulation	Water energy [kj/mol]	Octanol energy [kj/mol]	ΔG [kj/mol]	LogD
1	22.68022	-7.00584	-29.6861	5.200
2	19.48207	-7.48153	-26.9636	4.723
3	20.78674	-6.93362	-27.7204	4.856
			$\bar{x}$	4.926
			σ	0.201

Table S50 – Nfex

Simulation	Water energy [kj/mol]	Octanol energy [kj/mol]	ΔG [kj/mol]	LogD
1	23.17480	-6.916362	-30.091162	5.271
2	23.64633	-6.330258	-29.976588	5.251
3	21.28281	-7.552055	-28.834865	5.051
			$\bar{x}$	5.191
			σ	0.010

Table S51 – Nfn

Simulation	Water energy [kj/mol]	Octanol energy [kj/mol]	ΔG [kj/mol]	LogD
1	15.81482	-5.678048	-21.492868	3.765
2	16.51626	-4.974607	-21.490867	3.764
3	15.67659	-4.508709	-20.185299	3.536
			$\overline{x}$	3.688
			σ	0.108

Table S52 – Nf[naph]

Simulation	Water energy [kj/mol]	Octanol energy [kj/mol]	ΔG [kj/mol]	LogD
1	28.64359	-8.260299	-36.903889	6.464
2	31.94029	-9.118527	-41.058817	7.192
3	31.64883	-10.35277	-42.0016	7.357
			$\overline{x}$	7.004
			σ	0.388

Table S53 – Nfe[4Cl]

Simulation	Water energy [kj/mol]	Octanol energy [kj/mol]	ΔG [kj/mol]	LogD
1	23.51337	-7.75421	-31.2676	5.477
2	24.11048	-8.3002	-32.4107	5.677
3	23.40154	-7.69121	-31.0927	5.446
			$\overline{x}$	5.533
			σ	0.102

Table S54 – Nfe[4Br]

Simulation	Water energy [kj/mol]	Octanol energy [kj/mol]	ΔG [kj/mol]	LogD
1	23.94346	-8.15858	-32.102	5.623
2	24.56152	-8.1246	-32.6861	5.725
3	24.03651	-8.32673	-32.3632	5.669
			$\overline{x}$	5.672
			σ	0.042

Table S55 – Nk

Simulation	Water energy [kj/mol]	Octanol energy [kj/mol]	ΔG [kj/mol]	LogD
1	8.017939	1.324048	-6.69389	1.173
2	7.655092	0.752617	-6.90248	1.209
3	7.788909	1.808323	-5.98059	1.048
			$\bar{x}$	1.143
			σ	0.069

Table S56 – Nke

Simulation	Water energy [kj/mol]	Octanol energy [kj/mol]	ΔG [kj/mol]	LogD
1	3.665132	3.769994	0.104862	-0.018
2	4.3885	3.800343	-0.58816	0.103
3	4.033832	3.497304	-0.53653	0.094
			$\bar{x}$	0.060
			σ	0.055

Table S57 – Nab

Simulation	Water energy [kj/mol]	Octanol energy [kj/mol]	ΔG [kj/mol]	LogD
1	16.01986	-3.64546	-19.6653	3.445
2	16.84876	-3.94692	-20.7957	3.643
3	14.38903	-4.14805	-18.5371	3.247
			$\bar{x}$	3.445
			σ	0.162

Table S58 – Nw

Simulation	Water energy [kj/mol]	Octanol energy [kj/mol]	ΔG [kj/mol]	LogD
1	19.30856	-4.080147	-23.388707	4.097
2	20.99385	-3.304055	-24.297905	4.256
3	19.7299	-3.930853	-23.660753	4.144
			$\bar{x}$	4.166
			σ	0.067

Table S58 – Nwe

Simulation	Water energy [kj/mol]	Octanol energy [kj/mol]	ΔG [kj/mol]	LogD
1	20.51027	-4.306285	-24.816555	4.347
2	22.97705	-4.216702	-27.193752	4.763
3	22.46331	-5.638476	-28.101786	4.922
			$\bar{x}$	4.677
			σ	0.242

8. Assembly Studies

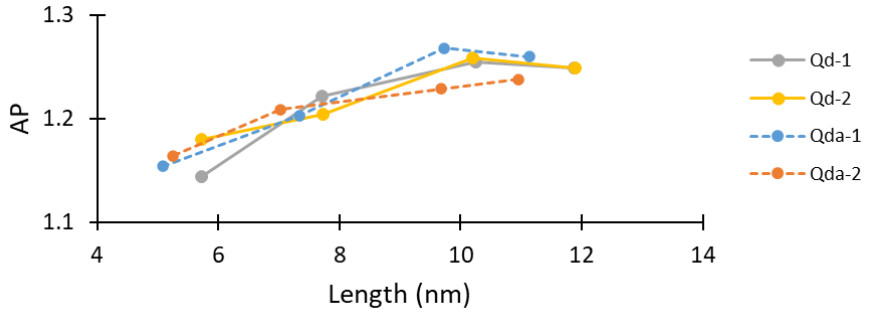

Figure S93. Equilibrium fibre length and associated AP score with either a Qd or Qda bead at the N-terminus. The resultant behaviour is the same irrespective of this choice, indicating that packing of minimal peptoids can be reproduced with either choice. In this work we elected to use an Qd bead as this is also used for peptide N-termini in Martini 2.1.

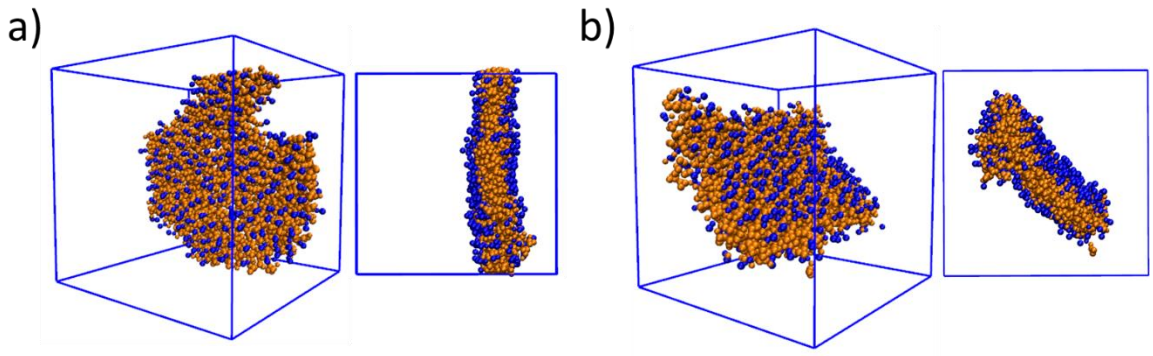

Figure S94. Resultant assembly structures formed from duplicate simulations of 300 Nf-Nke-Nf a 12.5 x 12.5 x 12.5 nm box for 250 ns of simulation time a) and b). in both cases flat bilayer like structures from with a well-defined aromatic core which agrees with other analyses of this system.[15]

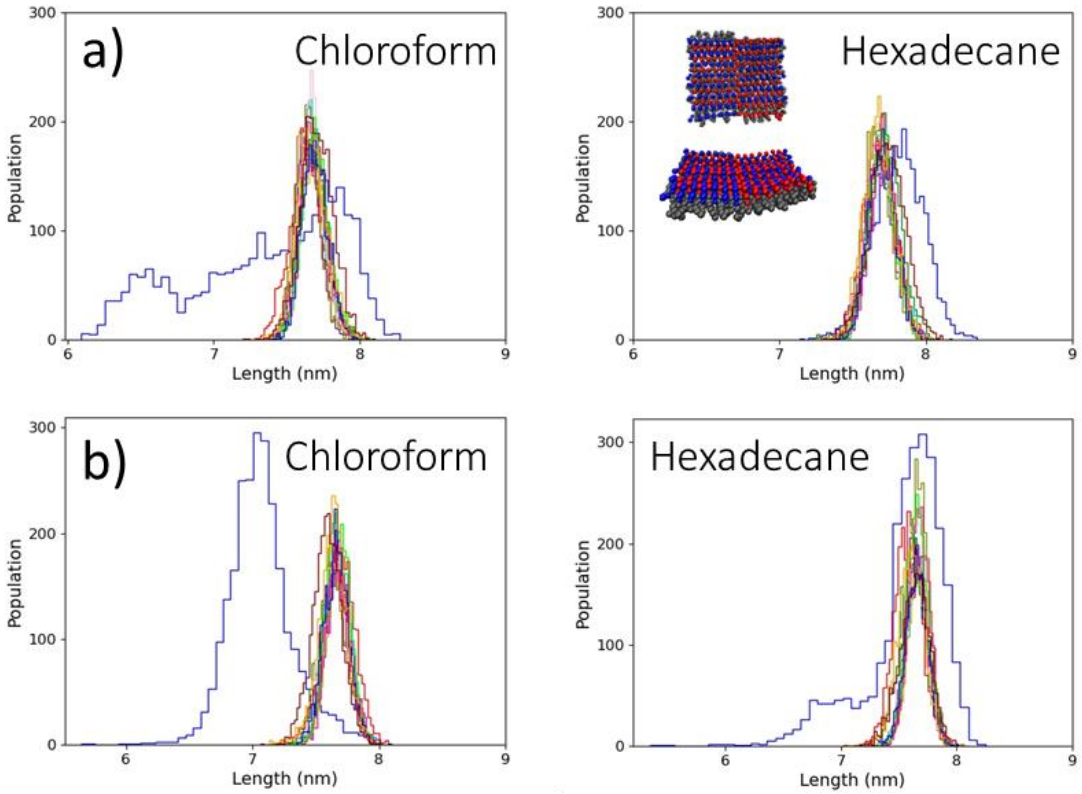

Figure S95. Histograms of end-to-end chain lengths measured for $(Nke\text{-}Nfe)_7$-$(Ne\text{-}Nfe)_7$ 28mer at air-chloroform and air-hexadecane interface, over 100 ns (2500 frames) duplicate experiments a) and b). In both cases the majority of the 14 chains are centred around 77 Å in length. Note the chain which is distinct from this (in blue) is at the edge and is not fully integrated into the sheet structure leading to distinct variations in length.

9. Dihedral Optimization

Prior to the use of Ns, Nt and NmO it was necessary to parameterise several dihedral torsions at the atomistic level. Here scans at the MP2/6-31G(d) level of theory were performed and dihedral angle potentials at the MD level were then selected to adequately reproduce the potential energy surface (PES) of the torsion. Partial charge fitting was done following the method we adopted for peptoid monomers previously and the energies of water interactions are detailed in Tables S60 – S62.[15] Additionally dihedral angle scans are shown in Figures S96 – S105.

In some cases, substantial differences exist between the QM and MD levels exist, this is due to structural changes through hydrogen bond formation, as well as unfavourable 'eclipsed protons' along a methylene chain which are beyond 1 – 4 exclusions (NmO, see Figure S96) however the global minima are reproduced and so this fit is reasonable.

Table S60 – NmO interaction energies (kcal mol^{-1}).

QM dipole magnitude: 1.703

MD dipole magnitude: 1.878 (deviation angle: 52.4°)

Complex	ΔE (HF)	ΔE (CGenFF)	ΔΔE
Interaction-1	-8.41	-8.38	-0.02
		MAE	0.02

Table S61 – Ns interaction energies (kcal mol^{-1}).

QM dipole magnitude: 2.118

MD dipole magnitude: 2.367 (deviation angle: 67.2°)

Complex	ΔE (HF)	ΔE (CGenFF)	ΔΔE
Interaction-1	-6.71	-6.52	-0.19
Interaction-2	-15.21	-15.33	0.12
		MAE	0.16

Table S62 – Nt interaction energies (kcal mol^{-1}).

QM dipole magnitude: 3.493

MD dipole magnitude: 5.419 (deviation angle: 3.9°)

Complex	ΔE (HF)	ΔE (CGenFF)	ΔΔE
Interaction-1	-6.35	-6.61	0.26
Interaction-2	-8.69	-8.37	-0.32
Interaction-3	-7.92	-7.99	0.06
		MAE	0.21

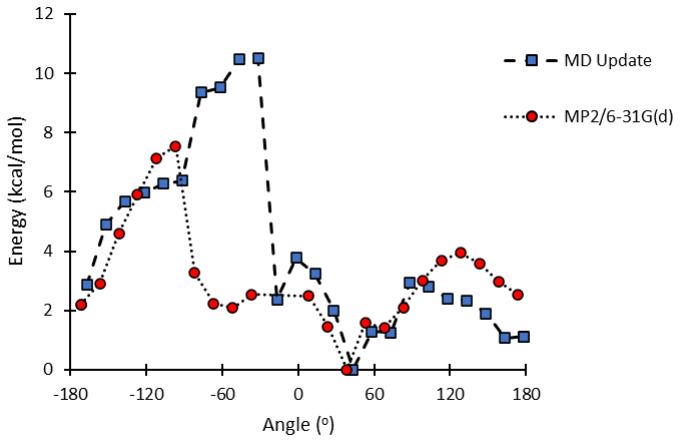

Figure S96. Torsion NTOID-CG321-CG321-CG3O1 along NmO sidechain branch.

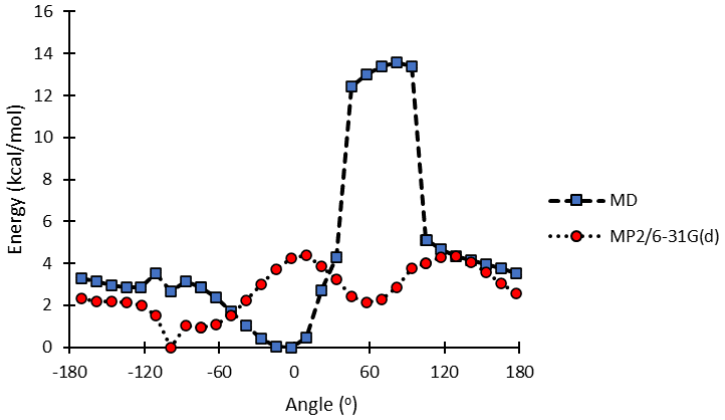

Figure S97. Torsion NTOID-CG321-OG311-HGP1 on Ns sidechain.

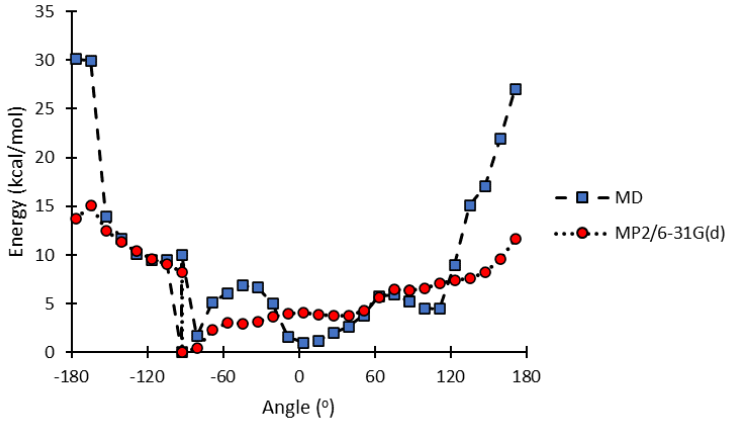

Figure S98. Torsion CG321-NTOID-CG321-OG311 on Ns sidechain.

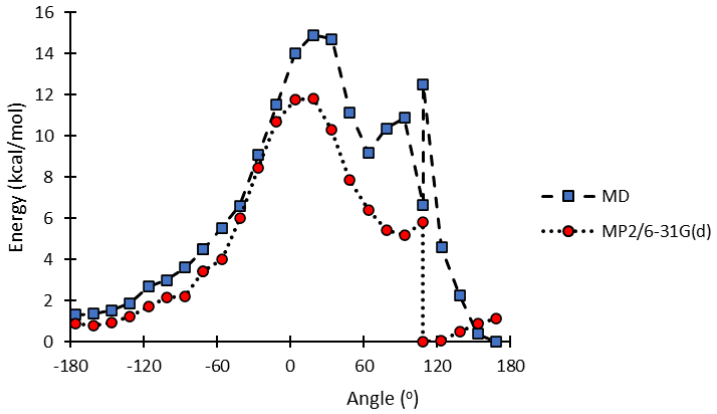

Figure S99. Torsion CG2O1-NTOID-CG321-OG311 on Ns sidechain.

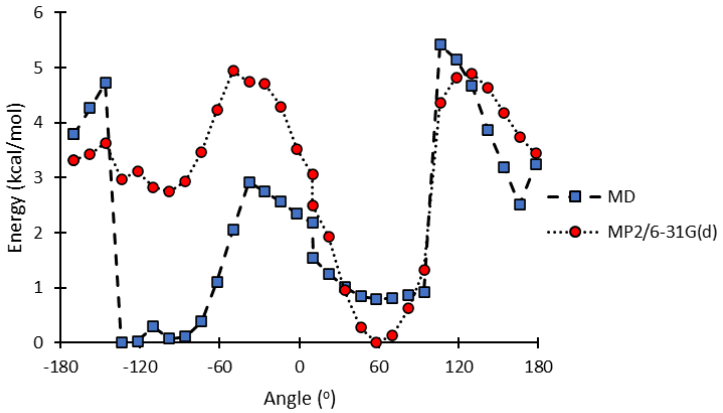

Figure S100. Torsion HGP1-OG311-CG311-NTOID on Nt sidechain.

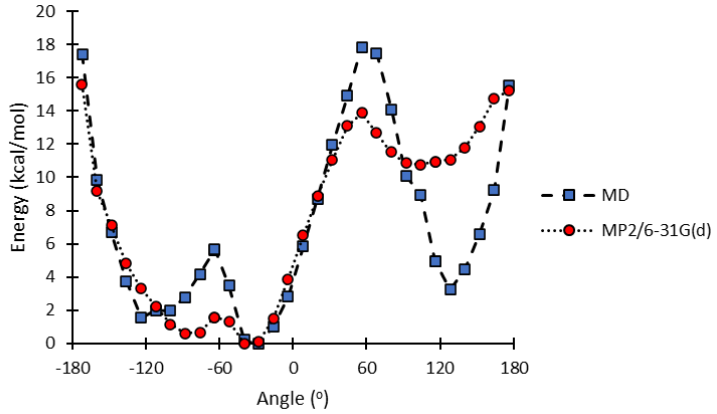

Figure S101. Torsion CG331-CG311-NTOID-CG321 on Nt sidechain.

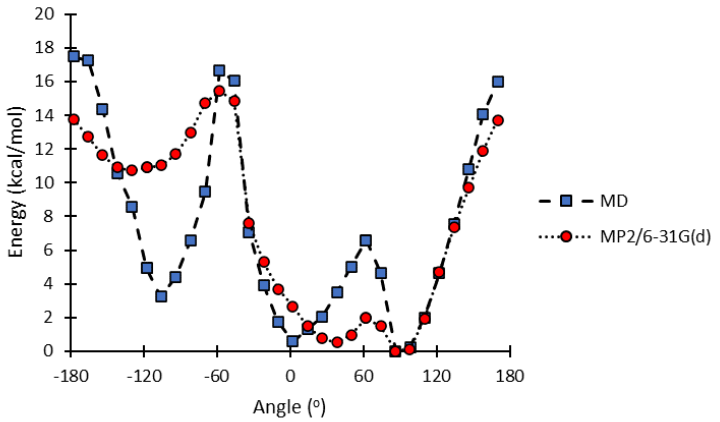

Figure S102. Torsion CG331-CG311-NTOID-OG311 on Nt sidechain.

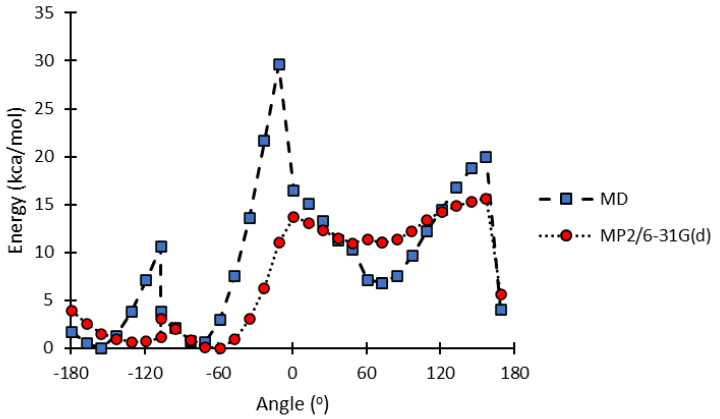

Figure S103. Torsion OG311-CG311-NTOID-CG2O1 on Nt sidechain.

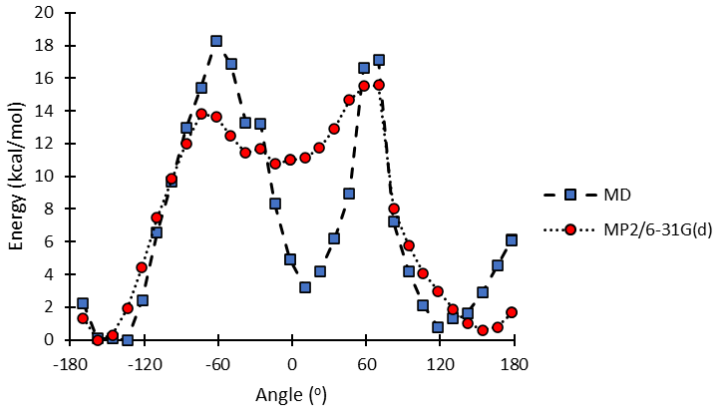

Figure S104. Torsion HGA1-CG311-NTOID-CG321 on Nt sidechain.

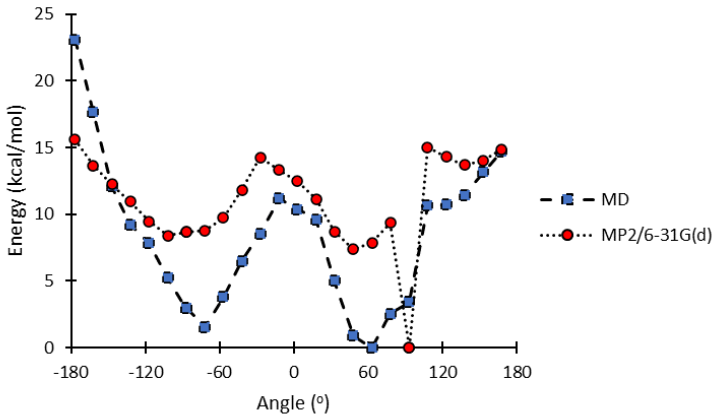

Figure S105. Torsion CG2O1-CG321-NTOID-CG311 on Nt sidechain.

10. References

1. R. N. Zuckermann, J. M. Kerr, S. B. H. Kent and W. H. Moos, *J. Am. Chem. Soc.*, 1992, **114**, 10646-10647.
2. A. Salaün, A. Favre, B. Le Grel, M. Potel and P. Le Grel, *J. Org. Chem.*, 2006, **71**, 150-158.
3. Y. Lee and J. Seo, *Tetrahedron Lett.*, 2018, **59**, 3946-3949.
4. H. L. Bolt, C. E. J. Williams, R. V. Brooks, R. N. Zuckermann, S. L. Cobb and E. H. C. Bromley, *Biopolymers*, 2017, **108**.
5. P. Pracht, F. Bohle and S. Grimme, *Phys. Chem. Chem. Phys.*, 2020, **22**, 7169-7192.
6. J. V. Vermaas, D. J. Hardy, J. E. Stone, E. Tajkhorshid and A. Kohlmeyer, *J Chem Inf Model*, 2016, **56**, 1112-1116.
7. Force fields in GROMACS, https://manual.gromacs.org/current/user-guide/force-fields.html, Accessed 2023.
8. B. Hess, H. Bekker, H. J. C. Berendsen and J. G. E. M. Fraaije, *J. Comput. Chem.*, 1997, **18**, 1463-1472.
9. M. F. Zhao, K. J. Lachowski, S. Zhang, S. Alamdari, J. Sampath, P. Mu, C. J. Mundy, J. Pfaendtner, J. J. De Yoreo, C. L. Chen, L. D. Pozzo and A. L. Ferguson, *Biomacromolecules*, 2022, **23**, 992–1008.
10. Martini tutorials: Free energy techniques http://cgmartini.nl/index.php/tutorials-general-introduction-gmx5/partitioning-techniques, Accessed 2023.
11. T. M. M. J. Abraham, R. Schulz, S. Páll, J. C. Smith, B. Hess, E. Lindahl, *SoftwareX*, 2015, **1**, 19 - 25.
12. W. Humphrey, Dalke, A. and Schulten, K., *J. Molec. Graphics* 1996, **14.1**, 33 - 38.
13. J. C. Phillips, R. Braun, W. Wang, J. C. Gumbart, E. Tajkhorshid, E. Villa, C. Chipot, R. D. Skeel, L. Kale and S. K., *J. Comp. Chem.*, 2005, **26**, 1781-1802.
14. J. L. Fauchere and V. Pliska, *European Journal of Medicinal Chemistry*, 1983, **18**, 369-375.
15. K. H. A. L. Hamish W. A. Swanson, and Tell Tuttle, *J. Phys. Chem. B*, 2023.